THE BIOENGINEERING OF HUMAN BLOOD AND LYMPHATIC CAPILLARIES IN DERMO-EPIDERMAL SKIN SUBSTITUTES

DISSERTATION

ZUR

ERLANGUNG DER NATURWISSENSCHAFTLICHEN DOKTORWÜRDE

(DR. SC. NAT.)

VORGELEGT DER

MATHEMATISCH-NATURWISSENSCHAFTLICHEN FAKULTÄT

DER

UNIVERSITÄT ZÜRICH

VON

JOACHIM LUGINBÜHL

VON

SCHLOSSWIL BE

PROMOTIONSKOMITEE

PROF. DR. REINHARD DUMMER (VORSITZ)

PROF. DR. MAX GASSMANN

PROF. DR. ERNST REICHMANN (LEITUNG DER DISSERTATION)

ZÜRICH, 2014

This work has been performed under the supervision of Prof. Dr. Ernst Reichmann at the Tissue Biology Research Unit, Department of Surgery, University Children's Hospital Zurich, Zurich, Switzerland.

TABLE OF CONTENTS

TABLE OF CONTENTS **5**

ABBREVIATIONS **7**

SUMMARY **9**

ZUSAMMENFASSUNG **11**

1 INTRODUCTION **13**

1.1 HUMAN SKIN **13**

1.1.1 STRUCTURE AND FUNCTION OF HUMAN SKIN 13

The epidermis 15
The dermo-epidermal junction 18
The dermis 21
The hypodermis 23

1.1.2 THE CUTANEOUS MICROVASCULATURE 23

The cardiovascular system 24
The lymphatic vascular system 33
Molecular markers of blood and lymphatic endothelium 36
Pericytes 37

1.2 CUTANEOUS WOUND HEALING **38**

1.2.1 INFLAMMATION 40
1.2.2 EPITHELIALIZATION 40
1.2.3 FORMATION OF GRANULATION TISSUE 41
1.2.4 NEOVASCULARIZATION 41
1.2.5 SCAR FORMATION 42
1.2.6 SEROMA FORMATION 43
1.2.7 ABNORMAL WOUND HEALING 43
1.2.8 OXYGEN AND WOUND HEALING 44

1.3 TISSUE ENGINEERING OF SKIN **46**

1.3.1 PRINCIPLES OF TISSUE ENGINEERING 46
1.3.2 THE BIOENGINEERING OF HUMAN SKIN 50

1.4 PREVASCULARIZATION OF ENGINEERED TISSUES IN VITRO 52

1.4.1 APPROACHES TO ACCELERATE REVASCULARIZATION OF TISSUE-ENGINEERED TISSUES AND ORGANS 53
1.4.2 ENDOTHELIAL CELLS PROVIDE INDUCTIVE SIGNALS INDEPENDENT OF BLOOD FLOW 57
1.4.3 PREVASCULARIZATION: STATE OF THE ART AND FUTURE PERSPECTIVES 58

2 RESULTS 62

2.1 BIOENGINEERING DERMO-EPIDERMAL SKIN GRAFTS WITH BLOOD AND LYMPHATIC CAPILLARIES 62

2.2 RAPID PERFUSION DIRECTS THE HEALING OF PRE-VASCULARIZED DERMO-EPIDERMAL SKIN SUBSTITUTES FROM SCAR FORMATION TOWARDS REGENERATION 75

2.2.1 ABSTRACT 77
2.2.2 INTRODUCTION 78
2.2.3 RESULTS 80
2.2.4 DISCUSSION 87
2.2.5 MATERIALS AND METHODS 89
2.2.6 FIGURES AND FIGURE LEGENDS 95

3 CONCLUSIONS 107

4 REFERENCES 111

5 ACKNOWLEDGEMENTS 121

6 CURRICULUM VITAE 122

7 PUBLICATIONS 124

8 CONTRIBUTIONS 125

ABBREVIATIONS

Ang	Angiopoietin
ATP	Adenosine triphosphase
BA	Branchial arteries
BEC	Blood endothelial cells
bFGF	Basic fibroblast growth factor
BM	Basement membrane
BMP	Bone morphogenic protein
BV	Blood vessel
CCL	CC chemokine ligand
CEA	Cultured epithelial autograft
CSF-1	Colony stimulating factor-1
DA	Dorsal aorta
dai	Days after integration
DEJ	Dermo-epidermal junction
DESS	Dermo-epidermal skin substitute
dpT	Days post-transplantational
E1	Embryonic day 1
EEC	Embryonic ectoderm
EGF	Epidermal growth factor
Eph	Eph receptor family
EXE	Extra-embryonic ectoderm
FGF	Fibroblast growth factor
GFR	Growth factor receptor
HDMEC	Human dermal microvascular endothelial cells
HUVEC	Human umbilical vein endothelial cells
ICA	Intercarotid artery
IGF	Insulin growth factor
ISV	Intersomitic vessel
KGF	Keratinocyte growth factor
LEC	Lymphatic endothelial cells

LV	Lymphatic vessel
LYVE-1	Lymphatic vascular endothelial hyaluronan receptor-1
NADPH	Nicotinamide adenine dinucleotide phosphate-oxidase
NG-2/MCSP	Neural/Glial Antigen 2/Melanoma chondroitin sulfate proteoglycan
Np	Neuropilin
NPDESS	Non-prevascularized dermo-epidermal skin substitute
OFT	Outflow tract
PCV	Posterior cardinal vein
PDESS	Prevascularized dermo-epidermal skin substitute
PDGF	Platelet-derived growth factor
PDMS	Polydimethylsiloxane
PLG	Polylactic glycol
PLGA	Polylactic-co-glycolic acid
PLLA	Polylactic acid
PPS	Posterior primitive streak
Prox-1	Prospero homeobox protein 1
ROS	Reactive oxygen species
RV	Right ventricle
SC	Stem cell
Shh	Sonic hedgehoc
TCP	Tricalcium phosphate
TEBG	Tissue-engineered bone graft
TGF-β	Transforming growth factor-beta
TNF-α	Tumor necrosis factor-alpha
UV	Ultraviolet
VEGF	Vascular endothelial growth factor
VEGFR2 (Flk-1)	Vascular endothelial growth factor receptor 2
vSMC	Vascular smooth muscle cells
α-SMA	Smooth-muscle-alpha-actin

SUMMARY

Slow vascularization of bioengineered organs after transplantation constitutes a major hurdle in tissue engineering and regenerative medicine. Providing these organs with functional blood and lymphatic capillaries prior to transplantation (henceforth referred to as prevascularization) may be an attractive solution for this problem, given that the bioengineered capillaries rapidly connect to the recipient's vasculature in the wound bed. Despite considerable progress in the bioengineering of functional blood capillaries, no data were available neither on the bioengineering of functional human lymphatic capillaries, nor on the integration of a dermal lymphatic network into a skin substitute. Moreover, it remained largely unknown how pre-existing blood and lymphatic capillaries affect the reconstitution of a dermo-epidermal skin substitute (DESS) after its transplantation.

The first part of my work aimed at bioengineering prevascularized DESS (PDESS) containing physiologically distinct blood and lymphatic capillaries. For this, human dermal microvascular endothelial cells (HDMEC), dermal fibroblasts and epidermal keratinocytes isolated from human skin biopsies were sequentially seeded into and onto rapidly polymerizing fibrin hydrogels. Within 3 weeks of *in vitro* culture, lumenized and interconnected capillary networks consisting of blood and lymphatic capillaries spontaneously assembled within PDESS. I found that during the process of prevascularization, the inoculated fibroblasts differentiated into pericytes and specifically stabilized blood capillaries, while they hardly associated with lymphatic capillaries. The lymphatic capillaries presented anchoring filaments, expressed all major lymphatic markers, and could be modulated by lymphangiogenic and anti-lymphangiogenic stimuli. In addition, the lymphatic capillaries took up fluid from the interstitial space *in vitro* and improved the drainage of fluids from PDESS *in vivo*. Analysis of PDESS after transplantation revealed a great acceleration of vascular regeneration involving two distinct mechanisms: rapid anastomosis of the bioengineered blood capillaries - followed by lymphatic anastomosis - and accelerated recipient blood and lymphatic angiogenesis.

In the second part of this work, I performed a broad analysis of the effects of prevascularization on several aspects of wound healing and skin morphogenesis of DESS.

By comparison of PDESS and non-prevascularized DESS (NPDESS) *in vivo*, I found that the rapid perfusion of the bioengineered blood capillary network increased proliferation and decreased apoptosis of transplanted cells, reduced graft shrinkage, induced the formation of rete ridges and capillary loops and promoted dermal remodelling. Furthermore, PDESS healed by the deposition of randomized collagen bundles instead of the scar-like parallel collagen bundle orientation found after transplantation of NPDESS.
Collectively, my data for the first time describe the bioengineering of clinically relevant PDESS containing human blood and lymphatic capillary networks that rapidly connect with the host vasculature after transplantation, thereby markedly accelerating perfusion of the graft. *In vitro* and *in vivo* studies indicate that the rapid perfusion of PDESS unlocks latent regenerative processes that shift the healing of DESS from typical scar formation towards regeneration.

ZUSAMMENFASSUNG

Die langsame Vaskularisierung künstlicher Organe stellt ein gravierendes Problem im Bereich Tissue engineering und Regenerative Medizin dar. Das Versetzen solcher Organe mit funktionalen Blut- und lymphatischen Gefässen vor der Transplantation (Prevascularization) repräsentiert eine attraktive Lösung für dieses Problem, bedingt jedoch, dass sich die künstlichen Gefässe nach der Transplantation schnell mit den Gefässen des Empfängers verbinden (Anastomose). Trotz bemerkenswerter Fortschritte in der Herstellung künstlicher Blutgefässe gab es bisher keine Berichte über die Herstellung von funktionalen lymphatischen Gefässen oder über die Versetzung von dermo-epidermalen Hautsubstituten (DESS) mit solchen lymphatischen Gefässen. Ausserdem war nur sehr wenig über den Effekt von konstruierten Blut- und lymphatischen Gefässen auf den Heilungsprozess eines dermo-epidermalen Hautersatzes bekannt.

Das Ziel des ersten Teils meiner Arbeit war die Herstellung von prevaskularisierten dermo-epidermalen Hautsubstituten (PDESS), die künstliche Blut- und lymphatische Gefässe beinhalten. Dafür wurden human dermal microvascular endothelial cells (HDMEC), dermale Fibroblasten und epidermale Keratinocyten von einer Hautbiopsie isoliert und zuerst in und dann auf ein schnell polymerisierendes Fibrin Hydrogel gesäht. Innert 3 Wochen entstand so spontan ein Netzwerk verbundener Kapillaren mit Lumen, bestehend aus Blut- und lymphatischen Gefässen. Die Fibroblasten differenzierten während der Prevaskularisierung zu Perizyten und stabilisierten spezifisch die Blutkapillaren, während sie kaum mit lymphatischen Gefässen assoziierten. Die lymphatischen Gefässe entwickelten Anchoring filaments, exprimierten alle wichtigen lymphatischen Marker und konnten mittels lymphangiogenen und anti-lymphangiogenen Stimuli moduliert werden. Ausserdem waren sie fähig zur Flüssigkeitsaufnahme *in vitro* und verbesserten den Flüssigkeits-Abtransport *in vivo*.

Die Analyse von PDESS nach der Transplantation hat gezeigt, dass Prevaskularisierung die vaskuläre Regeneration mittels zwei verschiedener Mechanismen beschleunigt: schnelle Anastomose der Blutgefässe – gefolgt von der Anastomose der lymphatischen Gefässe – und Beschleunigung des Einwuchses von Blut und lymphatischen Gefässen des Empfängers in das Hautsubstitut.

Im zweiten Teil meiner Arbeit führte ich eine ausgiebige Analyse der Effekte von Prevaskularisierung auf die Heilung und Hautmorphogenese von PDESS durch. Mittels eines Vergleichs von PDESS und nicht-prevaskularisierten DESS (NPDESS) *in vivo* habe ich herausgefunden, dass die schnelle Perfusion der künstlichen Blutgefässe die Proliferation der transplantierten Zellen unterstützt und deren Apoptose vermindert, die Schrumpfung des Hautsubstituts reduziert, die Entwicklung von Rete ridges und Capillary Loops induziert und das dermale Remodelling fördert. Ausserdem heilten PDESS mittels Deposition von zufällig orientierten Kollagenbündeln anstatt von parallelen, Narben-Kollagenbündeln wie nach der Transplantation von NPDESS.

Diese Arbeit beschreibt zum ersten Mal ein klinisch relevantes dermo-epidermales Hautsubstitut, welches sowohl Blut- als auch lymphatische Gefässe beinhaltet, durch deren schnelle Anastomose die Perfusion des Transplantats merklich beschleunigt wird. *In vitro* und *in vivo* Studien deuten darauf hin, dass die schnelle Perfusion ruhende regenerative Prozesse in PDESS aktiviert, welche den Heilungsprozess von einer typischen Narbenformation in Richtung Regeneration leiten.

1 INTRODUCTION

1.1 HUMAN SKIN

1.1.1 STRUCTURE AND FUNCTION OF HUMAN SKIN

All living organisms possess a circumferential "skin" that separates their body from the environment and defines their place in space. Whereas in more primitive organisms, this skin consists of a simple bio-membrane (e.g. the outer membrane of gram-negative bacteria[1]), human skin exhibits a high complexity and functions as an organ: it is composed of different cell-types and tissues that perform specific functions like the recognition and defense against other organisms, the maintenance of body temperature, the protection from the harmful effects of the external environment or the sexual attraction to preserve the species[2-5].

Structurally, human skin can be divided into three tissue layers (Figure 1). There is a rapidly replicating avascular epidermis that can be readily repaired from any damage it may suffer. Underneath the epidermis lies the dermis, a highly vascularized connective tissue that provides the skin with pliability, elasticity and tensile strength. Loss of dermal tissue usually leads to the formation of a scar, the typical end point of mammalian tissue repair[6]. As the last of the three layers of the human skin, the hypodermis consists of highly vascularized adipose tissue[7]. This skin layer serves as an energy reservoir, cushions and protects the skin, and enables mobility over underlying structures[8]. Each layer is essential and contains a specific set of specialized cell types of different embryonic origin that contribute to the maintenance of the various functions of the skin. Another precondition for the maintenance of the function of skin is the presence of various skin appendages and adnexal structures, like hair follicles, sebaceous and sweat glands that serve to provide the skin with sensation, contractility, lubrication and heat regulation[2].

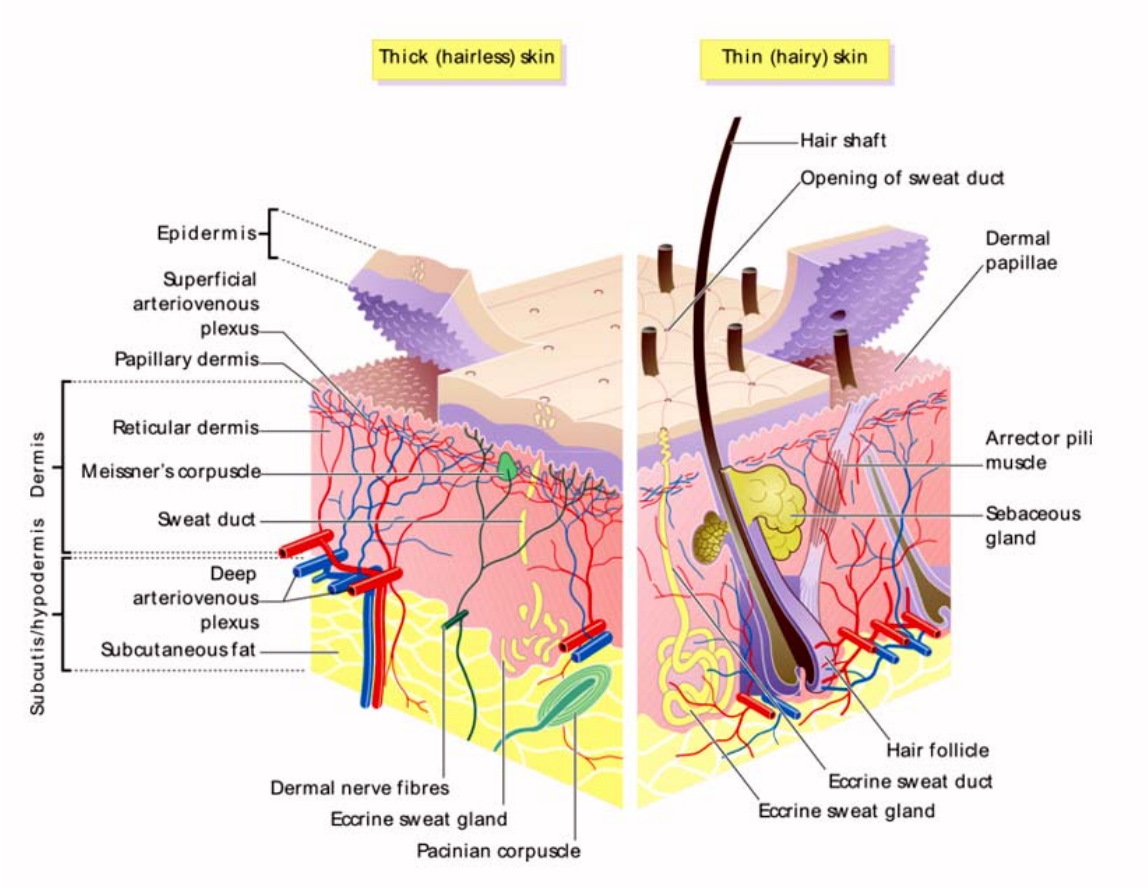

Figure 1 | Layers of hairless and hairy skin. View of all the essential components of the human epidermis, dermis and hypodermis in hairless and hairy skin. [http://en.wikipedia.org/wiki/Skin]

The epidermis

Approximately 90-95% of all cells in the epidermis are keratinocytes. Together with melanocytes, Langerhans cells and Merkel cells, they build up a stratified, continually renewing epithelium that exhibits progressive differentiation in a basal to superficial direction (Figure 2). Furthermore, the keratinocytes in the epidermis organize into different layers and each layer is characterized by a different keratinocyte morphology[9].

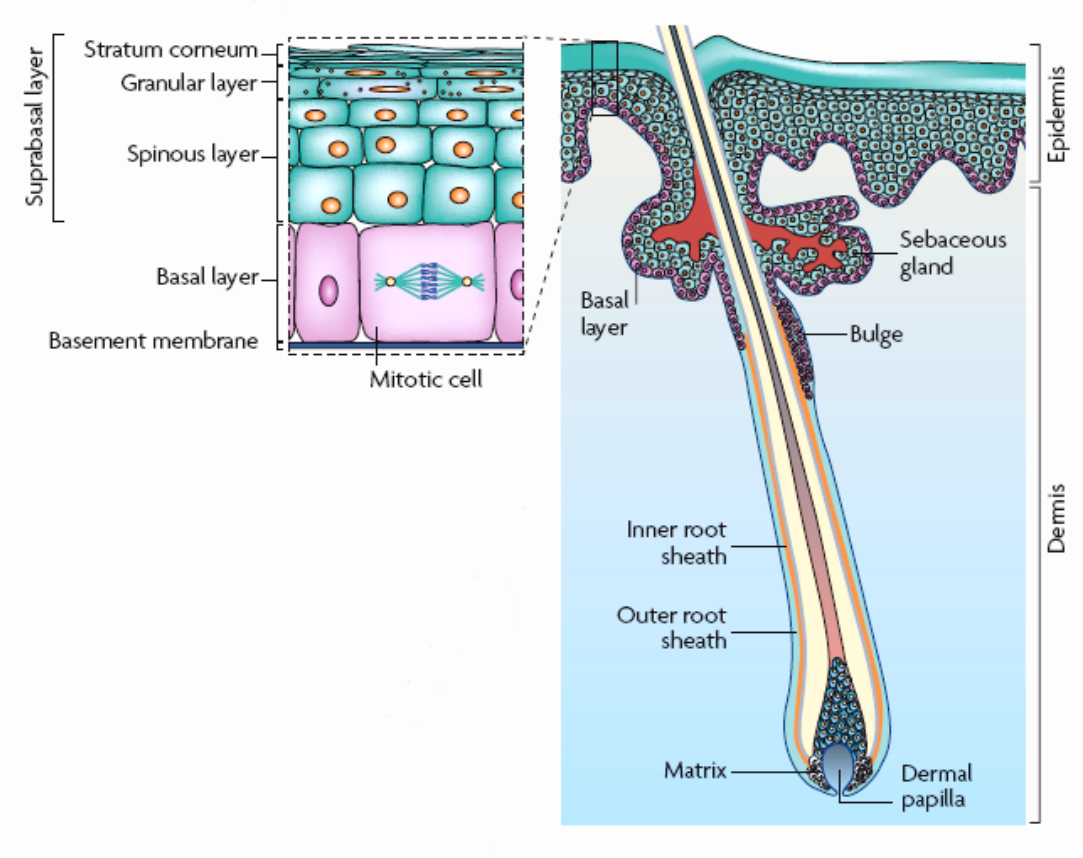

Figure 2 | Architecture of the epidermis. The outermost layer of the skin, the epidermis, is organized into layers of keratinocytes, which comprise the interfollicular epidermis, interspersed with hair follicles. Proliferating cells (pink) are believed to be confined to the basal layer, whereas differentiated cells occupy the suprabasal layers (blue)[10].

The basal layer usually is described as a single, continuous layer of keratinocytes which is structurally and functionally associated with components of the underlying basement membrane[2]. In certain conditions like in glabrous skin and hyperproliferative epidermis, however, the basal cell layer increases to several layers[11]. Keratinocytes in the basal cell layer exhibit heterogeneity in their proliferative potential. Approximately 10% of basal keratinocytes are long-living stem cells that exhibit a slow cell cycle. Keratinocyte stem cells are dispersed within the basal cell layer and are responsible for the replenishment of the epidermis throughout life[9]. After the division of a keratinocyte stem cell, one daughter cell is destined to differentiate and move upwards, while the other remains in the basal cell layer as the new stem cell (Figure 3). Potentially, one epidermal keratinocyte stem cell has the capacity to give rise to enough cells to cover the complete body surface[12]. Among all cells of the basal cell layer, it is the stem cell population that is prone to accumulation of deleterious mutations for example due to prolonged sun exposure, which is associated with the formation of skin neoplasias resulting in skin tumors[3,13].

Apart from keratinocytes, the basal cell layer harbours at least two different types of specialized cells, Merkel cells and melanocytes. Merkel cells mediate the proper neural encoding of touch stimuli essential for the detection of texture, shape and curvature[14]. They are attached to keratinocytes by desmosomal junctions, which are composed of intracellular keratin filaments linked to a cell surface molecule spanning the cytoplasmatic membrane called desmoglein and desmocolin[15] (Figure 4), and at some locations assemble into specialized structures called tactile discs or touch domes. Merkel cells may also contribute to the development of eccrine sweat glands, hair follicles, nails and nerves of skin[16].

Melanocytes are melanin-producing cells derived from the neural crest that protect the skin from ultraviolet (UV) radiation. Once established in the epidermis after migration through the mesenchyme, they extend dendritic processes to about 36 keratinocytes[17], allowing them to transfer melanin that protects from UV via its optical and chemical filtering properties. In contrast to Merkel cells, melanocytes are attached to keratinocytes via E-cadherin[18].

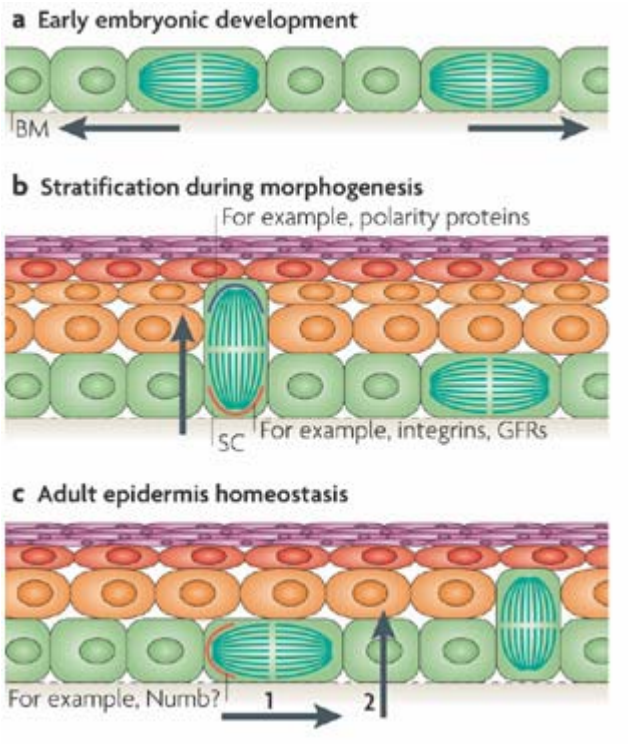

Figure 3 | Asymmetrical stem cell division during development and homeostasis. (**a**) During embryonic skin development, divisions are symmetric and parallel to the basement membrane (BM), ensuring coverage of surfaces. (**b**) During epidermal stratification, about 70% of cell divisions become asymmetric to allow stratification and differentiation and to establish a skin barrier. The basal cell segregates integrins and growth factor receptors (GFR), which provide survival and proliferative cues to the stem cell (SC). (**c**) During epidermal homeostasis in adult skin, asymmetric cell divisions occur with the plane of division parallel to the BM, such that only one daughter cell inherits a cell fate determinant and remains a SC. The other cell becomes committed to terminal differentiation.

Right above the basal layer lies the spinous layer. The abundance of focal desmosomes between neighboring keratinocytes in this layer results in the formation of spines during tissue processing. Another specialized cell type of the skin, the Langerhans cells, is also located in this suprabasal layer. Langerhans cells are dendritic cells that have been shown to be derived from the bone marrow[19]. Langerhans cells are responsible for the processing and presentation of foreign antigens, building a first line of defence against the constant attacks of the environment.

The spinous layer is followed by the granular layer which contains two to three layers of granular cells characterized by cytoplasmatic basophilic keratohyalin granules[20]. These granules are composed of profillagrin and keratin intermediate filaments and promote the cross-linking and hydration of keratin. Loricrin, a protein of the cornified cell envelope and a terminal differentiation marker of keratinocytes, is also found within these granules[21]. At the border to the next layer, the stratum corneum, keratinocytes secrete lamellar bodies containing lipids and proteins into the extracellular space. As a result, a hydrophobic lipid envelope, responsible for the skin's barrier properties, is deposited[4]. Subsequently, cells progressively loose their nuclei and organelles and differentiate into non-viable corneocytes in the stratum corneum.

The stratum corneum is the outermost epidermal layer that is directly exposed to the external environment, thus, it provides protection against water loss, invasion of environmental substances[5] and mechanical stress. It is composed of multiple layers of non-viable, terminally differentiated keratinocytes, the corneocytes. The barrier function is provided by lipid-depleted, protein-rich corneocytes sourrounded by a continuous extracellular lipid matrix. As corneocytes move toward the outer skin surface, they change their structure, composition and function. In deeper layers of the stratum corneum, cells are thicker and contain more densely packed parallel arrays of keratins, a more brittle cornified cell envelope and present a greater diversity of modifications for cell attachment compared with the outer stratum corneum[5]. Cells in the outermost stratum corneum have a rigid cornified envelope and undergo proteolytic degradation of the desmosomes. This degradation of the desmosomes promotes the shedding of the outer layers[22].

The dermo-epidermal junction

The main component of the dermo-epidermal junction (DEJ) is the cutaneous basement membrane, which separates the epidermis from the dermis and provides adhesion, mechanical stability and a dynamic interface between these two distinct compartments of the skin[23]. The DEJ restricts the transport of molecules between the epidermis and the dermis based on their size and charge, but permits the passage of migrating cells under normal (i.e. melanocytes[24] and Langerhans cells[25]) or pathological (i.e. tumor cells[26]) conditions.

The DEJ shows characteristic undulations, the papillae-rete ridge pattern (Figure 5 and Figure 6), whose features are specific for different regions of the skin surface. The function of rete ridges is not entirely understood, but it is believed to contribute to the mechanical stability of the skin, increase the surface area of the epidermis that is exposed to the vascularized dermis and, together with the capillary loops projecting into the papillae, to provide a protective niche for the proliferative basal keratinocyte layer that optimizes the delivery of nutrients and oxygen[27].

Ultrastructurally, the DEJ can be devided into four distinct zones (Figure 5):

1. The basal cell plasma membrane with its special attachment structures, the hemidesmosomes. Hemidesmosomes differ from the desmosomes found in the epidermis and contain a completely different set of molecules[28] (Figure 4).
2. The lamina lucida zone of the basement membrane that contains structures beneath the hemidesmosomes called anchoring filaments. Together with the hemidesmosomes, they form a continuous structural link between the basal keratinocyte's keratin intermediate filaments and the underlying basement membrane and dermal components.
3. The lamina densa, also called the basal lamina
4. The fibrous elements of the sub-basal lamina contain anchoring fibrils, microfibrils arranged in bundles, and collagen fibers.

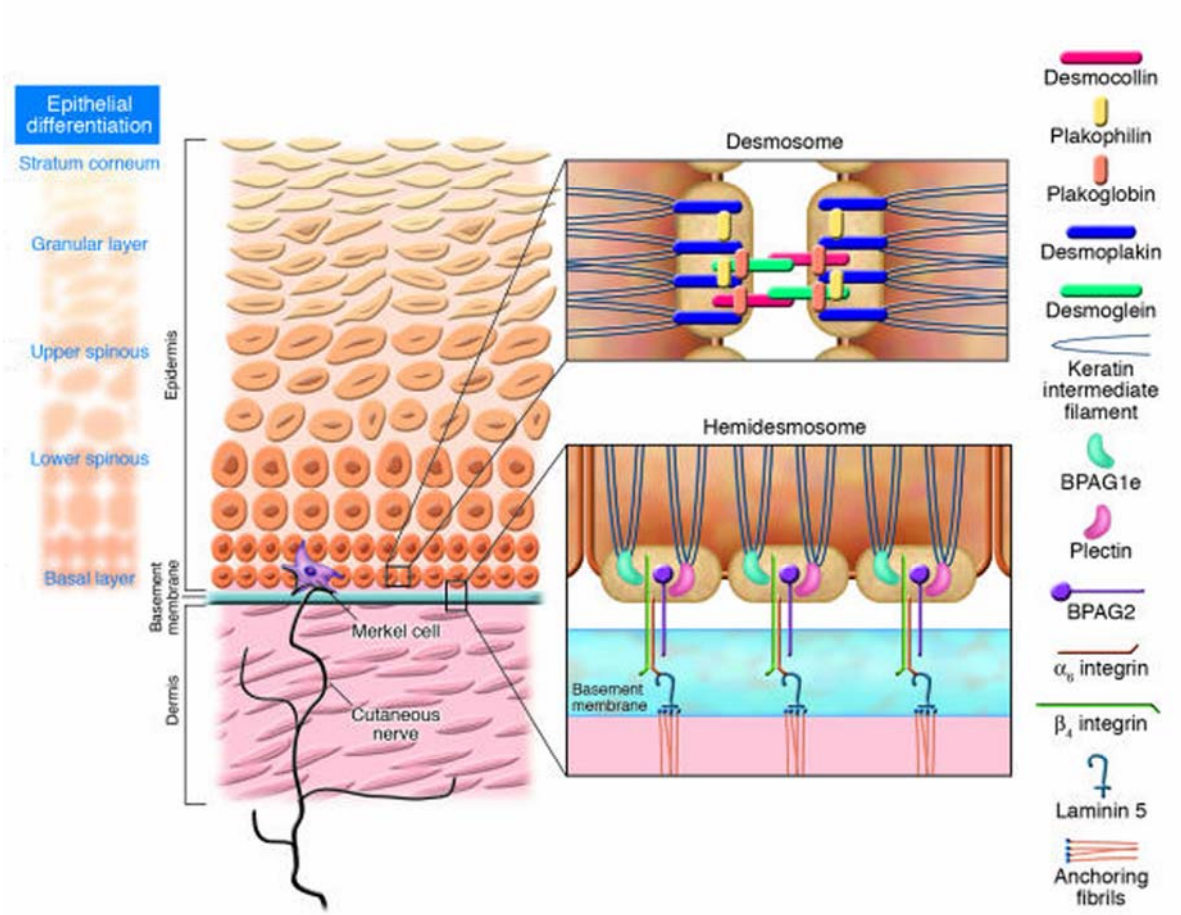

Figure 4 | Desmosomes and Hemidesmosomes. Desmosomes connect two neighbouring keratinocytes and consist of cadherins, such as desmogleins 1 and 3, that build an extracellular bridge. Hemidesmosomes tether the basal keratinocytes to the basement membrane trough integrins that attach to the anchoring fibrils in the sub-basal basement membrane[28].

Cultured epidermal autografts (CEA) applied on burned wounds are fragile and sensitive to mechanical shearing forces for at least 2 month after transplantation due to the lack of a well established DEJ[29]. This often leads to the formation of mechanically induced blisters which can result in substantial loss of transplanted material. Furthermore, mutations in genes encoding for molecular components of the DEJ can cause blistering skin diseases (Epidermolysis bullosa) characterized by the physical detachment of the epidermis and the dermis. As a result, patients can suffer from a range of symptoms, including mild blistering, extensive bulla formation, erosions, scarring and even death[30]. It is therefore obvious that an intact DEJ is of crucial importance for the proper function of the skin.

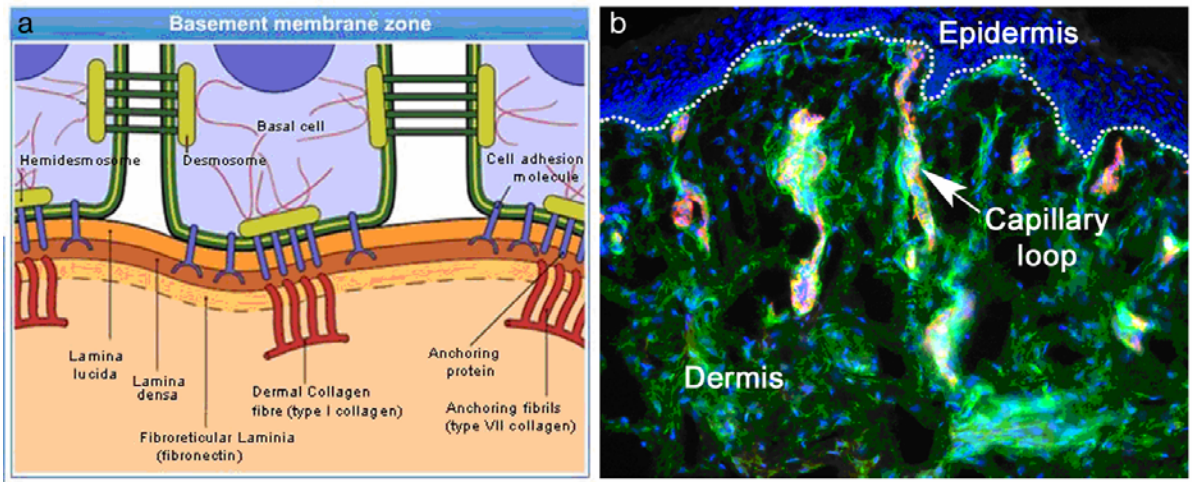

Figure 5|**The dermo-epidermal junction (DEJ).** (**a**) Schema of the main components of the DEJ including the hemidesmosomes, desmosomes, anchoring proteins and anchoring fibrils. (**b**) Immunofluorescence staining for the fibroblast marker CD90 (green) in combination with the pan-endothelial marker CD31 of normal human skin showing the rete ridge pattern of the DEJ and capillary loops (arrow; right). The white dotted line marks the DEJ. [http://www.kelownadermatology.ca/index.php]

The dermis

In contrast to the epidermis, the dermis is highly vascularized and exhibits a reduced cellular density. It is composed primarily of fibrous and amorphous extracellular matrix surrounding the epidermally derived appendages, neurovascular networks, sensory receptors and dermal cells (Figure 1). The majority of cells in the dermis are fibroblasts derived from the mesenchyme, which show increased proliferative and synthetic activity during wound healing and hypertrophic scar formation[31,32]. Monocytes, macrophages and dermal dendrocytes are other examples of cells of the dermis which represent the mononuclear phagocytic group of cells in the skin. Structurally, the dermis shows two distinct regions: the upper papillary dermis and the lower reticular region (Figure 6a). The structural organization of the papillary dermis reflects its primary function to optimally support the overlying avascular epidermis and to accommodate to mechanical stress. It is characterized by a high abundance of dermal papillae, nipple-like extensions of the dermis into the epidermis that greatly increase the surface area between epidermis and dermis, thereby increasing the exchange of oxygen, nutrients and waste products. Furthermore, dermal papillae prevent the mechanical seperation of the dermis and epidermis and provide better resistance to mechanical sheer stress. Intriguingly, connective tissue with the same organization and composition as the papillary dermis surrounds hair follicles., another situation where matrix underlies an epithelium.

The main extracellular matrix component of the dermis are collagens, which on histological sections show a typical basket-wave pattern (Figure 6b). The reticular dermis is characterized primarly by large-diameter collagen fibrils as compared to the fine but dense organization of collagen fibrils in the papillary dermis (Figure 6c). The two fiber systems of the papillary and reticular dermis are integrated and provide the dermis with strong and resilient mechanical properties.

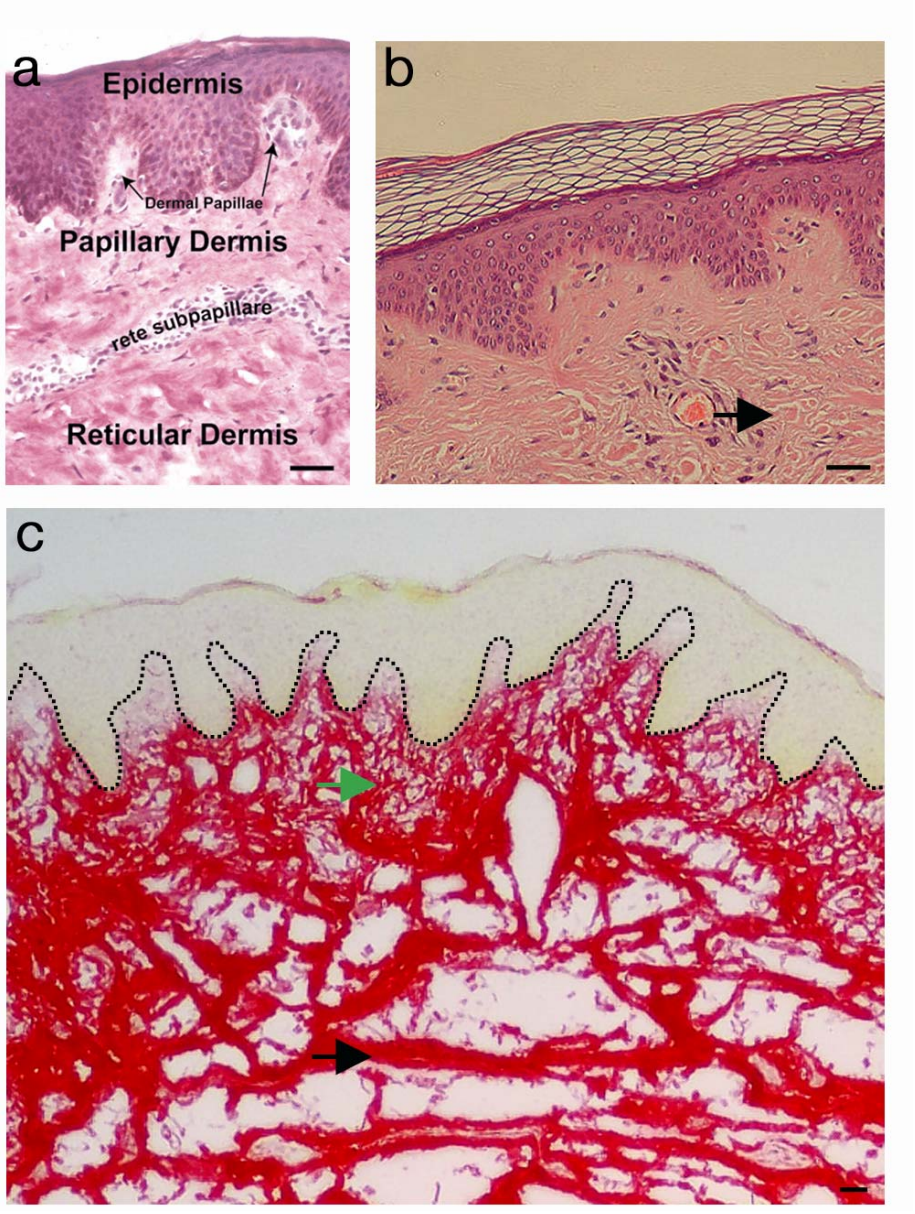

Figure 6 | The dermal architecture.
(**a**) The papillary and reticular dermis are separated by a vascular plexus, the rete subpapillare. From the papillary dermis, dermal papillae extend into the epidermis (arrows). (**b**) The main extracellular matrix component of the dermis is collagen, which is organized in a basket-wave pattern (arrow).
(**c**) Visualization of dermal collagen by picrosirius red staining reveals the different appearances of the collagen fibers in the papillary dermis (green arrow) and the reticular dermis (black arrow). Black dotted line marks the DEJ. All scale bars are 45um

(a)[http://www.biologyonline.org/articles/fibroblast_heterogeneity_skin_deep/figures.html[
(b)[http://en.wikipedia.org/wiki/File:Normal_Epidermis_and_Dermis_with_Intradermal_Nevus_10x.JPG]

The hypodermis

Underneath the dermis, as the lowermost layer of the integumentary system, lays the hypodermis (Figure 1). The hypodermis cushions and protects the skin and acts as an energy reserve. The fat contained in the adipocytes can get channeled back into the circulation and be metabolized in response to increased activity or when there is a lack of energy producing substances[33]. In patients with Werner's syndrome, a disease characterized by the absence of hypodermis in lesional areas over the bone, wounds ulcerate and heal poorly. This reflects the importance of this tissue layer for proper wound healing[34].

The dermis and the hypodermis are structurally and functionally well integrated through nerve and vascular networks and the continuity of epidermal appendages (Figure 1). The most abundant cell types of the hypodermis are adipocytes, fibroblasts and macrophages.

1.1.2 THE CUTANEOUS MICROVASCULATURE

The cutaneous microvasculature consists of vessels of the cardiovascular system, which distribute blood, and the vessels of the lymphatic vascular system, which transport lymph (filtered blood plasma, cells and macromolecules). All vertebrates have a closed cardiovascular system including a central pump, the heart, that delivers blood cells, oxygen, nutrients and hormones to all cells of the organism (Figure 7). In contrast, the lymphatic vascular system is a one-way, open-ended system without a central pump that channals fluid, cells, macromolecules, microbes and other substances from interstitial spaces back to the circulation. The main cellular components that constitute the cutaneous microvasculature are the HDMEC and pericytes (Figure 8). HDMEC is a collective term for both, blood and lymphatic endothelial cells.

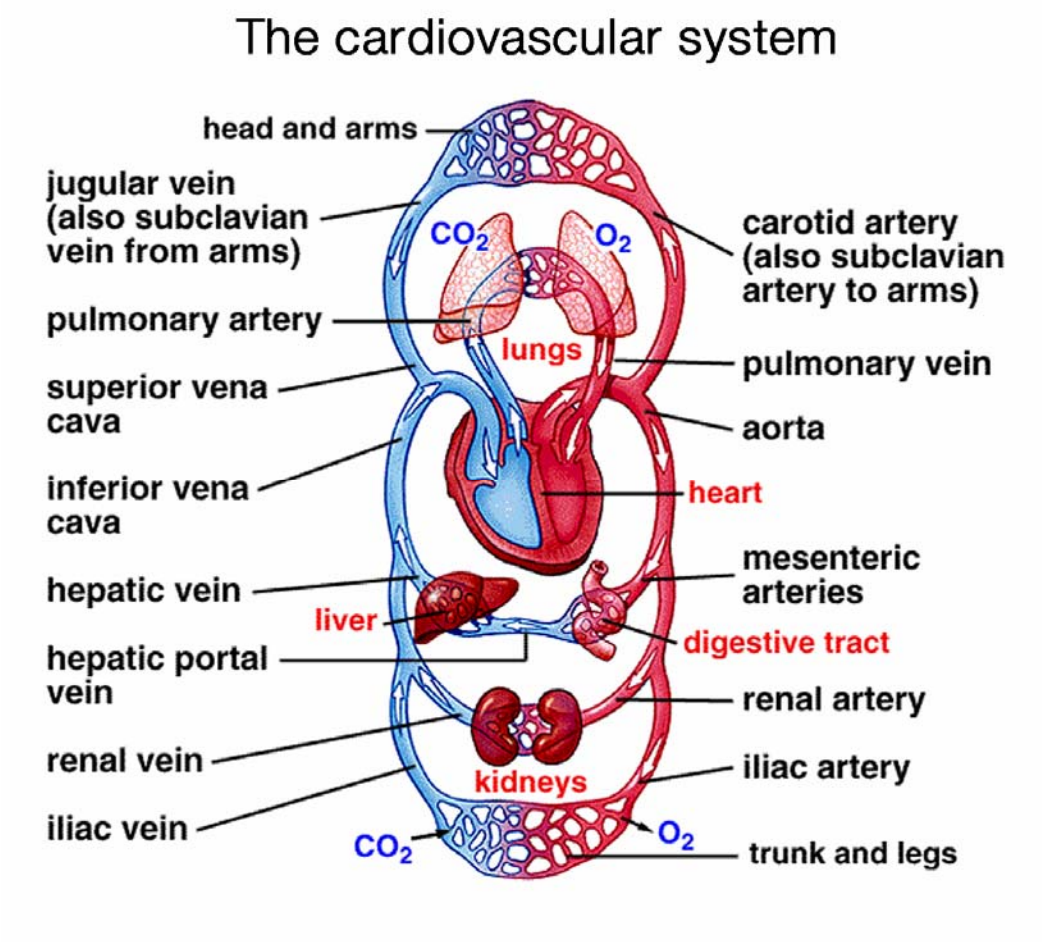

Figure 7 | The cardiovascular system. Scheme of the closed mammalian cardio-vascular system with all essential components. [http://www.mhhe.com/biosci/ap/dynamichuman2/content/cardio/visuals.mhtml]

The cardiovascular system

The three types of blood vessels are arteries, veins and capillaries (Figure 9) and the main cell type of the cardiovascular system is the blood endothelial cell[35]. Each type of blood vessel has distinct features to serve a different purpose[36]. Arteries are the first blood vessels the blood enters after leaving the heart. Since arteries experience high blood pressure, they present a thick and elastic muscular wall. These characteristics ensure the maintainance of a round shaped lumen[37] as well as a high degree of expansion potential in oder to adjust to the spike in blood volume that occurs with every heartbeat. After expanding, the arteries quickly contract back to their original size and push the blood along its way. From the arteries, the blood flows through successively smaller arteries and arterioles. In contrast, veins carry blood from various tissues to the heart. Since veins are

exposed to low blood pressure, they present a thinner layer of muscle than arteries[37].and contain one-way valves that ensure unidirectional blood flow.

Between the arterial and the venous blood system, an extensive network of very thin-walled blood vessels, the capillaries, is found. These allow for the rapid diffusion and exchange of nutritional molecules, growth factors, cytokines, hormones and oxygen from the blood to the tissue.

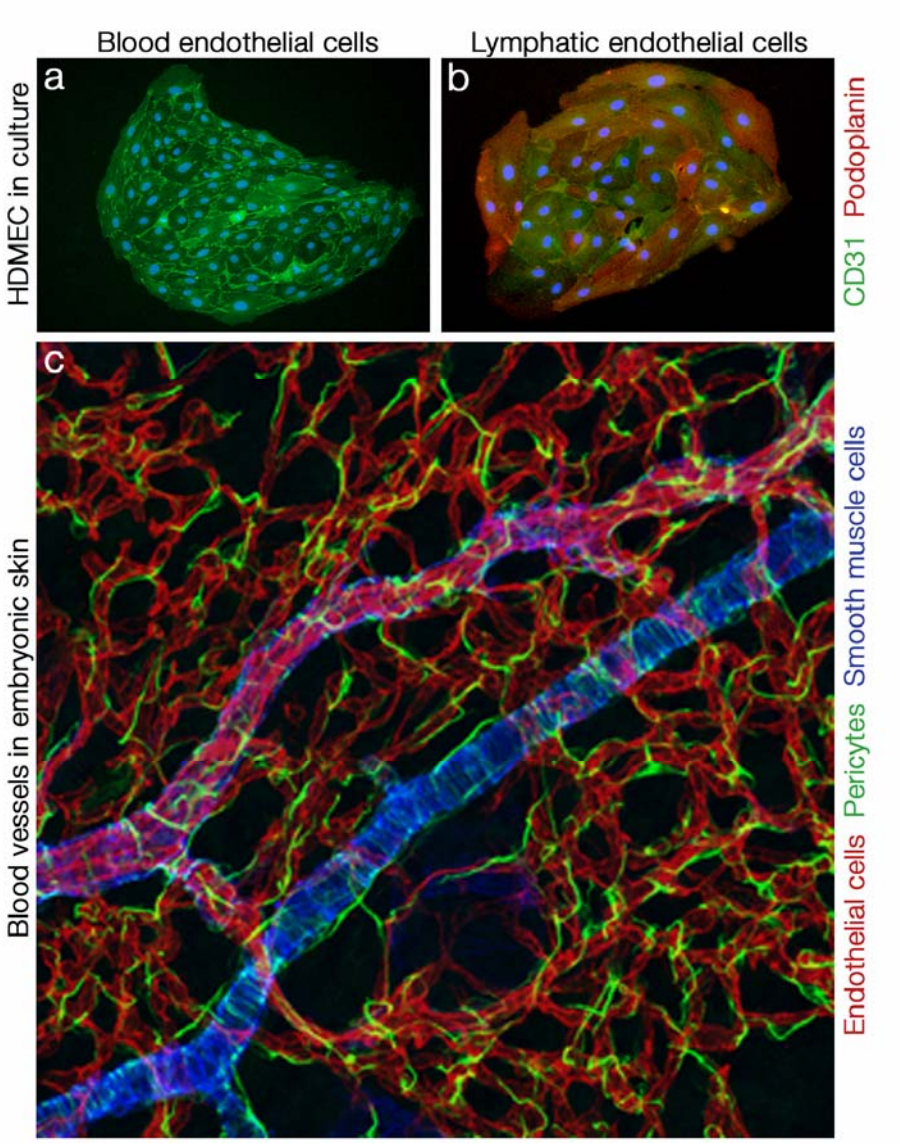

Figure 8 | The dermal vascular unit. (**a**) Immunofluorescence staining for CD31 and Podoplanin of a colony of blood endothelial cells (BEC) in culture. BEC do not express the lymphatic marker podoplanin. (**b**) Immunofluorescence for CD31 and Podoplanin of a colony of lymphatic endothelial cells (LEC) in culture. LEC express both CD31 and podoplanin. (**c**) View of the vasculature of emryonic skin. Blood vessels are stained in red, pericytes in green and smooth muscle cells in blue. [http://www.mpimuenster.mpg.de/en/research/teams/adams/projects/index.html]

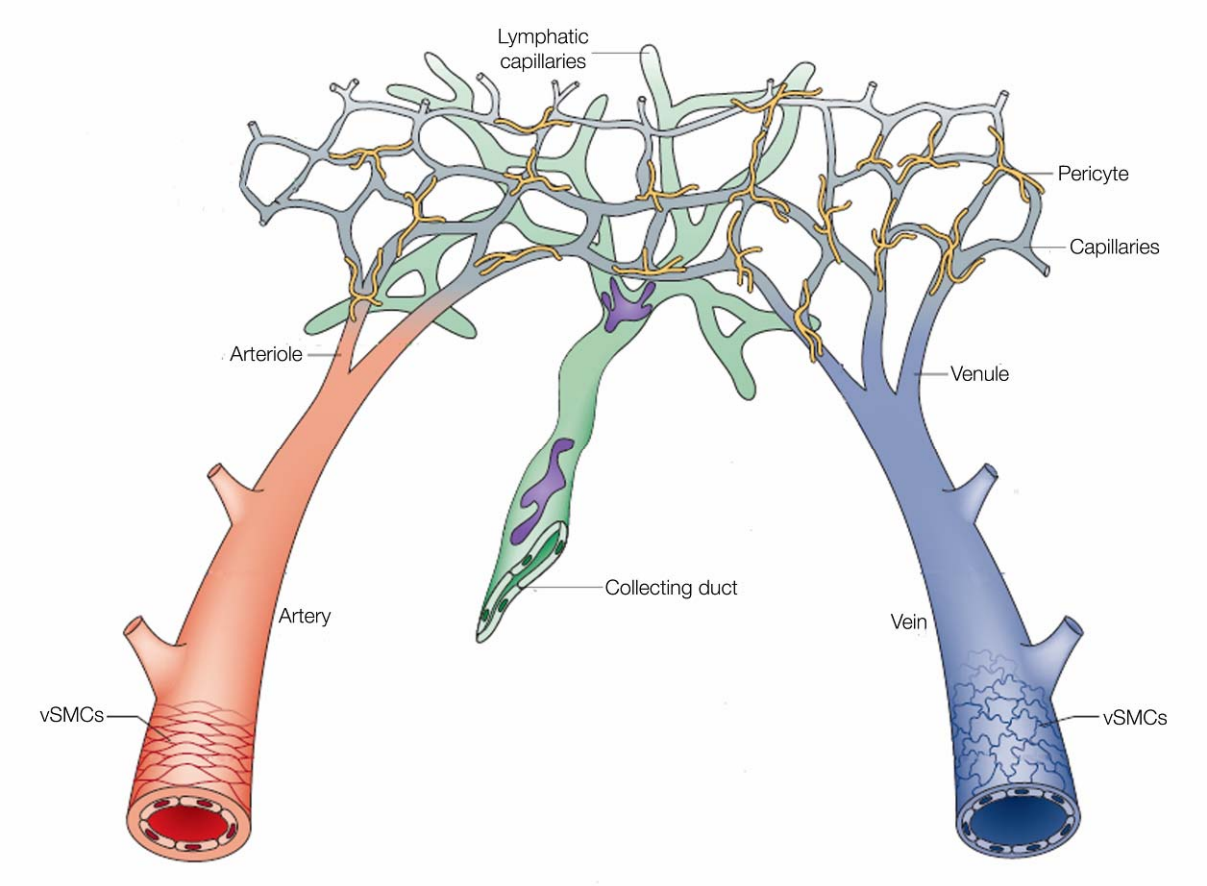

Figure 9 | Blood and lymphatic vessel types. Shown are the main blood and lymphatic vessel types in the human body. From the heart, blood enters into thick-walled arteries that are covered with vascular smooth muscle cells. Subsequently, blood flows through smaller arteries, the arterioles, into the capillaries where the exchange of nutrients and oxygen to the tissue occurs. In contrast to arteries, capillaries are covered by pericytes. After transport through the capillary network, venules and later veins which are also covered with vascular smooth muscle cells (vSMCs), but contain a thinner wall than arteries, transport the blood back to the heart[38].

There are three types of blood capillaries (Figure 10):

1. The most common capillary type is the continuous capillary. This type of capillary shows an uninterrupted lining of endothelial cells, which only allows the passage of small molecules like water and ions via intercellular clefts, gaps between the tight junctions that join neighbouring endothelial cells.
2. Large molecules and proteins can diffuse through fenestrated capillaries which contain pores with a diameter of 60-80nm. The pores are stabilized by a diaphragm of fibrils which serves as a molecular filter.
3. Sinusoidal capillaries are a special type of fenestrated capillary which contain larger pores (30-40µm), allowing the passage of white and red blood cells. This transport is further facilitated by a discontinuous basement membrane.

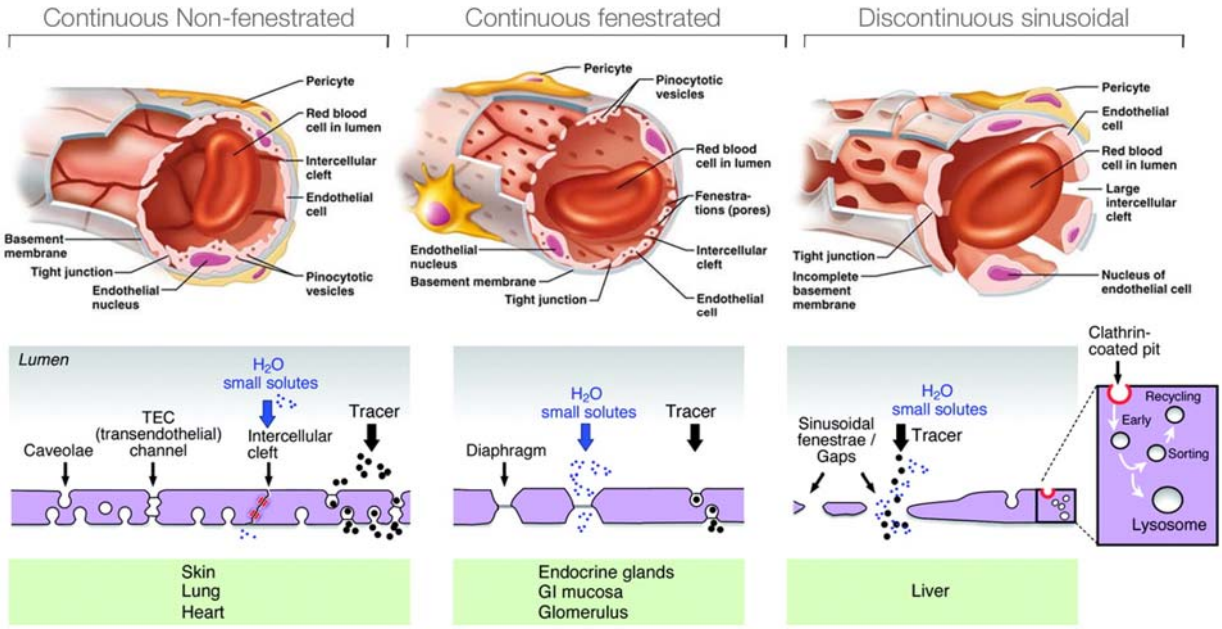

Figure 10 | The three types of capillaries in the human body. The main type of capillary in human skin is the continuous non-fenestrated capillary, which allows small molecules to enter via intercellular clefts. The continuous fenestrated capillary is mainly found in endocrine glands and allows larger molecules to enter the capillary via pores. The discontinous sinusoidal capillary is mainly found in the liver. These capillaries contain much larger pores than continuous fenestrated capillaries and show a discontinuous basement membrane, both of which enable the transport of white and red blood cells. [http://classes.midlandstech.edu/carterp/Courses/bio211/chap19/chap19.html]

Organization of the cutaneous blood microvasculature

The cutaneous microvasculature is composed of two plexuses of arterioles and venules, a superficial and a deep plexus. These plexuses are connected by communicating vessels that arise from arterioles and lead to veinules in the subcutaneous fat[39] (Figure 11). The deep plexus is located in the lower part of the reticular dermis, whereas the superficial plexus is located in the upper part of the reticular dermis right underneath the papillary dermis. From the superficial plexus, capillary loops project into each dermal papilla[40]. A capillary loop within such a dermal papilla is composed of an ascending arterial component and a descending venous limb. From the venous portion of the capillary loop, the blood empties into postcapillary venules and, successively, into dermal communicating venules and the small veins of the subcutaneous fat.

Through the permeable membranes of arterioles and venules, oxygen, water, nutrients and hormones enters from the blood into the tissues, and cabon dioxide and other metabolic byproducts are transported from it to excretory organs[37,39]. Postcapillary venules are the predominant type of vessel in the upper part of the dermis. They are highly permeable and represent the site of pathological changes in a variety of cutaneous inflammatory diseases (e.g. Cutaneous small-vessel vasculitis)[41,42]. In a postcapillary venule, a single pericyte, the cell type that provides blood flow regulation to most of the capillaries in the human body, forms tight junctions with two to four neighboring endothelial cells through breaks in the basement membrane[43].

Generally, the degree of vascularization is related to the metabolic demands of a given tissue. For example, the hyperproliferative epidermis in psoriasis is associated with tortuous, hyperplastic papillary loops and numerous endothelial cell fenestrations, reflecting the increased metabolic activity of the tissue[44]. In normal skin, however, up to 60% of cutaneous blood flow travels through shunts and not through exchange vessels[39]. This probably reflects the function of the skin as an organ of heat exchange and temperature regulation.

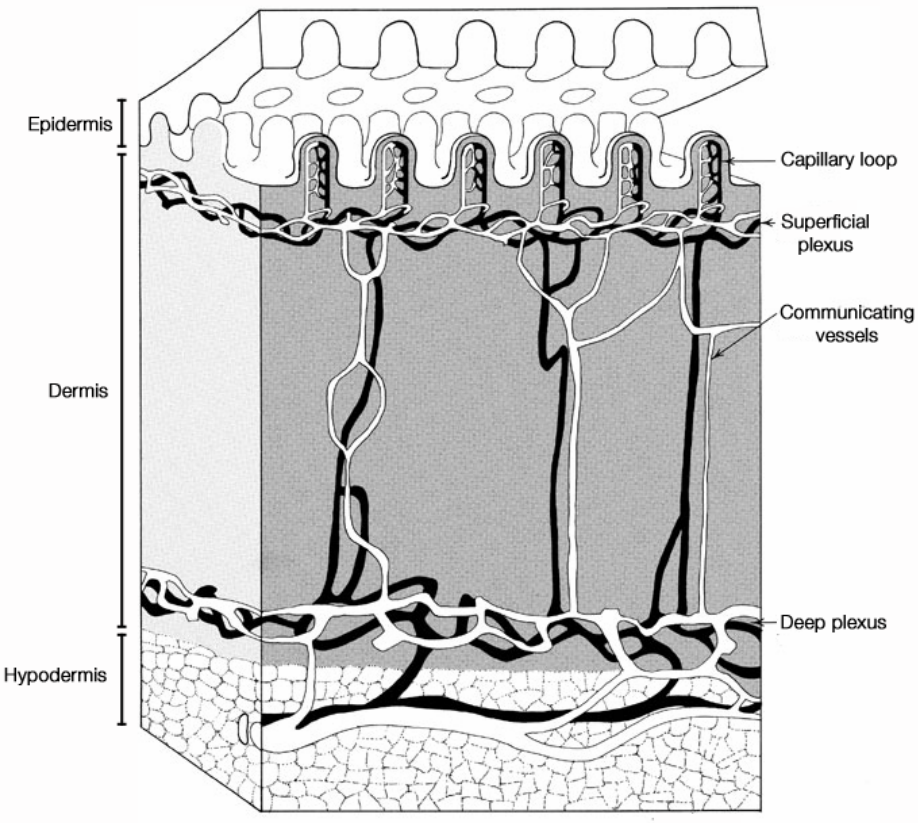

Figure 11 | Organization of the cutaneous vasculature. The cutaneous vasculature consists of a network of two plexuses that parallel the skin surface. The superficial plexus is located in the upper part of the reticular dermis, whereas the deep plexus is positioned in the lower part of the reticular dermis. Both plexuses are connected by communicating blood vessels oriented perpendicular to those plexuses. Capillary loops emanate from the superficial plexus and project into each dermal papilla. [http://derm101.com/Popups/FigurePopup.aspx?id=ack01f072&aid=13586]

Blood vascular development

Endothelial cells are thought to arise from a blast-like bipotential cell, the hemangioblast[45,46]. The hemangioblast differentiates into an intermediate pre-endothelial cell that then gives rise to either a commited hematopoietic cell or an endothelial cell[47]. Furthermore, endothelial cells are able to transdifferentiate into mesenchymal cells and intimal smooth muscle cells[48,49]. The initial step of embryonic vascular development is believed to include the formation of blood islands by angioblasts that fuse and sprout to form primary plexuses[35,50]. These primary plexuses thereafter slowly remodel and refine into the major vessels and capillary beds of the embryo. However, the dorsal aorta (DA) and the cardinal veins develop directly from angioblasts, without a plexus intermediate (Figure 12). These angioblasts differentiate from the mesoderm tissues and form the primary plexus by both vasculogenesis and angiogenesis. For a long time, vasculogenesis (the development of vessels from endothelial progenitor cells) was believed to happen only during embryonic development and the formation of new blood vessels in post-embryonic development was thought to solely be governed by angiogenesis, the sprouting, bridging and intussusceptive growth of existing vessels[51]. However, growing evidence supports the hypothesis that vasculogenesis also occurs during adult life[52-54]. Several studies demonstrated the presence of precursors of angioblasts and haematopoietic cells, the hemangioblasts, in the adult[55,56]. Hemangioblast were found in the bone marrow and express haematopoietic stem-cell markers such as CD34 and CD133 together with the endothelial marker vascular endothelial growth factor receptor 2 (VEGFR2). Upon mobilization with cytokines such as stromal-cell-derived factor-1 and VEGF, these hemangioblast precursors are released from the bone marrow into the periperal blood and home to sites of growing vasculature, for example in response to an injury or the growth of a tumor[57]. At the desired site, the hemangioblasts can differentiate into endothelial cells which participate in the formation of new blood vessels. The bone marrow has been shown to contain mesenchymal stem cells with the ability to differentiate into endothelial cells[58]. Additionally, haematopoietic stem-cell-derived myeloid cells can give rise to endothelial cells and form tube-like structures *in vitro*[59]. Other cell populations, derived from fat tissue, cardiac tissue and neural tissue can differentiate into endothelial cells, suggesting that multiple tissue-resident stem cells can contribute to vascular growth in post-embryonic development [60-62].

The mechanisms that lead to the formation of new blood vessels are not yet fully understood. Sonic hedgehoc signalling has been shown to play a central role in organizing specified angioblasts into vascular tubes[63]. VEGF-A is one of the most important signalling molecules involved in early blood vessel formation and acts through its high-affinity receptor VEGFR2 (Flk-1). The proper regulation of VEGF signaling patways is crucial for the formation of endothelial tubes[64,65]. Once primitive vascular plexuses have been developed, maturation of the vasculature continues by extensive remodelling including pruning, angiogenesis and investment with extravascular cell types[66]. Finally, a mature vasculature containing different blood vessel types like arteries, veins and capillaries is formed.

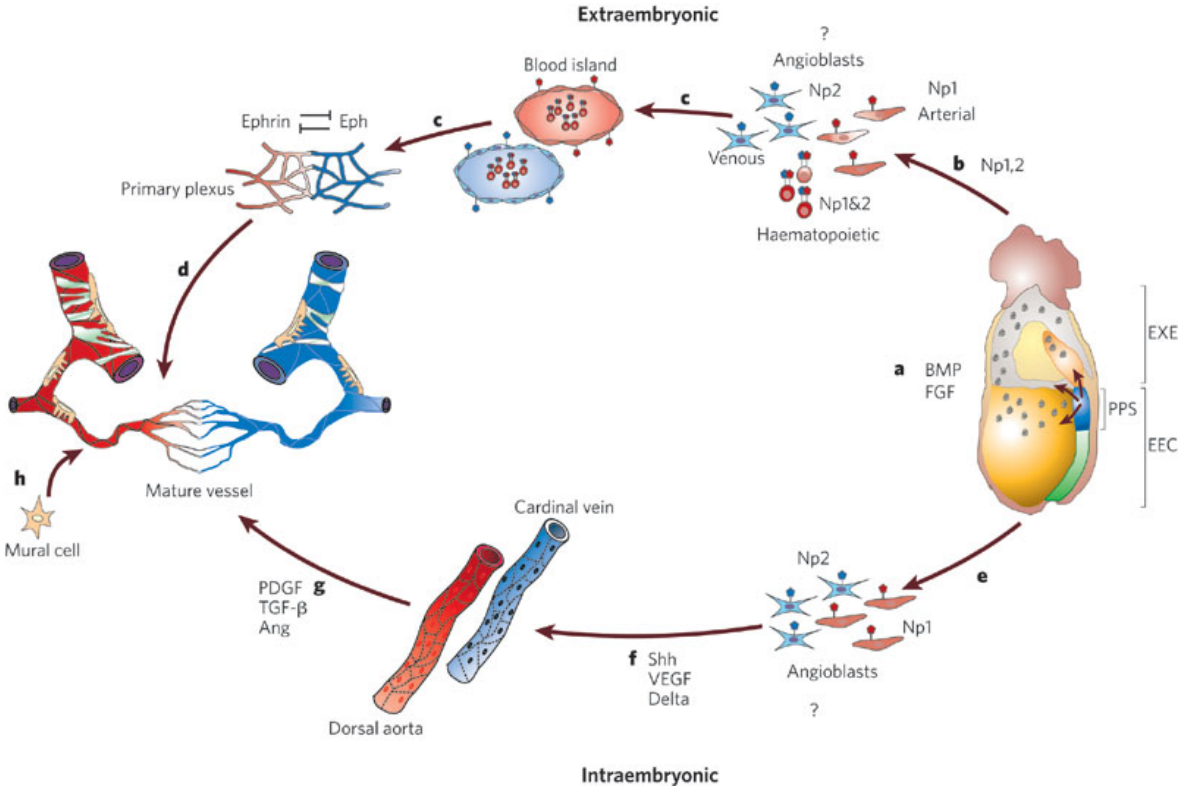

Figure 12 | Formation of a functional circulation in the embryo. (**a**) In response to FGF and BMP, vascular progenitors appear in the posterior primitive streak (PPS) of the embryo. These vascular progenitors are vascular endothelial growth receptor-2 (VEGFR-2) positive mesodermal cells. (**b**) The vascular progenitors then give rise to both blood and endothelium (haemangioblasts) and are restricted to haematopoietic or angiogenic fate after the migration into the extra-embryonic ectoderm (EXE), the yolk sac and the allantois and the embryonic ectoderm (EEC). (**c**) The formed blood islands fuse and give rise to a primary capillary plexus. (**d**) Later, the primary vascular plexus is remodelled and forms a mature circulation. (**e**) For the formation of the dorsal aorta and cardinal vein, intra-embryonic angioblasts migrate along distinct pathways before (**f**) directly forming these vascular structures, without a plexus intermediate. (**g**) The primary vessels (capillary plexus, dorsal aorta and cardinal vein) subsequently remodel, together with the extra-embryonic plexus, to form a mature vasculature, which involves VEGF, Notch and the angiopoietins and Tie receptors[67]. (**h**) Pericytes and smooth-muscle cells proliferate and differentiate in response to transforming growth factor-beta (TFG-beta) signalling, and are recruited to vessels by platelet-derived growth factor (PDGF) secreted by endothelial cells. Ang: angiopoietin; Eph: Eph receptor family; Shh: sonic hedgehoc; Np: neuropilin[47].

The lymphatic vascular system

The lymphatic vascular system - present in the skin and in most internal organs, with some exeptions (e.g. epidermis, nails, cartilage, brain) - consists of lymphoid organs such as the lymph nodes, spleen, thymus and tonsils, and the lymphatic vessels (Figure 13). Blind-ended lymphatic capillaries collect and transport the lymph (extravasated protein-rich fluid that originates from blood serum) to precollector lymphatic vessels[68]. From there, the lymph is transported into collecting lymphatic vessels that converge into lymphatic trunks to finally return the lymph to the venous circulation via the thoracic duct[69]. In addition, the lymphatic vascular system transports antigens and antigen-presenting cells to the lymph nodes where they are presented to B and T cells[70].

Initial lymphatic capillaries present neither a basement membrane nor pericyte/smooth muscle cell coverage. They are attached to the extracellular matrix via fibrillin-containing anchoring filaments[71], which are essential to pull open the lymphatic capillaries under high interstitial pressure[72]. From the initial lymphatic capillaries, the lymph flows unidirectionally into the collecting lymphatic capillaries. In contrast to initial lymphatic capillaries, collecting lymphatic capillaries contain a discontinuous basement membrane and exhibit smooth muscle cell coverage. Together with respiratory movements and skeletal muscle action, the smooth muscle cells generate the necessary pressure needed for the transport of the lymph into the lymphatic trunks[73]. Overlapping primary valves within the lymphatic collectors prevent the lymph from escaping the capillaries[74,75].

The lymphatic vascular system is involved in a variety of human pathological conditions, such as lymphedema, inflammation, cancer metastasis and hypertension[76,77].

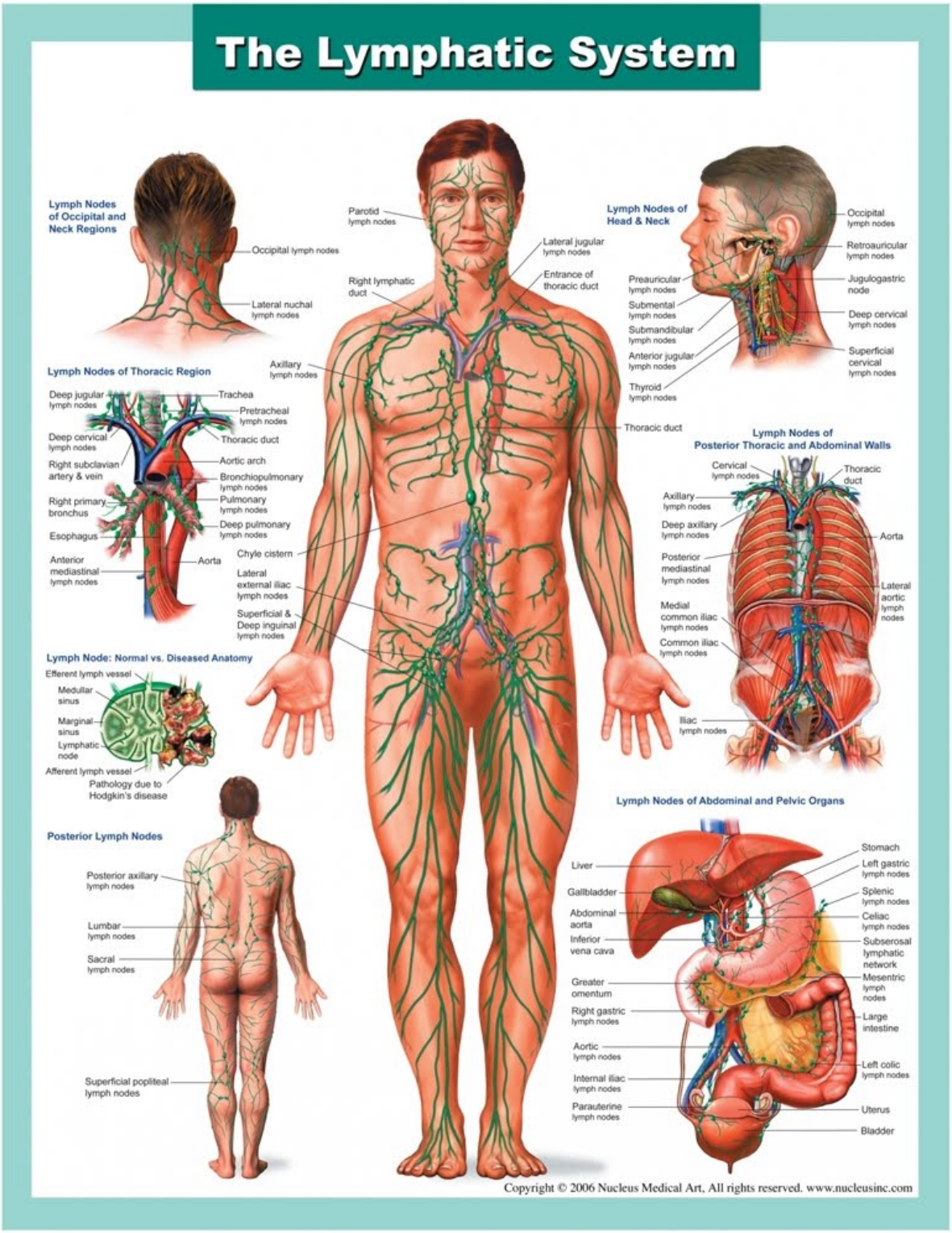

Figure 13 | The human lymphatic system. Display of all the essential components of the human lymphatic system. [http://www.higherpurposehealing.com/lymphatic-system/]

Organization of the cutaneous lymphatic microvasculature

Similar to the cutaneous blood microvasculature, the cutaneous lymphatic microvasculature is organized into two plexuses[78]. From the superficial plexus, lymphatic capillaries project into dermal papillae, but they do not form structures like capillary loops and are located more distant from the epidermis. From the superficial plexus, lymphatic capillaries project vertically downwards into the lower dermis and connect to the deep lymphatic plexus. In contrast to cutaneous blood capillaries, lymphatic capillaries are not found in the subcutaneous fat tissue[79]. Althoug lying adjacent to each other in many tissues, blood and lymphatic capillaries never anastomose.
The most important molecular promoters of lymphangiogenesis is VEGF-C which binds to VEGFR-2/3. In contrast, transforming growth factor (TGF-β) has been shown to inhibit dermal lymphangiogensis[80].

Lymphatic vascular development

In the mouse embryo, lymphatic vessels appear after blood vessels, which was a first indication that lymphatic vessels are derived from the blood vasculature[81]. Indeed, recent lineage-tracing experiments in mice[82] have solidified the concept that lymphatic endothelial cell progenitors are derived from venous BEC. At around embryonic day (E) 9.5, a subpopulation of venous BEC start to express the lymphatic specific marker Prox-1 at a defined location[83]. After that, these Prox-1-positive LEC leave the cardinal vein by directed budding in response to VEGF-C, migrate away and form lymph sacs and lymphatic vessels. Importantly, the expression of Prox-1 is not only required for lymphatic specification, but also for the maintenance of the lymphatic identity in the adult[84]. By E14.5, the lymphatic vascular network is present troughout the whole body. Postnatally, this primitive lymphatic vascular network is remodelled to give rise to a mature lymphatic vascular network consisting of initial lymphatic capillaries, pre-collector and collector lymphatic vessels.

Molecular markers of blood and lymphatic endothelium

By the establishment of pure blood and lymphatic endothelial cell populations isolated from human dermal tissues[85], it has been shown that LECs and BECs maintain their lineage-specific profile even after several passages in culture[86]. Recentyl, genome expression profiling experiments have revealed a number of lymphatic and blood vascular specific markers (Table 1).

Table 2.1.2 Lymphatic and blood vascular lineage-specific markers

Markers	Function	LV	BV	References
Prox1	Transcription factor	++		(Wigle et al. 1999)
Podoplanin	Transmembrane glycoprotein	++		(Wetterwald et al. 1996; Breiteneder-Geleff et al. 1999)
LYVE-1	Hyaluronan receptor	++		(Banerji et al. 1999)
VEGFR-3	Growth factor receptor	+	/(+)	(Kaipainen et al. 1995)
Neuropilin-2	Growth factor receptor	+	/(+)	(Yuan et al. 2002)
Macrophage mannose receptor-1	Adhesion molecule	+		(Irjala et al. 2001; Irjala et al. 2003)
CCL21	CC-chemokyne	+		(Gunn et al. 1998)
CCL20	CC-chemokyne	(++)	(++)	(Kriehuber et al. 2001; Hirakawa et al. 2003)
Desmoplakin	Anchoring protein of adherent junctions	+		(Ebata et al. 2001)
Plakoglobin	Connect cadherins to cytoskeleton in cell-cell junction	+		(Petrova et al. 2002; Hirakawa et al. 2003)
Integrin α9	Adhesion molecule, VEGFR3 co-receptor	+		(Huang et al. 2000; Petrova et al. 2002)
CD44	Hyaluronan receptor		+	(Kriehuber et al. 2001)
VEGF-C	Growth factor		+	(Kriehuber et al. 2001; Hirakawa et al. 2003)
VEGFR-1	Growth factor receptor		+	(Hirakawa et al. 2003)
Neuropilin-1	Growth factor receptor		+	(Hong et al. 2002; Petrova et al. 2002)
Endoglin	TGF-b receptor		++	(Hirakawa et al. 2003)
CD34	Adhesion molecule	/(+)	++	(Young et al. 1995)
IL-8	CXC-chemokine		+	(Petrova et al. 2002)
N-cadherin	Adhesion molecule		+	(Petrova et al. 2002; Hirakawa et al. 2003)
ICAM	Adhesion molecule		+	(Erhard et al. 1996)
Integrin α5	Adhesion molecule		+	(Petrova et al. 2002; Hirakawa et al. 2003)
Collagen IV	ECM protein	/(+)	++	(Hirakawa et al. 2003)
Versican	Proteoglycan		+	(Petrova et al. 2002; Hirakawa et al. 2003)
Laminin	Basement membrane molecule	/(+)	++	(Barsky et al. 1983; Petrova et al. 2002)
Collagen XVIII	Basement membrane molecule	/(+)	++	(Petrova et al. 2002; Hirakawa et al. 2003)

Table 1 | Lymphatic and blood vascular lineage-specific markers. BV=blood vessels; CCL=CC chemokine ligand; LV=lymphatic vessels; LYVE-1=lymphatic vascular endothelial hyaluronan receptor-1; VEGF=vascular endothelial growth factor; VEGFR= VEGF-receptor[87].

Pericytes

In contrast to other cell types, pericytes show a unique relation and interface with the microvascular basement membrane and the endothelial cells. Although related to vascular smooth muscle cells, they differ from these cells by their location (being embedded within the endothelial basement membrane), their morphology, and, to some extent, by their marker expression[88]. Similar to the pericytes in other organs, such as lung, placenta and kidney, which are primarily involved in gas exchange, nutrient transport, filtration and secretion[89,90], dermal pericytes are distributed to minimally hinder the exchange of gas and metabolites between blood vessels and the environment[91,89,90].

Several markers have been identified for pericytes, including smooth muscle alpha-actin (α-SMA), desmin, NG-2, platelet-derived growth factor receptor (PDGFR-beta), aminopeptidase A and N, RGS5, and the promoter trap tran[43]. However, none of these markers is entirely specific for pericytes. State-of-the-art identification of pericytes, therefore, is a combination of methods, including the use of different markers and high-resolution confocal imaging or electron microscopy. By this approach, immature angiogenic sprouts and tumor vessels, which have been thought to show only minimal pericyte coverage, have been shown to present abundant pericytes on their walls[88,92-94].

Furthermore, pericytes are believed to be able to differentiate into other cell types of mesenchymal origin, including vascular smooth muscle cells, fibroblasts, osteoblasts, chondrocytes and adipocytes[95]. They have been suggested to escape from the capillary basement membrane and differentiate into fibroblast-like cells that may contribute to the collagenous matrix of scars in wound healing, to chronic inflammation-related fibrosis, and to the formation of fibrous tumor stroma in cancer[96].

Mice lacking PDGF-B or PDGFR-beta die at embryonic stage due to microvascular leakage and hemorrhage caused by a severe deficit in pericytes, indicating that PDGF-B plays a central role in the recruitment of pericytes to the developing vasculature[97,98]. This is corroborated by the finding that PDGF-beta is expressed by the sprouting endothelium and PDGFR-beta is expressed by pericyte-progenitors[99].

1.2 CUTANEOUS WOUND HEALING

Because the primary function of the skin is to serve as a protective barrier against the outside world, any loss of the integrity of the skin may lead to major disability or even death and, therefore, must be mended rapidly and efficiently. Generally, the wound healing that follows a skin injury is very similar to the healing of a myocardial infarction or a spinal-cord injury, despite the different organs and cell types affected[31]. Wound healing is a highly dynamic process involving multiple cell types and can be divided into 3 main phases – inflammation, new tissue formation (granulation tissue) and remodelling – that overlap in time (Figure 14).

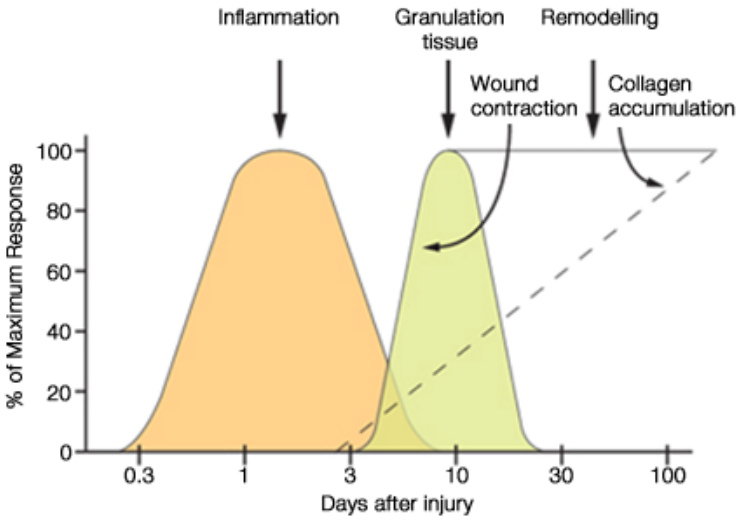

Figure 14 | Physiological stages of wound healing. Wound healing occurs in distinct phases that overlap in time. [http://www.clinimed.co.uk/WoundCare/Education/Wound-Essentials/Phases-of-Wound-Healing.aspx]

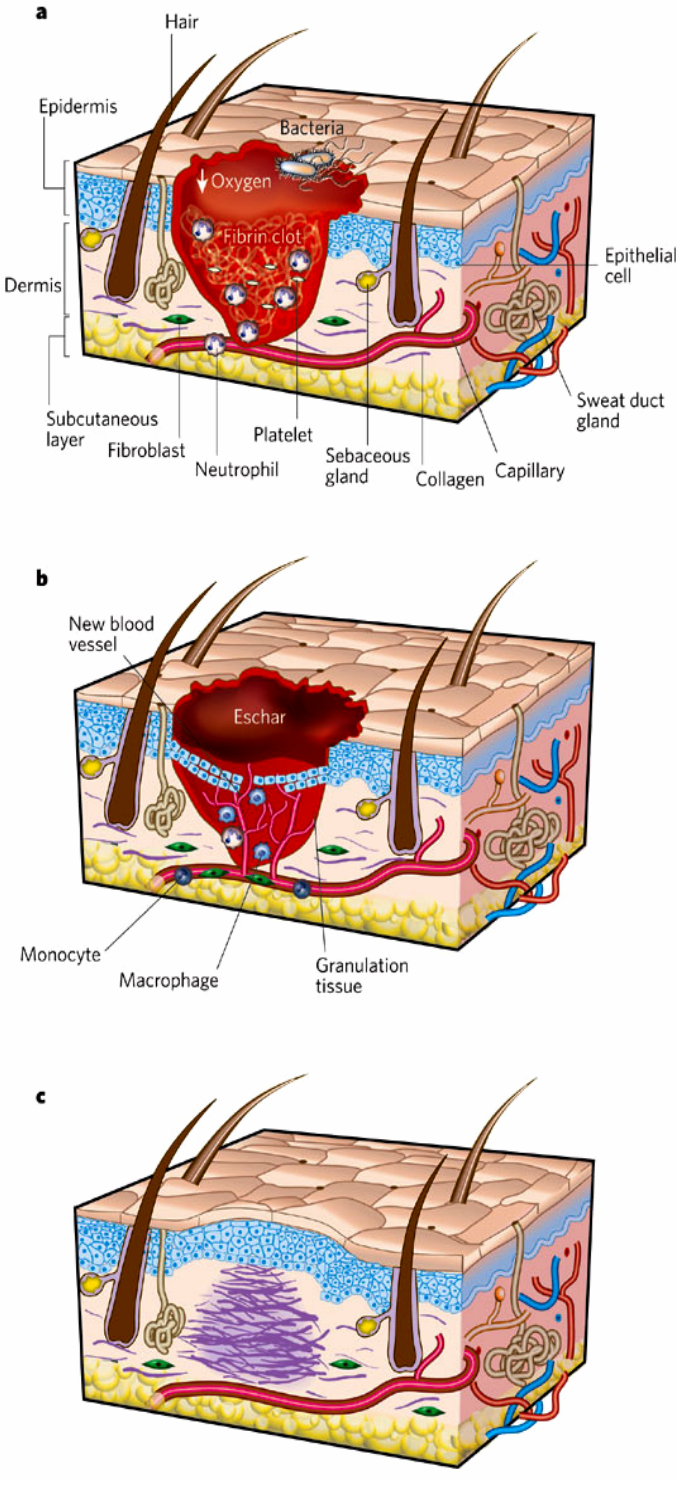

Figure 15 | Classic stages of wound repair. There are three classic stages of wound repair: inflammation (a), new tissue formation (b) and remodelling (c). (a) Inflammation. This stage lasts until about 48h after injury. Depicted is a skin wound at about 24-48h after injury. The wound is characterized by a hypoxic (ischaemic) environment in which a fibrin clot has formed. Bacteria, neutrophils and platelets are abundant in the wound. Normal skin appendages (such as hair follicles and sweat duct glands are still present in the skin outside the wound. (b) New tissue formation. This stage occurs about 2-10 days after injury. Depicted is a skin wound at about 5-10 days after injury. An eschar has formed on the surface of the wound. Most cells from the previous stage of repair migrated from the wound, and new blood vessels now populated the area. The migration of epithelial cells can be observed under the eschar. (c) Remodelling. This stage lasts for a year or longer. Depicted is a skin wound about 1-12 month after repair. Disorganized collagen has been laid down by fibroblasts that have migrated into the wound. The wound has contracted near its surface, and the widest portion is now the deepest. The re-epithelialized wound is slightly higher than the surrounding surface, and the healed region does not contain normal skin appendages or typical rete ridges[31].

1.2.1 INFLAMMATION

A first temporary repair of wounded skin is achieved in the form of a blood clot that plugs the defect (Figure 15). This clot re-establishes hemostasis and provides a provisional matrix for subsequent cell migration. The platelets of the blood facilitate the formation of this clot and secrete several mediators of wound healing[100]. Indeed, growing evidence suggests that platelets have a much more diversified role in the wound healing cascade. In addition to the induction of blood coagulation, platelets have been shown to aid in recruiting leucocytes, induce changes in cell permeability and promote cell migration and chemotaxis, essential steps in wound repair[101]. Together with numerous vasoactive mediators and chemotactic factors generated by the platelets and injured parenchymal cells and in response to molecular changes in the surface of endothelial cells, activated inflammatory leukocytes and fibroblasts are attracted to the site of injury[102]. Infiltrating neutrophils clean the wounded area from foreign particles and bacteria and are subsequently extruded with the eschar or phagocytosed by macrophages. By binding to specific proteins of the extracellular matrix through integrin receptors, macrophages are stimulated to phagocytose microorganisms[103]. At the same time, adherence of monocytes to the exracellular matrix stimulates them to differentiate into inflammatory or reparative macrophages. This is mediated by the expression of colony-stimulating factor 1 (CSF-1), tumor necrosis factor alpha (TNF-α) and PDGF. In addition, monocytes and macrophages express TGF-α/β, interleukin-1 and insulin growth factor 1 (IGF-1)[104]. The monocyte- and macrophage-derived growth factors are crucial for the propagation of new tissue formation during wound healing, as macrophage-depleted animals have defective wound repair[105]. However, the importance of neutrophils and macrophages in the initiation of wound repair is incompletely understood. Recent data imply that a deficiency in either cell type can be compensated[106] and that, if both cell types are absent, small wounds can still heal properly and scar formation is even reduced[107].

1.2.2 EPITHELIALIZATION

Shortly after injury, keratinocytes start to migrate over the wounded area and initiate re-epithelialization. Epidermal cells from skin appendages such as hair follicles start to remove clotted blood and damaged stroma. In order to crawl over the provisional fibrin clot deposited in the wound area, the hemidesmosome and desmosome junctions of the

keratinocytes have to be dissolved and keratinocytes at the edge of the wound have to change their set of integrin receptor expression[108-110] and retract their intracellular tonofilaments[111]. This rearrangment of integrin receptor expression most likely accounts for the lag of several hours before re-epithelialization begins. The migrating epidermal keratinocytes separate desiccated eschar from viable tissue. One to two days after the initiation of wound repair, wound margin keratinocytes start to proliferate in response to the local release of growth-factors, like epidermal growth factor (EGF), transforming growth factor alpha, and keratinocyte growth factor[112,113].

1.2.3 FORMATION OF GRANULATION TISSUE

Granulation tissue, which refers to the new stromal matrix deposited in the wound, begins to develop in the wound space about 4 days after injury. The new provisional fibrin matrix containing structural molecules like fibrin, fibronectin and hyaluronic acid[114-116] is deposited by invading fibroblasts and serves to support cell ingrowth and proliferation. This provisional extracellular matrix, consisting mainly of cross-linked fibrin, is steadily replaced with a collagenous matrix. After deposition of an abundant collagen matrix and a stop in collagen production, the fibroblast-rich granulation tissue is replaced by a relatively acellular scar.

1.2.4 NEOVASCULARIZATION

The formation of new blood vessels is pivotal to sustain the metabolic demands of the newly formed granulation tissue[117]. Angiogenesis has been shown to be induced through the concerted action of multiple angiogenic growth factors, including vascular endothelial growth factor, transforming growth factor beta, angiogenin, basic fibroblasts growth factor and Ang-1[118,119]. Furthermore, the ingrowth of new blood vessels is promoted by local low oxygen tensions (hypoxia)[120] and elevated lactic acid. Most of these growth factors are secreted by macrophages, endothelial cells, fibroblasts and activated keratinocytes.

Other prerequisites for angiogenesis are appropriate extracellular matrix molecules and endothelial cells expressing the receptors for the provisional matrix. In response to a skin injury, endothelial cells in and in close proximity to the wound secrete increased amounts of fibronectin[121]. Since the endothelial expression of functional fibronectin receptors is

crucial for angiogenesis, the deposited fibronectin could act as a conduit for the invasion of endothelial cells into the wound[122].

An injury of the skin leads to the damage of the tissue and, due to the impairment of the local vasculature, to hypoxia. In response to the disruption of tissue, macrophages release angiogenic factors such as acidic and basic fibroblast growth factor (bFGF). In response to local hypoxia, keratinocytes start to secrete vascular endothelial growth factor. Endothelial cells in the wound are further stimulated to release plasminogen activator and pro-collagenase, which leads to the digestion of the basement membrane. Upon fragmentation of the basement membrane, endothelial cells are induced to form new blood vessels in the wound. After the deposition of granulation tissue, angiogenic activity decreases through apoptosis[123].

1.2.5 SCAR FORMATION

Tissue remodelling is the longest phase of wound healing, which can take up to several years to complete. If this phase completes without serious problems, the result of tissue remodeling usually is a normotrophic scar, that serves to rapidly restore the main functions of the skin[124]. About 2 weeks after an injury, wound fibroblasts differentiate into myofibroblasts and wound compaction and contraction are initiated. Collagen remodeling during scar formation is dependent on continued synthesis of collagens at a relatively low rate, whereby initially deposited collagen-III is remodelled into collagen-1[125]. Degradation of wound collagen is mediated by matrix metalloproteinases, which are secreted by endothelial cells, keratinocytes, fibroblasts and macrophages.

Scar formation has evolved through the urge to most rapidly restore the barrier function of the skin. However, a scar never attains the same breaking strength as uninjured skin, often is unaesthetic and can lead to considerable tissue dysfunction and reduction of life quality. Furthermore, scar formation can become uncontrolled and lead to malignant tissue transformation[126]. Certainly, the optimal result of wound healing would be perfect regeneration, or with other words, scar-free healing. Indeed, there are examples of scar-free healing in nature, like the fetal wound healing of mammals[127] or the perfect regeneration of urodeles[128]. Accordingly, these examples have been extensively analyzed with the hope to find strategies that prevent scar formation in the adult mammal. A great number of studies has revealed the following differences between the scar-free fetal wound healing and the healing of post-natal wounds: Fetal skin has a higher ratio of

collagen type III to collagen type I[129], fetal wounds contain higher ratios of TGF-b3 to TGFb1 and TGFb2[130], fetal fibroblasts do not produce collagen in response to TGF-b1 [131], fetal skin is more hypoxic than adult skin[132], fetal fibroblasts are capable of proliferating simultaneously while producing collagen which leads to delayed collagen deposition and scar formation in adult wounds[133], fetal wounds show a reduced inflammatory response[134] and fetal mammals show a higher activity of transcription factor patterning genes, such as homeobox genes[135]. However, despite the growing knowledge about differences in fetal and adult mammalian wound repair, the field of regenerative medicine has failed to induce the perfect regeneration of skin so far.

1.2.6 SEROMA FORMATION

After wounding, also the dermal lymphatic endothelium is ruptured, thus, the draining capacity of the lymphatic vessels is compromised. As a consequence, accumulation of tissue fluid, i.e. seroma, arises. Persistent local interstitial fluid as well as delayed removal of local debris and inflammatory cells impede wound healing. In contrast, induction of lymphangiogenesis and immune cell recruitment were shown to accelerate skin regeneration[136]. By overexpression of VEGF-C, it was shown that increased lymphangiogenesis leads to a faster wound closure in genetically diabetic mice.

1.2.7 ABNORMAL WOUND HEALING

Abnormal wound healing in humans can appear either as delayed wound healing (e.g. as a consequence of diabethes[137] or after radiation exposure[138]) or as an excessive healing response (hypertrophic and keloid scars[126]). Excessive deposition of large amounts of extracellular matrix and alterations in local vascularization leads to the formation of an abnormal scar. After burns for example, excessive healing often leads to the formation of a hypertrophic scar[139]. Another example of abnormal wound healing are diabetic ulcers. They usually occur in patients who are unable to sense and relieve cutaneous pressure because of the damage of the local nerve system[137]. Secondary to vascular disease, ischemia also impedes the healing of diabetic ulcers by diminishing the supply of oxygen and other nutrients.

Approaches to modify and improve wound healing have mainly been focussed on TGF-β, since scar formation is accompanied by the presence of increased amounts of this

factor[140]. This has led to clinical efforts to block scar formation using antibodies and small molecules against TGF-beta and other pro-inflammatory mediators[141]. However, no strategy so far has led to significant advances in patient care.

The ultimate solution to both delayed and excessive healing might be the administration of a bio-engineered organ that elaborates the full complexity of biological signalling. After transplantation onto the wound, cells within the bioengineered organ can provide the proper sequence of extracellular factors to accelerate tissue repair and regeneration. Therefore, tissue engineering attracts more and more interest and is likely to eventually deliver approaches to prevent abnormal healing and even direct normal healing from fibrosis towards tissue regeneration.

1.2.8 OXYGEN AND WOUND HEALING

Normal homeostatic human skin is considered mildly to moderately hypoxic[142]. Given the avascular nature of the epidermis, it is not surprising that there is a progressive increase in the hypoxic state in the direction from the dermis to the epidermis, which peaks in the metabolically inactive outermost layer of the epidermis, the stratum corneum[143]. However, it is well established that the perturbation of the local skin's vasculature by disease or wounding exacerbates the hypoxic status of the skin and obstructed blood flow hampers proper wound healing and fosters the development of chronic wounds[144,145]. Oxygen is a basic requirement for almost every step of the wound healing cascade. The most obvious and best known role of oxygen in wound healing is its essential involvement in the production of biological energy equivalents like adenosine triphosphase (ATP)[146]. Sufficient wound oxygenation therefore is crucial for the maintenance of an adequate energy level to support cellular function. However, oxygen has various other functions in different phases of wound healing, like the inflammatory phase. The oxygen-dependent NADPH-linked oxygenase catalyses the production of reactive oxygen species (ROS). ROS are essentially involved in oxidative bacterial killing through the stimulation of cytokines and chemokines which attract and activate neutrophils and macrophages[147,148]. Furthermore, these inflammatory cells are extremely active and require high amounts of oxygen for their cell function. Oxygen is also essential for the collagen synthesis of fibroblasts during the remodelling phase of wound healing[149]. The hydroxylation of proline and lysine residues during collagen production requires oxygen. Re-epithelialization of the wound by keratinocytes requires restructuring of their

cytoskeleton, a process that is oxygen dependent. In addition, injury-induced release of chemokines such as KGF, EGF and IGF that initiate re-epithelialization also requires oxygen. Finally, the differentiation of fibroblasts into myofibroblasts during tissue remodelling is triggered by oxygen[150].

Generally, it can be said that hypoxia following an injury triggers the wound healing cascade for example by boosting ROS activity, but prolonged hypoxia due to a failure in the rapid recovery of wound tissue oxygenation impairs physiological wound healing and can lead to chronic wounds.

1.3 TISSUE ENGINEERING OF SKIN

1.3.1 PRINCIPLES OF TISSUE ENGINEERING

The need for donor organs nowadays far exceeds the availability of organs for transplantation. The urge of finding new organs has led to the development of new surgical techniques, like whole organ transplantation from living, related donors (e.g. kidneys) and splitting adult organs (e.g. part of the liver or a lung from a parent to a child). Despite excellent progress in these techniques and high success rates, the problem of organ shortage still remains and, due to the increasing average expectancy of life of humans, is constantly rising.

Tissue engineering has emerged as a new alternative for organ transplantation and, because of the use of autologous cells isolated from the patient's own body, completely avoids the risk of immunological responses such as rejections[151]. The basic concept of tissue engineering consists of a scaffold or extracellular matrix (ECM) that provides a provisional architecture onto or into which isolated and expanded cells are seeded. These then can organize and develop into the desired organ or tissue prior or after transplantation (Figure 16). The scaffold or ECM mimics the extracellular environment and provides an initial biomechanical grid for the replacement tissue until the cells produce an adequate secondary extracellular matrix. Usually, the scaffold is either degraded or metabolized during the formation of the newly generated matrix.

For the isolation of the cells, there are two basic approaches. The first way to obtain autologous, organ-specific cells is by the dissection of a biopsy. This technique is commonly used for most organ structures, such as skin, liver, heart, blood vessels, bone, bone marrow and cartilage. However, for the engineering of certain other tissues or organs, the dissection of a biopsy is technically demanding or even dangerous for the patient. Thus, other strategies like harvesting the cells from a related tissue, must be considered (e.g. the peripheral vein segments for heart valve engineering)[152].

Recent progress in stem cell biology has opened the exciting possibility to differentiate all the desired cell types using a unique source of stem cells like bone marrow-derived stem cells[153]. Further refinement of the understanding of how to induce, control and maintain a certain cell type differentiated from stem cells is critical for a broad use of this technique in tissue engineering.

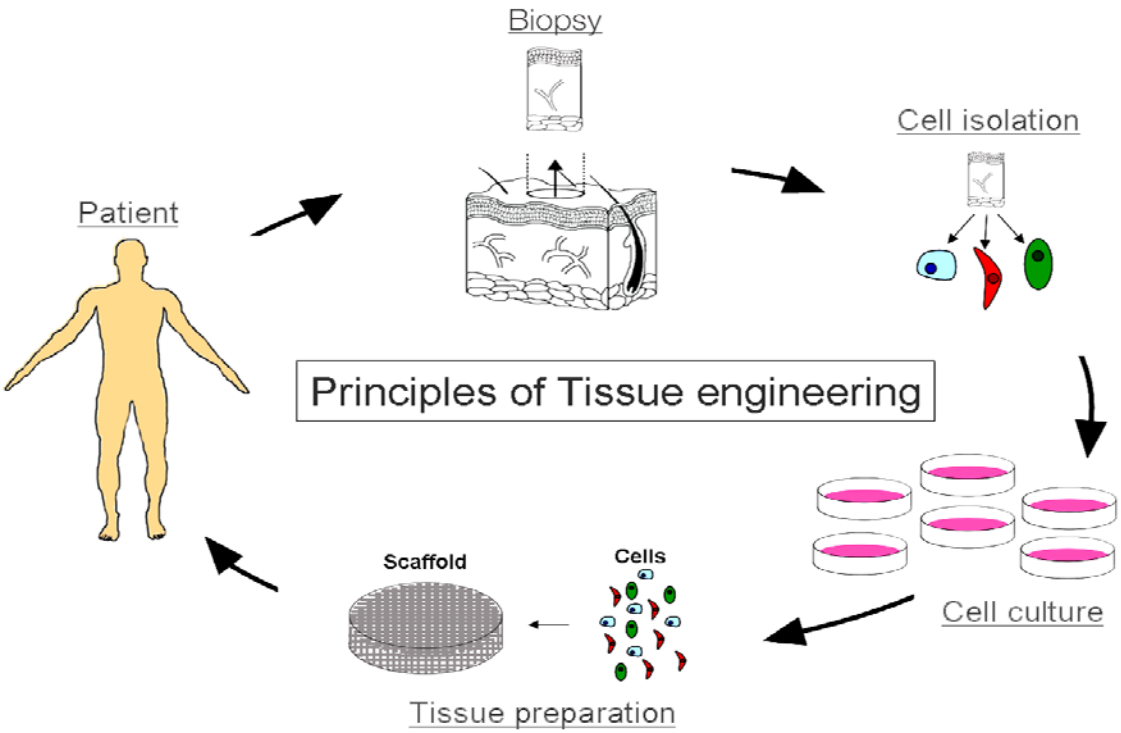

Figure 16 | Principles of Tissue engineering. Scheme showing the typical sequence of steps in tissue engineering. Usually, a biopsy of the patient is taken, cells are isolated and propagated using cell culture. Finally, employing an appropriate scaffold like a hydrogel, the desired engineered tissue is assembled and transplanted back onto the patient.

Induced pluripotent stem cells

In 2006, Takahashi and Yamanaka presented an approach to alter cell fates of differentiated cells[154]. By overexpression of a defined set of factors such as Oct-3/4, Klf4, Sox-2 and c-Myc, they could induce a stem cell phenotype in adult, differentiated mouse fibroblasts, transforming them into induced pluripotent stem cells (iPS). Since then, a great number of papers have delivered advances in reprogramming technology, including alternative methods for reprogramming and the successful derivation of iPS cells from various differentiated cell types[155]. For the field of regenerative medicine, iPS cells hold great potential, as they can substitute for patient cells that otherwise would have to be gained by taking biopsies (Figure 17). It is therefore not surprising that quite a number of recent studies have focussed on the generation of cardiomyocytes using iPS[156-158]. Indeed, despite considerable challenges, the generation of disease-specific and patient-specific iPS has become almost routine. Disease-specific iPS cell provide a unique opportunity to

study a variety of diseases, to carry out *in vitro* drug screenings and to evaluate potential therapeutics.

In a landmark study, Wernig et al. gained dopaminergic neurons from iPS cells. These cells, after transplantation into the brain, became functionally integrated and furthermore improved the condition of a rat model of Parkinson's disease[159]. This study reflects the therapeutic value of pluripotent stem cells for cell-replacement therapy in the brain. The application of iPS cells in regenerative medicine is one of the most promising areas for the future of iPS-cell application.

One of the most important questions that still remains is to what degree iPS cells differ from embryonic stem cells. Initially, a remarkable similarity between iPS cells and embryonic stem cells was reportet. However, more recent reports have revealed some differences. For example, Chin et al. identified hundreds of genes that were differentially expressed in iPS cells and embryonic stem cells[160]. In another study, it was shown that there are differences in the DNA methylation between two types of pluripotent stem cell lines[161]. On the other hand, several studies had difficulties to distinguish between iPS cells and embryonic stem cells by gene expression or DNA methylation[162,163]. Clearly, further studies are required to get a more complete picture about these differences in order to better evaluate the therapeutic potential of iPS cells. Such studies will bring the field closer to patient-matched cells and tissues for clinical transplantation.

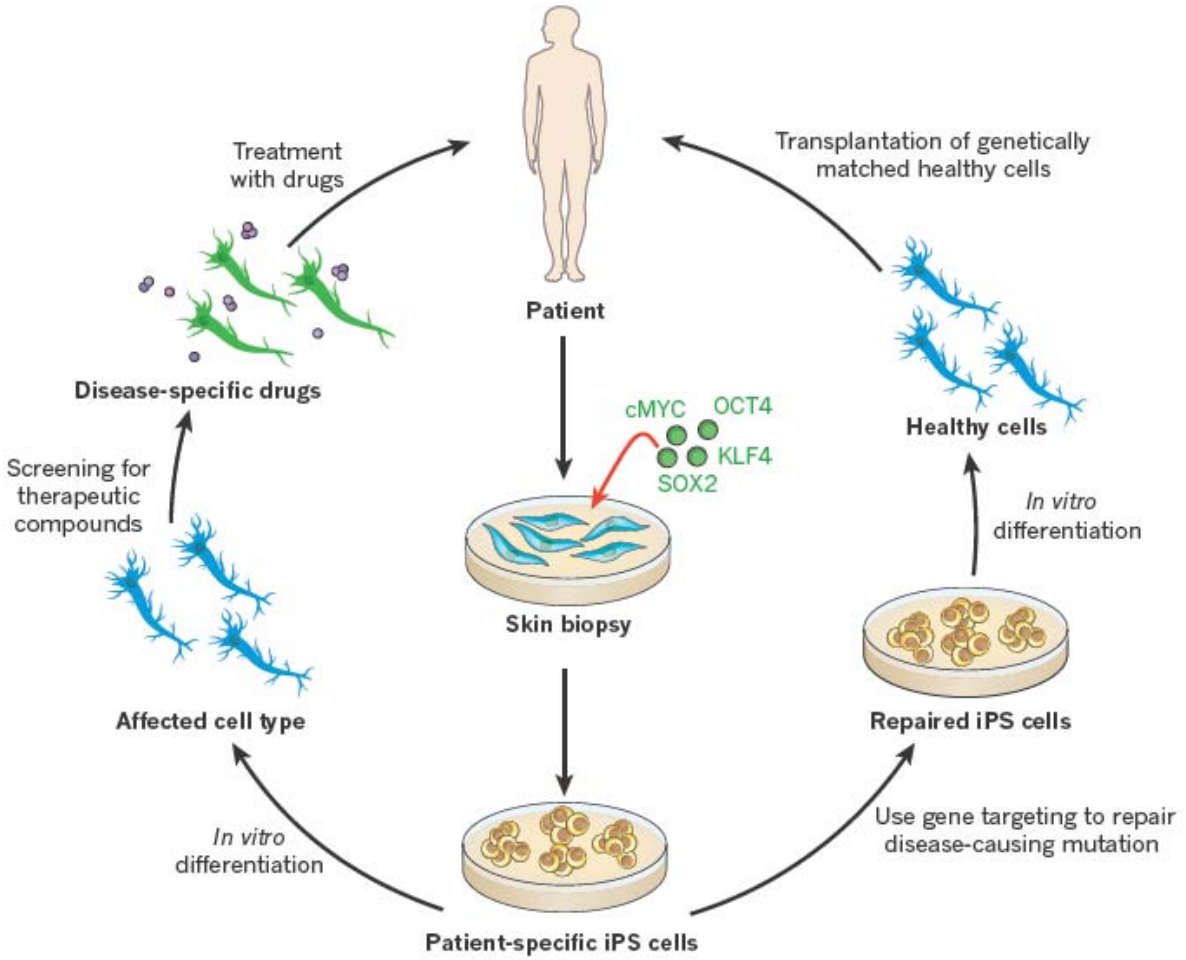

Figure 17 | Medical applications of iPS cells. Example of a medical application of iPS cells. In this case, the patient has a neurodegenerative disorder. Parient specific iPS cells are gained from cells isolated from a skin biopsy using the overexpression of c-Myc, Oct4, Sox2 and Klf4. Thereafter, there are two possibilities to proceed. If the mutation underlying the disease is known, gene targeting to repair these mutations could be applied and the resulting healthy cells could be transplanted back into the patient. Another possibility is to generate affected cell types from these iPS cells that can be used in models for drug screening to develop disease-specific drugs. [http://www.nature.com/nature /journal/v481/n7381/pdf/nature10761.pdf]

1.3.2 THE BIOENGINEERING OF HUMAN SKIN

The current gold standard for the treatment of large skin wounds is the application of autologous split-thickness skin containing only little dermis. However, probably as a consequence of the limited amount of dermis contained in split-thickness skin, these grafts usually develop into scars or show insufficient pigmentation. Additionally, in severely injured patients, the defect may cover more than 50-60% of the total body surface area. As a result, donor sites for the removal of split-thickness skin are very limited. In these cases, tissue-engineered skin becomes a vital option, especially since the harvesting of split-thickness skin can also lead to disfiguring scars, which often is the case in children that are prone to the development of hypertrophic scars and keloids[164]. Furthermore, tissue-engineered skin may significantly support the healing of chronic wounds[165], they can be used for reconstructive sugery e.g. scar revisions, correction of pigmentation defects such as vitiligo, and congenital nevi[166].

Usually, skin is engineered by the expansion of skin cells in the laboratory originally isolated from a biopsy of the patient's own skin. These are then used to generate complex allogenic or, in our case, autologous skin grafts to restore the function of skin as completely as possible (especially in burns patients) or to close chronic, non-healing ulcers[167].

Essential for the initiation of skin tissue engineering was the development of a technique to enzymatically separate the epidermis and the dermis[168] and the successful *in vitro* propagation of keratinocytes[169]. Since the first successful growth of human primary epidermal cells in serial culture[170], enormous progress in the pursuit of developing engineered skin has been made. In 1981, the first DESS was tested in an animal model[171] and since then, the development of DESS has been constantly improved. However, there are still significant problems to be solved for a successful use of engineered autologous DESS in the clinics, like the addition of skin appendages, such as sweat glands, hair follicles, and sebaceous glands or melanocytes for pigmentation. Further approximating the complexity of human skin would greatly contribute to achieve similar results with engineered skin as with the transplantation of the patient's own full thickness skin.

The development of tissue engineered skin substitutes was initially triggered by the clinical need of large amounts of autologous skin graft to treat patients with extensive burns to cover large areas of the body. Burn wounds cause water, electrolyte and protein

loss in the affected wound area and are prone to bacterial invasion. The modern treatment concept for extensive burns involves the surgical removal of heat denaturated proteins and devitalized tissue[172]. This procedure turns the burn wound into an excisional wound, thus triggering the normal wound healing cascade[173]. Primary excision, when compared to results obtained by awaiting spontaneous separation of eschar with later grafting, has reduced mortality, morbidity and later reconstructive measures by 50%[174]. Especially in burns affecting large areas of the body, split-thickness skin grafts are not always available in sufficient quantity[175]. This has given rise to the clinical need for tissue-engineered alternatives. Initial attempts to treat burn wounds with tissue engineered skin consisted in CEA that were grafted directly onto the wound[176]. Other more recent approaches that include only keratinocytes without dermal component were keratinocyte suspensions that were sprayed onto the wound[177]. However, it rapidly became clear that rapid and efficient attachment of the keratinocytes to the underlying dermis is of key importance for a successful healing. Precondition for an efficient attachment of the keratinocytes is a good preparation of the wound bed to achieve a highly vascularized dermis[178,179]. The importance of an optimal wound bed has led to the development of an acellular collagen-glycosaminoglycan-based dermal substitute, called Integra[180]. Integra in combination with split-thickness skin has found wide use in the clinics and has considerably improved the life of burn patients. Even though the use of Integra leads to the most reliable take of split-thickness skin, an obvious disadvantage of this procedure is the involvment of two surgical interventions. In a first step, Integra is applied, after which a certain amount of time is needed for this dermal template to heal and integrate. Thereafter, the split-thickness skin is sutured on top in a second surgical intervention.

For the patient, these issues are important and other solutions are required. Obviously, a better solution is the engineering of a DESS that approximates the complexity and quality of full thickness skin. DESS, in which the epidermal and dermal layers are firmly attached prior to transplantation, can optimally be transplanted in only one surgical intervention. Additionally, since rapid and tight attachment of the epidermal and dermal layers is crucial for a successful outcome of skin transplantations[166], DESS might significantly improve take rates when compared to epithelial or dermal grafts.

The necessity of a well-vascularized wound bed indicates that another main determinant of a successful treatment of burned wounds with skin substitutes is angiogenesis. Skin is commonly thought to be less dependent on angiogenesis than other tissue engineered

organs like bone or skelletal muscle. However, if the thickness of a DESS exceeds 0.3 – 0.4 mm, ingrowth of new blood vessels into the transplant is too slow to provide the whole tissue with oxygen and nutrients[181]. Lack of a blood supply in these cases can lead to necrosis and loss of grafts. Indeed, if skin substitutes are placed directly over fat or poorly vascularized wound beds, the graft may be lost as well. The importance of angiogenesis and the fact that both the dermal and epidermal layer demand a continuous provision of nutrients from dermal capillaries close to the DEJ has led to an advanced form of DESS containing a pre-formed microvascular network[182-185]. In the last decade, engineering of a pre-formed microvascular network in different engineered organs has made remarkable progress, but further optimization and analysis of the benefit of prevascularization for the transplantation of a given organ were needed.

1.4 PREVASCULARIZATION OF ENGINEERED TISSUES IN VITRO

Once tissue engineering had progressed from creating thin cell sheets to more and more complex tissues and organs exhibiting an increasing thickness, it rapidly became clear that a key challenge in tissue engineering will be to design strategies that accelerate the connection of an engineered organ to the vasculature after transplantation. Neovascularization, the ingrowth of new blood vessels into a transplanted tissue, is relatively slow, especially during the first period after transplantation, and therefore is not sufficient to efficiently support larger tissues[186]. As a result, transplantation of avascular and thicker engineered tissues and organs without an innate strategy to accelerate revascularization will inevitably lead to cell necrosis and graft failure. Nature itself has recongnized this inescapable fact and has designed vertebrate organogenesis accordingly: the cardio-vascular system is the primary organ to appear during the embryonic vertebrate development and thus can sustain the development of all subsequent tissues and organs[187]. However, nature has the tendency to assign different tasks to the same cell type and has provided endothelial cells, the main building blocks of the vasculature, with additional tasks beyond their nutritional role. Recently, several studies have shown that endothelial cells provide inductive signals to various tissues during organogenesis, such as the liver and the pancreas[187] (see below). Thus, promoting the revascularization of engineered

tissues is not only critical for the success of the transplantation, but may also be crucial in the decision whether or not the implant will develop into the desired tissue or organ after transplantation.

1.4.1 APPROACHES TO ACCELERATE REVASCULARIZATION OF TISSUE-ENGINEERED TISSUES AND ORGANS

Strategies for acceleration of tissue engineered organ revascularization can be divided into three main groups: 1. angiogenic growth factor-releasing scaffolds, 2. engineered vasculature using microfabrication techniques or decellularized matrices and 3. prevascularization of tissue *in vitro*.

Growth factor-releasing scaffolds

One approach to achieve tissue vascularization is the use of a polymer scaffold supplied with growth factors that are released in a controlled manner (Figure 18). Control of the growth factor release is achieved through the degradation process of the polymer. Several studies have shown that by this approach, angiogenesis could be achieved resulting in higher capillary numbers, blood vessel density and a higher degree of maturity[188,189]. Several materials have been used for the scaffold, including poly lactic glycol (PLG), and poly lactic-co-glycolic acid (PLGA). Scaffolds were supplied with growth-factor containing microspheres, matrigel or hydrogels like fibrin gels[190-194].
It is recognized, however, that the administration of a single growth factor is insufficient to induce the formation of mature blood vessels. Therefore, the release of a combination of different growth factors has been strived. Among these strategies, the combination of VEGF with either PDGF or FGF2 have given best results so far[195-197].

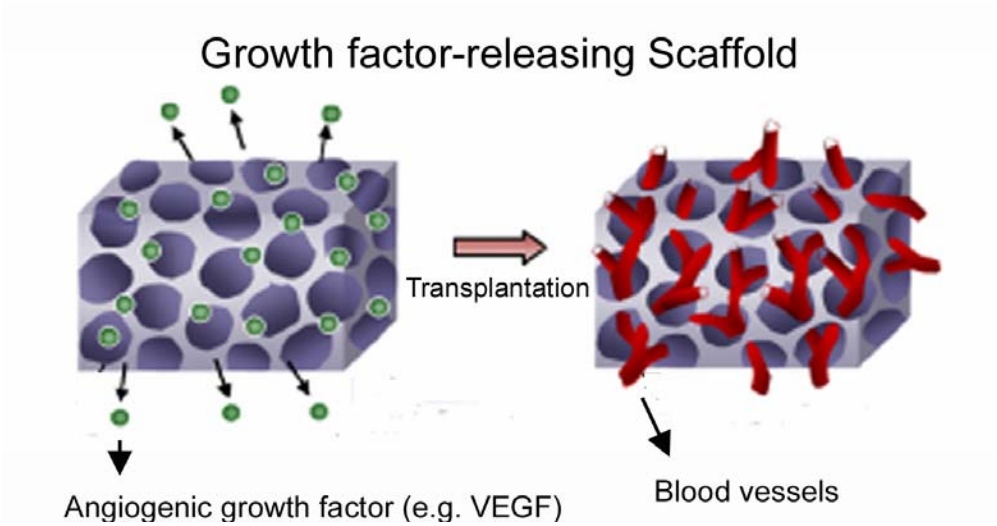

Figure 18 | Growth factor-releasing scaffold Scaffolds can be supplied with growth factors before transplantation. In this example, angiogenic growth factors like VEGF and/or FGF-2 can be used to promote the ingrowth of blood vessels[198].

Engineered vasculature using microfabrication techniques

Because more complex organs such as the heart or the lung contain a dense vasculature with diverse dimensions that are difficult to obtain through the seeding of randomly distributed endothelial cells, microfabrication methods were introduced (Figure 19). An example for that is a non-woven silk fibroin net that allows adhesion and spreading of endothelial cells along the fibres[199]. A breakthrough in the field of microchannels for engineered vasculature was achieved by Choi et al. by engineering microfluidic channels networks directly embedded within bovine chondrocyte-seeded alginate gels[200]. They used soft lithography of a silicon stamp as a master on which hydrogels with a definitive microstructure can be molded. Afterwards, cell seeded alginate was injected and crosslinked. Using this method, two matching parts of the scaffold were fabricated and eventually pressed against each other to form a sealed structure which allows the flow of solutions through the microchannels. Nahmias et al. introduced a laser guided direct writing using a weakly focused beam to trap and deliver particles, including living cells, to a non-absorbing surface[201]. They used this approach for patterning of HUVEC on Matrigel along a desired form. After self-assembly of the HUVEC into vascular structures, they were co-cultured with hepatocytes, resulting in an aggregated tubular structure similar to hepatic sinusoid.

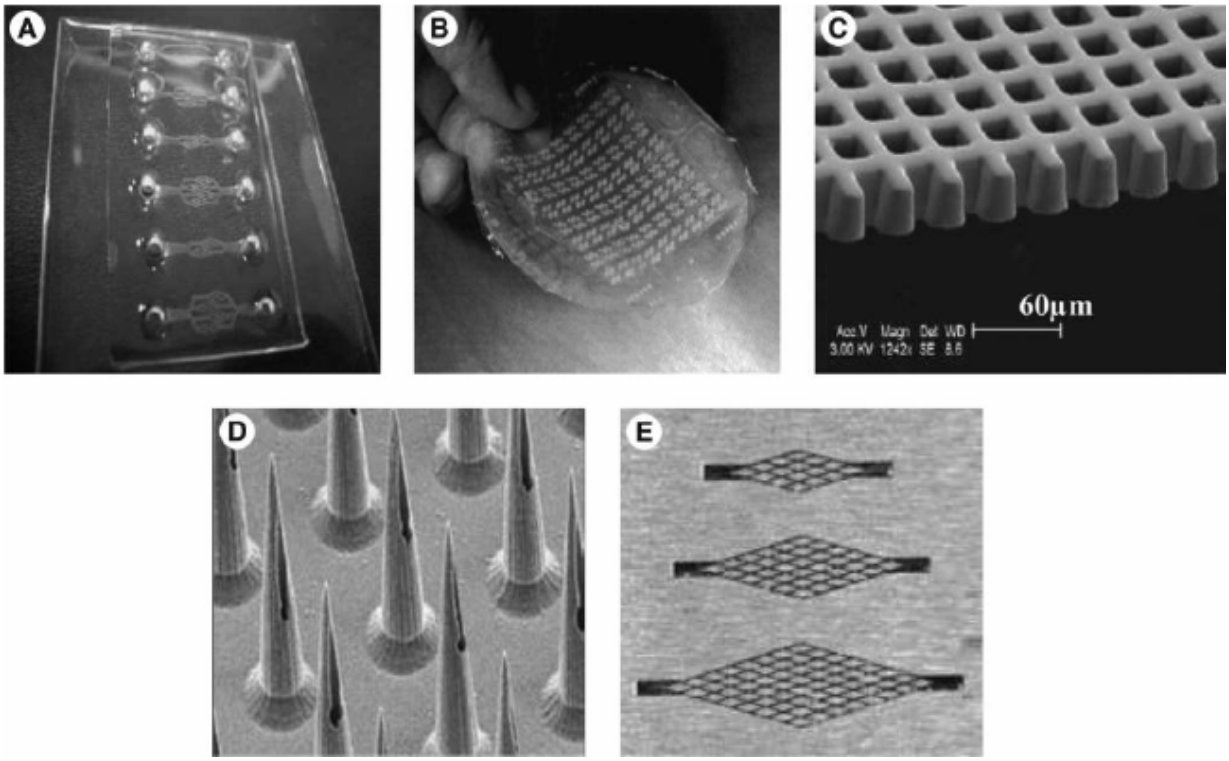

Figure 19 | Examples of microfabrication methods to create microvessel scaffolds (**A**) PDMS[202] and (**B**) PLGA—microchannels of 25–35 x 20–40 um^2 cross section. (**C**) Microchannels in 50/50 PLLA/PLGA[203]. (**D**) Microneedle arrays with fluidic channels at 20 um diameter[204]. (**E**) 20 x 60 um^2 Vascular network on stainless steel with 800 um in segment length[205,186].

Prevascularization of tissue in vitro

The basic idea of prevascularization is to seed the engineered tissue with endothelial (progenitor) cells to induce the formation of a vascular network *in vitro*. Several studies have underlined the necessity of adding a supportive mesenchymal cell source for prevascularization, such as dermal fibroblasts, pericytes or myoblasts[206,207]. The aim of *in vitro* prevascularization is to rapidly establish a natural connection of the *in vitro* generated vascular network with the wound bed vasculature after traslantation onto a living organism. The process of connecting the two systems is called anastomosis (Figure 20). A study analyzed the revascularization of a prevascularized reconstructed skin equivalent in comparison to an avascular reconstructed skin. They found that the connection of the prevascularized skin to the mouse vasculature after transplantation required only 4 days in comparison to the 14 days required to connect the avascular skin[185]. Clearly, the advantage of prevascularization over the use of growth-factor-releasing scaffold, in addition to the issues of factor degradation and fuctionality, lies in

the saving of time. Whereas in growth-factor-releasing scaffold still a complete vasculature has to be build de novo after transplantation, connection of the preformed vasculature in prevascularized tissue can save considerable time.

An alternative to *in vitro* prevascularization is *in vivo* prevascularization. In this approach, the avascular tissue is placed in a first surgical intervention under the skin of a living organisms in order to get it vascularized. In a second surgical intervention, the *in vivo* prevascularized tissue is placed into the ischemic target site of this same organism. A clear disadvantage of this approach, however, is the need for multiple surgical interventions.

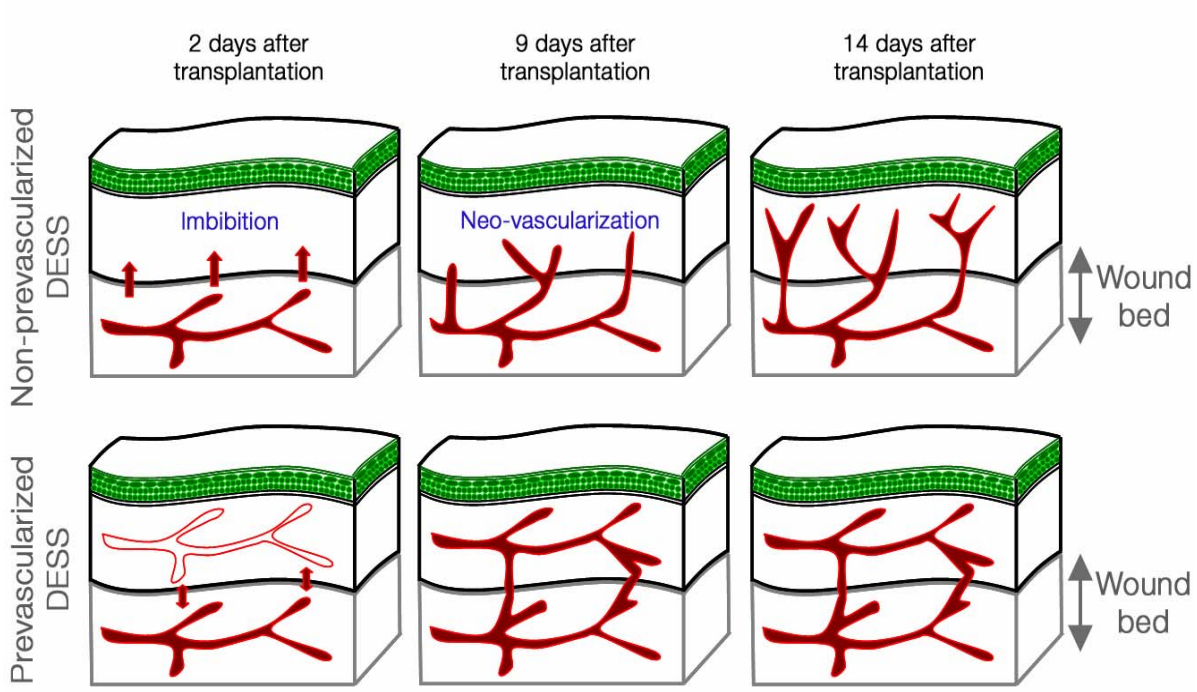

Figure 20 | The principle of prevascularization and anastomosis. Scheme despicting the principles of prevascularization using the example of a DESS. If a non-prevascularized DESS is transplanted, it initially has to survive solely by imbibition (diffusion), which is the passive diffusion of nutrients. Neovascularization will eventually take over, but can last up to 14 days to complete, depending on the thickness of the DESS. If a prevascularized DESS is transplanted, rapid (around 4 days) connection (anastomosis) of the pre-formed vessels with the wound bed vasculature highly accelerates functional neovascularization and is independent of the thickness of the reconstructed skin.

1.4.2 ENDOTHELIAL CELLS PROVIDE INDUCTIVE SIGNALS INDEPENDENT OF BLOOD FLOW

It is an intriguing finding that endothelial cells provide inductive signals during organ development in addition to their nutritional role[187]. Endothelial cells have been shown to play a critical role in defining the local immune response and provide tumor growth. Indeed, close association between the vasculature and developing organs have been observed for many years and it is this association that has led to the assessment of the possibility that endothelial cells could provide inductive signals. A first evidence of such reciprocal interactions between endothelial cells and sourrounding tissue during development was given by the study of heart development. Stainier et al. have found that in the zebra fish, the myocardial cell layer fails to mature in the absence of endothelium[208]. Furthermore, studies on embryonic liver development have revealed that the development of the hepatocyte primordium occurs in close proximity to primitive endothelial cells that express VEGFR2. In subsequent development, the hepatocytes divide and intermix with the endothelial cells. Using mice genetically deficient in endothelial cells, it was shown that the signals from endothelial cells promote hepatic endoderm budding independent of blood flow[209]. Studies of thyroid development have revealed that endothelial cells control the positioning of the thydoid primordium[210]. Furthermore, the pancreas develops in close apposition to blood vessels. It was shown that isolated murine dorsal endoderm only gives rise to insulin secreting cells in the presence of aortic explants[211]. Additionally, excision of the DA from Xenopus embryos abolishes the specific expression pattern of the pancreas[212]. Also, vascular cells participate in pancreatic development indirectly through ensuring stromal survival. At later stages in development, a circulation-dependent effect of the vasculature on dorsal pancreatic mesenchyme has been shown in mice[213].

Moreover, there is evidence that the similar paths of the vasculature and the nervous system in some locations arises from reciprocal chemotactic signals between these two tissue types[214,215]. In the central nervous system, the observation that neural stem cells are situated in close apposition to the endothelium indicated that endothelial cells may be important modulators of stem cell activity. Endothelial cells have been show to significantly affect the composition of embryonic neural stem cell cultures[216].

In combination with the crucial role of endothelial cells in circulation and nutrition, the finding that endothelial cells provide inductive signals for organogenesis attributes the rapid revascularization of *in vitro* generated organs a key role in tissue engineering.

1.4.3 PREVASCULARIZATION: STATE OF THE ART AND FUTURE PERSPECTIVES

The technique of prevascularization is currently under intense investigation. Several different prevascularized tissues and organs have been developed and analyzed (see below). In addition to the analysis of prevascularized tissues and organs, the prevascularization process itself has been investigated and improved. Chen et al. have engineered prevascularized fibrin gels using a coculture of HUVECs or endothelial progenitor cell-derived endothelial cells and dermal fibroblasts and analyzed the effects of varying fibroblasts densities on the degree of anastomosis after transplantation. They found that a high density of fibroblasts significantly promoted the formation of functional anastomoses of the engineered vessels with the mouse vasculature after transplantation. Indeed, the engineered network of mature capillaries was found to anastomose as early as 1 day after transplantation if a high density of fibroblasts was used instead of 4 days when a lower density of fibroblasts was used[217,218] . In another study, Alajati et al. showed that blood and lymphatic endothelial cells grafted as spheroids into a matrix give rise to a complex three-dimensional network of microvessels and showed that the blood vessels are able to anastomose to a living vasculature. They challenged their approach for usability as an experimental model system to study vessel formation originating from gain-of-function- or loss-of-function-manipulated endothelial cells to assess new candidate molecules of the angiogenic cascade. Furthermore, they probed the feasibility and robustness of the spheroidal approach as qualitative and quantitative angiogenesis assay and studied the activities of VEGF and FGF-2 on microvessel formation. Finally, they analyzed the effects of anti-angiogenic drugs on the formation of spheroid-based microvessels[218]. In a more recent study, the spheroid-based approach was used to engineer a minitumor model using a tri-culture of endothelial cells, fibroblasts and a breast cancer cell line. They showed that the growth of capillary-like structures was enhanced in the presence of the tumor cells and that the effects of inhibitors of angiogenesis and tumor growth on their system was similar to *in vivo* observations. Therefore, they suggested their

approach as a powerful new tool for the study of tumour angiogenesis *in vitro*[219]. Finally, Kang et al. engineered blood vessels and showed their ability, to get re-perfused in a second mouse after being perfused in a first mouse, thereby extending the potential applications of their prevascularization technology for transplantable tissue engineered constructs[220].

Skin

The first report about *in vitro* formed microvessels within an engineered tissue was described by Black et al. They engineered a skin equivalent by the co-culture of dermal fibroblasts, keratinocytes and HUVECs on chitosan/collagen scaffolds. The HUVECs formed a tubular network by self-organization and the skin equivalent formed a stratified epidermis with a pseudo-basal cell layer, stratum spinosum and stratum granulosum[182]. Shepherd et al. showed that endothelial cells, differentiated and expanded from circulating endothelial progenitor cells, can be used to promote vascularization of engineered human skin substitutes. They found that the development of the vessels in the engineered skin substitute is not prevented in a setting of impaired host angiogenesis/vasculogenesis and thus, the feasibility of their approach for patients with non-healing skin ulcers[183]. Finally, Gibot et al. developed an endothelialized reconstructed skin from autologous cells without any exogenous angiogenic growth factors or scaffold. They showed the ability of the *in vitro* generated microvessels to anastomose with the mouse vasculature after transplantation and found that the presence of pre-existing microvessels promoted revascularization of the reconstructed skin by mouse microvessels by exerting an angiogenic effect[184].

Bone

The interaction between bone and the vascular system is well known and there is a particular interest for bone prevascularization. Rouwkema et al. demonstrated the possibility to form a prevascular network of cord-like structures in a spherical model of human mesenchymal stem cells and HUVECs *in vitro*. The primitive network further matured *in vivo* and formed connections to the host vasculature 2 weeks after transplantation. The interaction of mesenchymal stem cells and HUVECs induced an

upregulation of the osteogenic marker alkaline phosphatase, suggesting an improved differentiation of osteoprogenitor cells[221].

In another study, a segmental defect in the femurs of rabbits was implanted with prevascularized tissue-engineered bone grafts (TEBG) generated by seeding mesenchymal stem cells into beta-Tricalcium phosphate (TCP) scaffolds. They found that the treatment with prevascularized TEBG led to a significantly higher volume of regenerated bone and a larger amount of capillary infiltration compared to non-vascularized TEBG and showed that this difference was accompanied with elevated expression of VEGF[222]. Mendes et al. used a cell sheed technology to create a scaffold free construct composed of osteogenic, endothelial and perivascular-like. They showed that the engineered microvessels anastomosed with the host vasculature and proved the osteogenic potential of the created construct. Furthermore, the perivascular cells differentiated from bone marrow-derived mesenchymal stem cells contributed to the stability of the vascular network[223].

Skeletal muscle

Levenberg et al. showed the possibility to prevascularize skeletal muscle tissue using a tri-culture system of endothelial, fibroblasts and myoblasts[207]. The endothelial cells formed lumenized microvessels stabilized by mouse embryonic fibroblasts that differentiated into smooth muscle actin-positive mural cells. A fraction of the mouse skeletal myoblasts were shown to differentiate into aligned, elongated multinucleated cells similar to muscle fibers. The prevascularized network anastomosed to the host vasculature within 14 days post-transplantation and improved the vascularization, blood perfusion and survival of the engineered tissue. In a subsequent study, Koffler et al. analyzed the influence of the degree of *in vitro* vascularization on the efficiency of vascularized muscle graft integration. They found that extended *in vitro* incubation, enabling the formation of a more structured vascular bed, allowed for a graft-host angiogenic collaboration that promoted anastomosis and vascular integration and supported enhanced muscle regeneration, maturation and integration[207].

Cardiac muscle

Using a tri-culture system including fibroblasts, cardiomyocytes and endothelial cells, Caspi et al. designed a muscle construct. They showed that the formed capillary structures were stabilized by mural cells derived from the fibroblasts and that the construct exhibited typical structural and functional properties of early-cardiac tissue[224,225] . Another study by Stevens et al. developed a scaffold-free prevascularized human heart tissue using cardiomyocytes, endothelial cells and fibroblasts that survived *in vivo* transplantation and integrated with the host coronary circulation. Functionally, vascularized patches actively contracted, could be electrically paced and exhibited passive mechanics, more similar to myocardium than patches containing only cardiomyocytes[225].

Future perspectives

There is no doubt that the major precondition for the success of tissue engineering in a daily clinical practice is the ability to guarantee an adequate and rapid blood supply to the implanted tissue constructs. Although vast research in this field has been done and considerable progress has been made, significant obstacles and challenges still remain. Because of the diversity of endothelial cell sources and the wide spectrum of engineered tissues and organs, further studies are needed to determine which endothelial cell source is best suited for the prevascularization of a given tissue or organ and at the same time most optimal for specific clinical solutions. Furthermore, strategies to optimize the prevascularization process and approaches to maximize the survival and functionality of the engineered vessels must be seeked. Novel insights into the regulatory mechanism of angiogenesis, vasculogenesis and network formation as well as further progress in the fields of computational modeling, biomaterial research and microsurgery will undoubtly contribute to the success of prevascularization of engineered tissues in the future.

2 RESULTS

2.1 BIOENGINEERING DERMO-EPIDERMAL SKIN GRAFTS WITH BLOOD AND LYMPHATIC CAPILLARIES

Daniela Marino[1,#], Joachim Luginbühl[1,#], Simonetta Scola[1], Martin Meuli[2], and Ernst Reichmann[1,*]

[1]Tissue Biology Research Unit, Department of Surgery, University Children's Hospital Zurich, August Forel-Strasse 7, 8008, Zurich, Switzerland
[2]Department of Surgery, University Children's Hospital, Steinwiesstrasse 75, 8032 Zurich, Switzerland

# Authors contributed equally to this work
*Corresponding author. Email: ernst.reichmann@kispi.uzh.ch

One sentence summary: Human lymphatic capillaries were engineered in a 3-D hydrogel system to improve dermo-epidermal skin grafting.

RESEARCH ARTICLE

BIOENGINEERING

Bioengineering Dermo-Epidermal Skin Grafts with Blood and Lymphatic Capillaries

Daniela Marino,[1]* Joachim Luginbühl,[1]* Simonetta Scola,[1] Martin Meuli,[2] Ernst Reichmann[1]†

The first bioengineered, autologous, dermo-epidermal skin grafts are presently undergoing clinical trials; hence, it is reasonable to envisage the next clinical step at the forefront of plastic and burn surgery, which is the generation of autologous skin grafts that contain vascular plexuses, preformed in vitro. As the importance of the blood, and particularly the lymphatic vascular system, is increasingly recognized, it is attractive to engineer both human blood and lymphatic vessels in one tissue or organ graft. We show here that functional lymphatic capillaries can be generated using three-dimensional hydrogels. Like normal lymphatics, these capillaries branch, form lumen, and take up fluid in vitro and in vivo after transplantation onto immunocompromised rodents. Formation of lymphatic capillaries could be modulated by both lymphangiogenic and anti-lymphangiogenic stimuli, demonstrating the potential usefulness of this system for in vitro testing. Blood and lymphatic endothelial cells never intermixed during vessel development, nor did blood and lymphatic capillaries anastomose under the described circumstances. After transplantation of the engineered grafts, the human lymphatic capillaries anastomosed to the nude rat's lymphatic plexus and supported fluid drainage. Successful preclinical results suggest that these skin grafts could be applied on patients suffering from severe skin defects.

INTRODUCTION

The critical importance of the lymphatic system in the human body becomes increasingly evident. Consequently, the tissue engineering of lymphatic organs (lymphatic vessels, lymph nodes, spleens, and cells derived from lymphatic organs) not only generates valuable ex vivo research models but also allows the transplantation of these organs to repair or improve lymphatic deficiencies caused by disease or injury (*1*).

Our research focuses on the bioengineering of full-thickness skin analogs: dermo-epidermal skin substitutes with physiological, structural, and functional properties (*2*). A central issue of this approach is the in vitro generation of a preexisting network of capillaries (*3*), which significantly supports perfusion of the dermal component, hence, providing rapid and efficient access to oxygen and nutrients, which assures rapid take, proliferation, and differentiation of the skin transplant (*2*). Prevascularized dermo-epidermal skin substitutes were generated using primary human endothelial cells and sophisticated biological matrices (*4*–*7*). So far, however, limited data are available on the bioengineering of functional human lymphatic capillaries or on the integration of a dermal lymphatic network in skin grafts.

In the human dermis, lymphatic vessels play a major role in tissue fluid homeostasis and immune cell trafficking (*8*). Dermal lymphatic capillaries exhibit a wide lumen, anchoring filaments, and no or an incomplete basement membrane, and lack mural cell coverage. These features enable lymphatic capillaries to respond to interstitial liquid pressure by taking up and removing excess tissue fluid (*8*, *9*). After wounding, also the lymphatic endothelium is ruptured; thus, the draining capacity of the lymphatic vessels is compromised. As a consequence, accumulation of tissue fluid, that is, lymphedema, seroma, or lymphoceles (*10*–*12*), arises. Persistent local interstitial fluid, as well as delayed removal of local debris and inflammatory cells, impedes wound healing. In contrast, induction of lymphangiogenesis and immune cell recruitment were shown to accelerate skin regeneration (*13*). Therefore, to achieve a physiologically relevant dermal tissue complexity, and accelerate skin tissue regeneration after graft transplantation, a skin graft containing both blood and lymphatic vessels would ideally serve to efficiently reconstitute a full-thickness skin defect.

This study demonstrates the in vitro bioengineering and in vivo grafting of a human dermo-epidermal skin substitute prevascularized by both lymphatic and blood capillaries. Both the pure population of human lymphatic endothelial cells (hLECs; isolated from human foreskin) and the hLEC fraction present in human dermal microvascular endothelial cells (HDMECs; isolated from human foreskin) developed into lumen-forming bona fide lymphatic capillaries in vitro within 21 days in either fibrin or collagen type I hydrogels. We confirmed the lymphatic nature of the engineered microvessels by showing that they presented anchoring filaments, expressed all major lymphatic markers, and could be modulated by both lymphangiogenic and anti-lymphangiogenic stimuli.

Lymphatic functionality was confirmed by demonstrating that the bioengineered lymphatic microvessels took up fluid from the interstitial space in vitro and triggered fluid drainage in vivo. Grafting studies in vivo revealed that the engineered lymphatic microvessels maintained their lumens as well as their typical characteristics, such as the absence of a complete basement membrane and the lack of mural cell coverage. We found that bioengineered human lymphatics anastomosed to the recipient's lymphatics as early as 14 days after transplantation. When transplanted onto immunoincompetent rats, the prevascularized dermis supported the development of the epidermis, indicating that it may, in the future, be possible to translate these prevascularized dermo-epidermal substitutes into clinical application.

RESULTS

Bioengineering of human lumen-forming lymphatic capillaries in three-dimensional hydrogels in vitro

The identification of markers specific for the lymphatic vascular lineage has made it possible to isolate hLECs at high purity from human dermis

[1]Tissue Biology Research Unit, Department of Surgery, University Children's Hospital Zurich, August Forel-Strasse 7, 8008 Zurich, Switzerland. [2]Department of Surgery, University Children's Hospital, Steinwiesstrasse 75, 8032 Zurich, Switzerland.
*These authors contributed equally to this work.
†Corresponding author. Email: ernst.reichmann@kispi.uzh.ch

by either fluorescence-activated cell sorting (FACS) or magnetic-activated cell sorting (*14*). Prox1, a marker of human lymphatic vessels (*15*, *16*), was homogeneously expressed by hLECs in conventional cell culture (Fig. 1A). Confluent hLEC monolayers assembled into cord-like structures when overlaid with collagen type I gels for up to 20 hours in vitro (Fig. 1B). These cords, often referred to as tube-like structures in a tube formation assay, are somehow reminiscent of the morphology of microvessels. However, under these in vitro circumstances, lumen formation did not occur (Fig. 1B).

Using a method that we had established previously for HDMECs (*7*), we investigated whether hLECs would similarly arrange into lumen-forming true capillaries in both fibrin and type I collagen hydrogel; indeed, hLECs developed into branching capillaries (Fig. 1, C, D, and F), as revealed by staining for CD31—a pan-endothelial cell marker—3 weeks after coculture with 40% human dermal fibroblasts. Notably, capillary formation did not occur in the absence of fibroblasts (Fig. 1, E and F). Likewise, neither fibroblast-conditioned medium, the addition of vascular endothelial growth factor–A (VEGF-A) or VEGF-C, nor the presence of fibroblasts on the underside of a Transwell system induced capillary formation in hLECs (Fig. 1F). Hence, the physical contact between human dermal fibroblasts and LECs was a requisite for the development of true branching lymphatic capillaries in the hydrogel. Histology revealed that the engineered capillaries developed a continuous lumen of physiological size (17 to 60 μm) (Fig. 1G), with an average lumen diameter of 28 + 10.67 μm (+SEM, 25 lymphatic vessels analyzed per five hydrogels) measured on whole-mount specimens.

The lymphatic nature of the capillaries was confirmed by double immunofluorescence staining performed on whole-mount hydrogel preparations. The bioengineered lymphatic capillaries expressed CD31 (Fig. 2A) and the lymphatic-specific nuclear transcription factor Prox1 (Fig. 2, A to D). Most of the capillaries showed a physiological size (10 μm in diameter) (*17*) of the nuclei (Fig. 2B). Two other lymphatic vascular markers, Lyve-1 (Fig. 2C) and podoplanin (Fig. 2D), confirmed the lymphatic nature of the bioengineered human capillaries.

Modulation of capillary formation by pro- and anti-lymphangiogenic stimuli in vitro

To investigate whether lymphatic vessel formation in vitro is modulated by known lymphangiogenic and anti-lymphangiogenic stimuli,

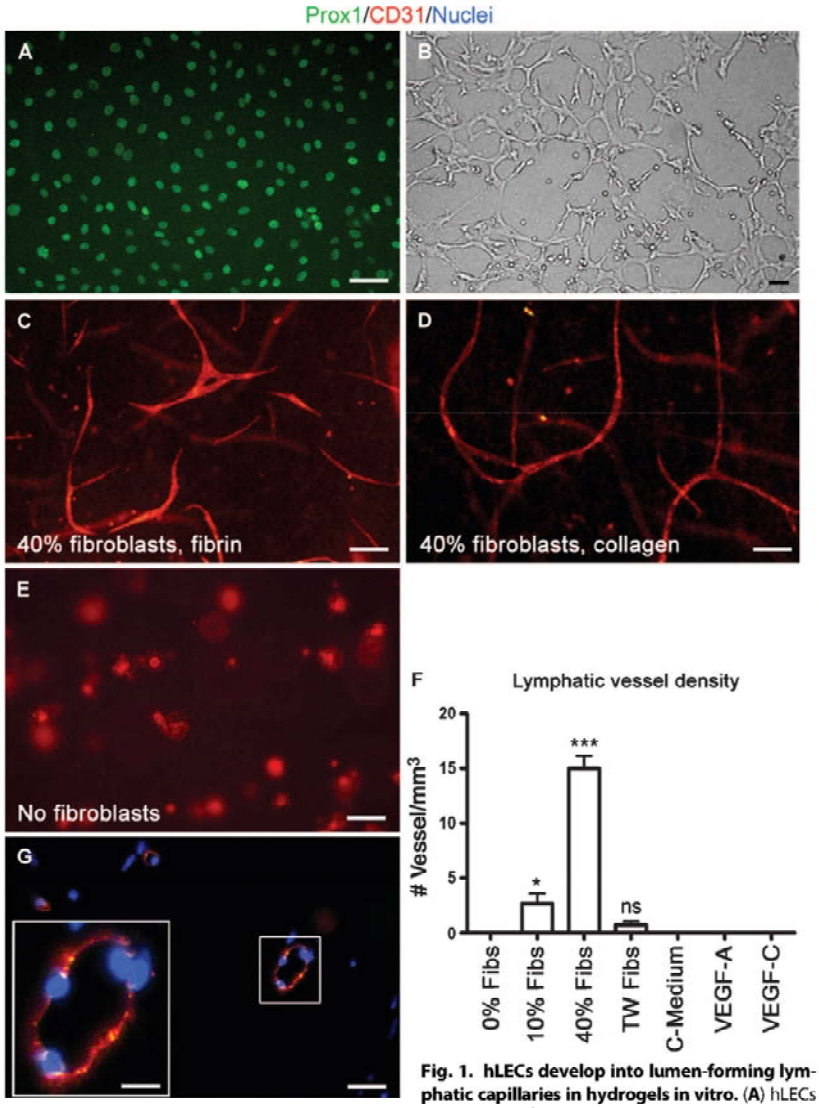

Fig. 1. hLECs develop into lumen-forming lymphatic capillaries in hydrogels in vitro. (**A**) hLECs express Prox1$^+$ (green). Scale bar, 50 μm. (**B**) hLECs assemble into cords in a 2D tube formation assay. Scale bar, 25 μm. (**C** to **E**) Whole-mount CD31 immunofluorescence analysis reveals that hLECs develop into capillaries when cocultured with human fibroblasts in either fibrin (C) or collagen (D) hydrogels, but not in the absence of human fibroblasts (E). Scale bars, 50 μm. (**F**) hLECs cultured in fibrin with 0 to 40% fibroblasts (Fibs), fibroblasts in a Transwell system (TW), human dermal fibroblasts–conditioned medium (C-Medium), VEGF-A, or VEGF-C. Data are means ± SEM ($n = 6$ hydrogels per group). *$P < 0.05$, ***$P < 0.001$, versus 0% fibroblasts using t test. ns, not significant. (**G**) Immunofluorescence analysis for CD31 (red) on paraffin sections shows lumen formation in lymphatic capillaries. Cell nuclei stained with 4′,6-diamidino-2-phenylindole (DAPI) (blue). Images are representative of $n = 18$ hydrogels. Scale bar, 10 μm (inset, 50 μm).

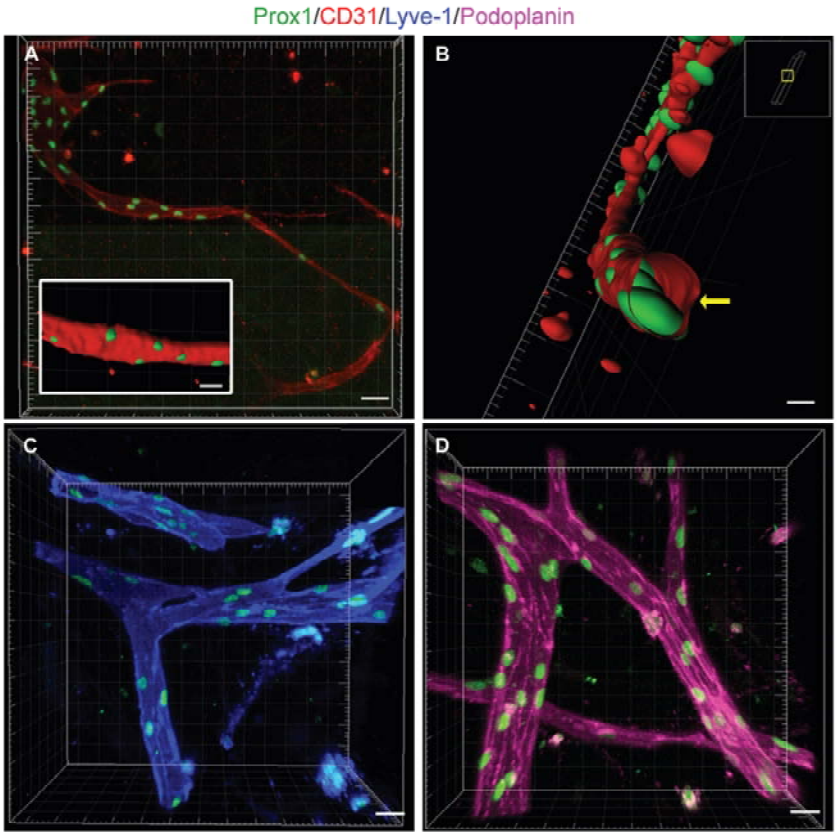

Fig. 2. In vitro bioengineered human lymphatic capillaries express lymphatic lineage-specific markers. (**A**) Whole-mount immunofluorescence analysis for CD31 (red) and Prox1 (green) confirms the lymphatic nature of the capillaries engineered in hLEC coculture with human dermal fibroblasts in fibrin hydrogels for 3 weeks in vitro. Scale bar, 50 μm (inset, 20 μm; digital surfacing caption). (**B**) The lymphatic capillary shown in (A) reveals the physiological distribution and size of Prox1$^+$ nuclei and the formation of a lumen (yellow arrow). Digital surfacing caption. Inset defines the spatial orientation of the snapshot. Scale bar, 3 μm. (**C** and **D**) Prox1$^+$ (green) lymphatic capillaries express both Lyve-1 (C, blue) and podoplanin (D, purple). Scale bars, 20 μm. Images are representative of $n = 12$ hydrogels. All images are confocal Z-stack captions; grids define the 3D space.

we investigated the effect of pro-lymphangiogenic VEGF-A and VEGF-C, as well as the effect of anti-lymphangiogenic transforming growth factor–β1 (TGF-β1) and the tyrosine kinase inhibitor SU5416 (*18*). Both VEGF-A and VEGF-C significantly promoted the formation of lymphatic capillaries in vitro compared to the factor-free control medium (Fig. 3, A to C and F). In contrast, exposure to SU5416 led to a significant inhibition of vessel formation (Fig. 3, D and F). Likewise, treatment with TGF-β1 significantly inhibited the formation of lymphatic microvessels (Fig. 3, E and F). Further analysis showed that hLECs tended to assemble into a slightly higher number of capillaries in type I collagen hydrogels compared to fibrin hydrogels in the presence or absence of VEGF-C (Fig. 3F). However, differences were not statistically significant.

Isolation of single-cell suspension from lymph-vascularized hydrogels

Studies on lymphatic vessel formation might necessitate specific molecular analysis at a cellular level to narrow down molecular pathways involved in lymphangiogenesis. Hence, we next investigated the possibility of retrieving single human cells from the lymph-vascularized hydrogels for further studies (Fig. 4A). Three weeks after in vitro culture, hLECs had assembled into CD31$^+$/Prox1$^+$ lymphatic capillaries as in Fig. 1D. At this stage, type I collagen hydrogels were digested using collagenase type II, and single cells were isolated and FACS-sorted into CD31$^+$/CD90$^-$ hLECs and CD31$^-$/CD90$^+$ fibroblasts (Fig. 4, B and C). After sorting, the individual populations of hydrogel-derived hLECs and fibroblasts were used to develop new lymph-vascularized hydrogels. The isolation/sorting procedure neither impaired the formation of the capillaries nor affected their lymphatic nature, as confirmed by whole-mount immunofluorescence staining for CD31 and Prox1 (Fig. 4, D and E).

Bioengineering a composite blood/lymphatic vascular plexus

On the basis of our ability to bioengineer blood capillaries and lymphatic capillaries in vitro, we focused on the generation of a complete dermal vascular plexus for skin grafting. This was achieved by coculturing HDMECs, isolated from human foreskin, in three-dimensional (3D) fibrin hydrogels. HDMECs consist of a mixture of both hLECs and human blood vascular endothelial cells (hBECs), as confirmed by a staining for Prox1 (Prox1$^+$ hLECs and Prox1$^-$ hBECs) (Fig. 5A). Coculture of HDMECs and human dermal fibroblasts in fibrin hydrogels for 3 weeks resulted in the formation of branching, lumenized capillaries (Fig. 5, B and C). Both Prox1$^+$/CD31$^+$ lymphatic capillaries and Prox1$^-$/CD31$^+$ blood capillaries were present in these hydrogels (Fig. 5D). In addition to Prox1, the two types of capillaries could also be discriminated using Lyve-1 (Fig. 5E). The two distinct types of microvessels were never found to anastomose in vitro; that is, they never formed hybrid blood-lymph capillaries. Similar to the hLEC cultures, HDMECs developed into lumen-forming capillaries in both fibrin (Fig. 5D) and collagen type I hydrogels (Fig. 5F).

To further investigate the functionality of the bioengineered lymphatic vessels, we determined whether the capillaries would react to interstitial pressure variations and resolve tissue fluid accumulation. Evans blue dye (20 to 80 μl) was injected into prevascularized hydrogels (Fig. 5G). After injection, CD31$^+$ and Lyve-1$^+$ lymphatic capillaries

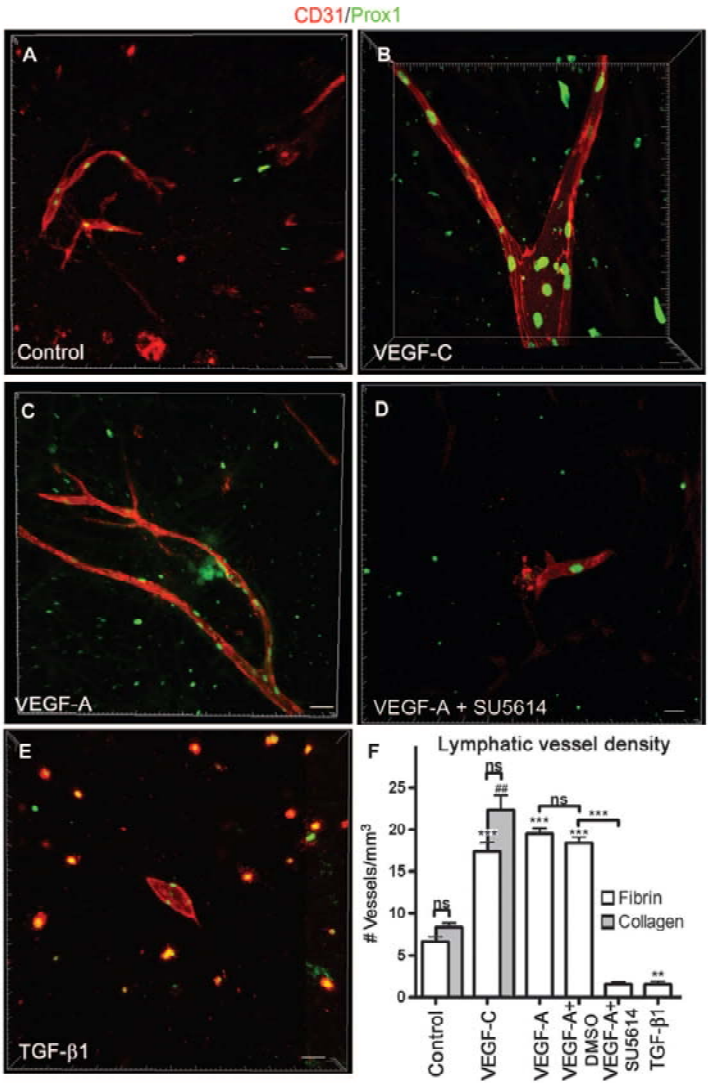

Fig. 3. In vitro bioengineered human lymphatic capillaries respond to lymphangiogenic and anti-lymphangiogenic stimuli. (**A**) Confocal microscopy of whole-mount immunofluorescence stainings for Prox1 (green) and CD31 (red) shows that hLECs, cultured in control medium, form capillaries in the fibrin hydrogels in vitro. Scale bar, 50 μm. (**B** and **C**) Exposure to VEGF-C (B) or VEGF-A (C) increases the density of branching lymphatic capillaries. (**D** and **E**) Exposure to SU5614 or TGF-β1 inhibits the formation of human lymphatic microvessels. Scale bars, 50 μm (C and E) and 20 μm (B and D). (**F**) The density of the lymphatic capillaries was quantified. Data are means ± SEM ($n = 6$ hydrogels per group). $^{**}P < 0.01$, $^{***}P < 0.001$ versus control fibrin hydrogels, unless otherwise indicated; $^{\#\#}P < 0.001$ versus control collagen hydrogels, *t* test. All *P* values were calculated against the respective control, unless otherwise specified. All images are displayed as Z-stack confocal captions; grid defines the 3D space.

were found to take up the dye from the extracellular space (Fig. 5H). Figure 5G shows that the area surrounding the lymphatic vessels was cleared from the dye after 20 minutes. These results show that the engineering of a dermal vascular plexus containing both blood and lymphatic capillaries is achievable and that the lymphatic capillaries exhibit their specific function, which is the uptake and removal of tissue liquid.

Human blood and lymphatic vascular plexus in bioengineered dermo-epidermal skin substitutes and in vivo grafting

Toward translation, we next monitored the transplantation of human dermo-epidermal skin grafts containing a composite vascular (blood and lymph) plexus onto rats. First, skin grafts were created in vitro using $CD31^+$ HDMECs, human $CD90^+$ fibroblasts, and human $keratin5^+$ ($K5^+$) keratinocytes in fibrin hydrogels. Figure 6A shows a confocal micrograph of a capillary (red) surrounded by fibroblasts (blue) in a fibrin hydrogel. Both cell types constituting the dermal compartment of the graft were arranged underneath several layers of keratinocytes (green), the epidermal compartment. These skin grafts were then transplanted onto wounded backs of immunoincompetent *nu/nu* rats using a Fusenig chamber to avoid competitive, lateral ingrowth/overgrowth of rat keratinocytes (Fig. 6B). The circular patch of the thin human epidermis was macroscopically visible. Two weeks after transplantation, the human skin substitute was surgically removed from the rat underlying tissue and analyzed for dermal structure and neovascularization. The vascularized neodermis supported stratification of the overlaying epidermis (Fig. 6C).

Immunofluorescence analysis after 2 weeks revealed the presence of both human blood and lymphatic microvessels in the neodermis (Fig. 6, D to H). Most of the bioengineered $Prox1^+/CD31^+$ lymphatic microvessels maintained their lumen in vivo (Fig. 6D, asterisks). Human microvessels expressing Lyve-1 and podoplanin were detected, indicating that human lymphatic capillaries remained intact 2 weeks after transplantation (Fig. 6E, arrow, and F to H). Blood microvessels that solely expressed CD31 were also detected (Fig. 6E, arrowhead). Notably, the two distinct types of microvessels were never found to anastomose. $Podoplanin^+$ lymphatic capillaries did not stain for laminin1,2 (Fig. 6F, arrow) but partially stained for collagen IV (Fig. 6G, arrows). Our analyses of mural cell (vascular smooth muscle cells and pericytes) coverage confirmed that the bioengineered human lymphatic capillaries were devoid of α-smooth muscle actin (αSMA)–expressing cells (Fig. 6H, arrows).

Further analysis of the capillary revealed that $podoplanin^+$ human lymphatic microvessels presented $fibrillin^+$ anchoring filaments (Fig. 6I, arrows). The presence of anchoring filaments strongly suggests that the capillaries could react to interstitial pressure variations and resolve tissue fluid accumulation in vivo. The presence of anchoring filaments and no or discontinuous basement membrane as well as the absence of mural cell coverage are major characteristics of lymphatic microvessels (*8*).

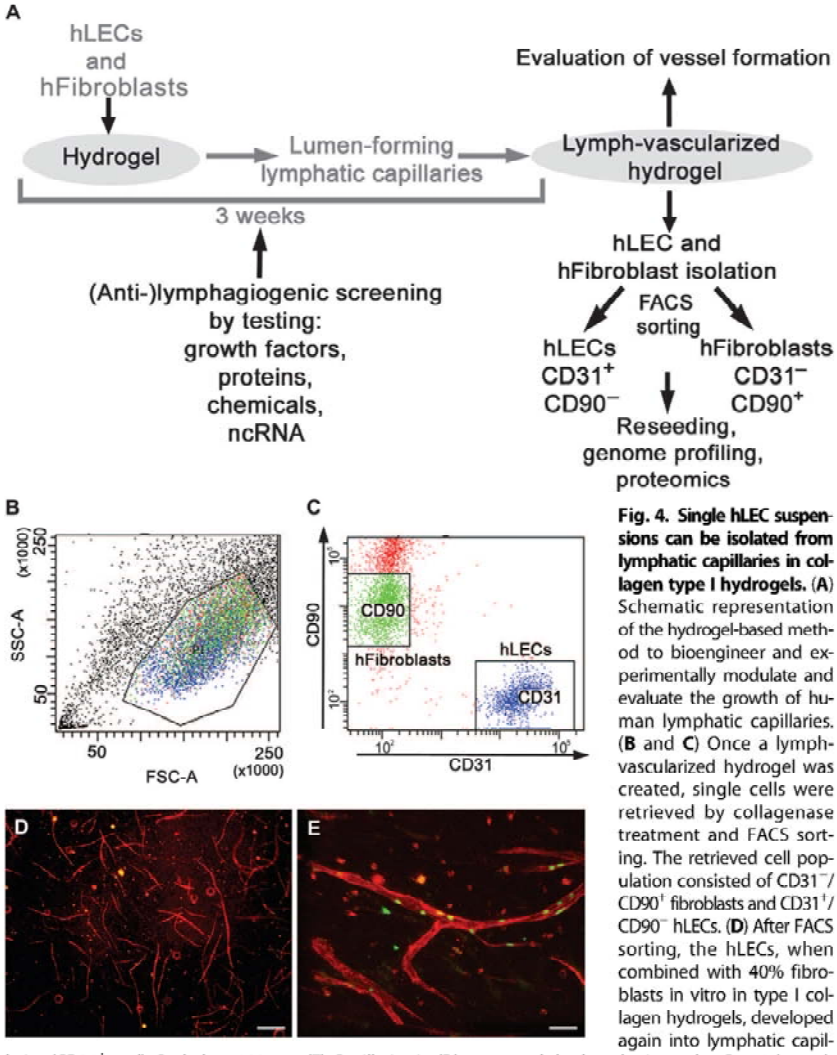

Fig. 4. Single hLEC suspensions can be isolated from lymphatic capillaries in collagen type I hydrogels. (**A**) Schematic representation of the hydrogel-based method to bioengineer and experimentally modulate and evaluate the growth of human lymphatic capillaries. (**B** and **C**) Once a lymph-vascularized hydrogel was created, single cells were retrieved by collagenase treatment and FACS sorting. The retrieved cell population consisted of $CD31^-$/$CD90^+$ fibroblasts and $CD31^+$/$CD90^-$ hLECs. (**D**) After FACS sorting, the hLECs, when combined with 40% fibroblasts in vitro in type I collagen hydrogels, developed again into lymphatic capillaries ($CD31^+$, red). Scale bar, 100 μm. (**E**) Capillaries in (D) expressed the lymphatic marker Prox1 (green). Scale bar, 40 μm. Images are representative of $n = 12$ hydrogels.

Anastomosis of bioengineered human lymphatic capillaries and in vivo functionality

Bioengineered blood vessels have been shown to connect to the host blood vasculature after in vivo grafting (*19*). We set out to investigate whether bioengineered lymphatic capillaries would also anastomose to the lymphatic vascular plexus of immunoincompetent recipient rats. The hydrogels were grafted to the wounded backs of *nu/nu* rats as in Fig. 6B. Immunofluorescence analyses of the expression of human- and rat-specific podoplanin showed that the human lymphatic capillaries, present in the bioengineered human dermis, connected to the host rat lymphatic vessels (3.5 + 2.6 SD anastomoses within a 0.5-mm stretch of bioengineered skin, total $n = 8$ animals) as early as 14 days after grafting (Fig. 7, A and B).

Hybrid anastomosis between human lymphatic capillaries and rat blood capillaries was never observed. We found two types of anastomoses among human and rat lymphatics: a direct connection type (Fig. 7A, arrow in inset) and a wrapping connection type (Fig. 7B, arrowheads in inset). The direct connection appeared to occur by linking of the blunt ends of a human and a rat lymphatic capillary. In the wrapping connection, the human and rat LECs wrapped around each other to form a hybrid vessel (Fig. 7B). Notably, rat lymphatics were found in close proximity to human lymphatic microvessels rather than randomly throughout the tissue (Fig. 7B).

To investigate whether the bioengineered lymphatic capillaries would be functional in vivo, we performed lymphatic drainage experiments by injecting small amounts (25 μl) of Evans blue into grafts 15 days after transplantation. When analyzing the grafts 30 minutes after injection, about five fold more Evans blue was retained in the hydrogels containing human fibroblasts only (Fig. 7C) compared with hydrogels containing human lymphatic and blood capillaries (Fig. 7, D and E), indicating lymphatic drainage function in the prevascularized grafts. These data suggest that the grafted human lymphatics were recognized by and anastomosed to the recipient's lymphatics and that the newly developed lymphatic plexus efficiently drained fluid in vivo.

DISCUSSION

Although structurally distinct, the blood and lymphatic vascular systems are functionally closely interconnected to ensure fluid and protein balance, cell nutrition, and immunologic functioning in tissues. The main function of the lymphatic system is the absorption of fluid and proteins that escaped from the blood circulation, hence, returning them back into the bloodstream. Impairment of lymphatic function leads to a number of diseases that are characterized by edema, seroma, lymphoceles, impaired immunity, and fibrosis (*8*). As the critical importance of the lymphatic system in the human body becomes more evident, tissue engineers are getting increasingly motivated to generate both blood and lymphatic vessels, side by side in bioengineered tissue and organ grafts (*20*).

Skin grafting is applied to treat defects caused by accident, such as burns, or in elective cases, such as scar revisions and removal of congenital nevi, or to treat chronic ulcers. Skin grafts may fail because of the development of infections, insufficient vascularization, hematoma,

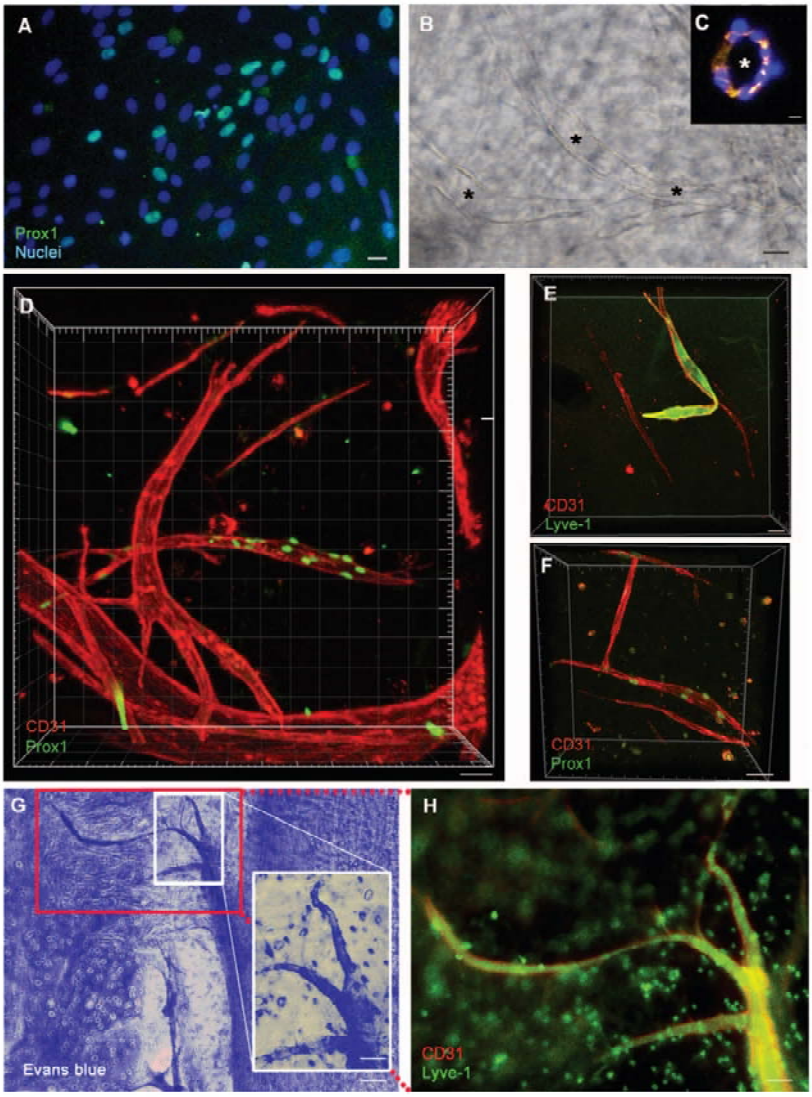

Fig. 5. HDMECs develop into blood capillaries as well as into functional lymphatic capillaries in fibrin hydrogels in vitro. (**A**) Immunofluorescence staining for the lymphatic marker Prox1 confirms that HDMECs isolated from human foreskin contain both Prox1$^+$ lymphatic (teal) and Prox1$^-$ blood vascular endothelial cells (blue only, for DAPI-stained nuclei). Scale bar, 25 μm. (**B** and **C**) Culture of HDMECs for 3 weeks in fibrin hydrogels resulted in the development of capillaries that presented a lumen (marked by asterisks). (B) Light microscopy of the hydrogel. (C) Immunofluorescence staining for CD31 [red cell nuclei (blue) of a paraffin-embedded hydrogel cross-section]. Scale bars, 10 μm (B and C). (**D**) Both Prox1$^+$/CD31$^+$ lymphatic and Prox1$^-$/CD31$^+$ blood capillaries were present in the 3D fibrin cultures. (**E**) Only the human lymphatic capillaries expressed the lymphatic marker Lyve-1 in the hydrogel. (**F**) HDMECs developed into both lymphatic and blood capillaries also in collagen type I hydrogels. Scale bars, 50 μm (D to F). (**G** and **H**) Evans blue dye injection into prevascularized fibrin hydrogels ($n = 6$) revealed that bioengineered human lymphatic capillaries take up fluid from the interstitial space (G). The same lymphatic vessel in (G) stains for CD31 and Lyve-1 (H). Scale bars, 50 μm [(G); inset, 20 μm] and 25 μm (H).

or seroma. Seromas occur by the accumulation of serous fluid underneath the graft because of the lack of sufficient drainage by the lymphatic system (*21*, *22*). Bioengineering a preformed network of lymphatic capillaries into dermo-epidermal skin grafts should help circumvent seroma formation by improving lymphatic drainage and accelerating the establishment of tissue fluid homeostasis.

In contrast to the large body of work done on the generation of blood vessels, only few studies have focused on engineering human lymphatic vasculature (*23*, *24*), including using a constant interstitial flow exerted by a bioreactor (*25*–*27*). The use of bioreactors is technically demanding, and, although it certainly represents a valid in vitro test system, no data are yet available on such engineered capillaries in vivo. A second pilot approach to tissue-engineered lymphatics indicated that hLECs could serve as seed cells to be combined with poly(glycolic acid) scaffolds (*28*). The developed tissue-engineered tubular structures showed very preliminary characteristics of a lymphangion (3-mm diameter); however, lymphatic capillaries, 10 to 60 μm in diameter (*29*), are required to constitute a functional, liquid-collecting, lymphatic plexus. The bioengineered lymphatic capillaries described herein showed exactly this range in diameter.

Our goal was to develop permanent, autologous dermo-epidermal skin grafts for clinical use. There are bioengineered grafts containing autologous keratinocytes and fibroblasts that are close to the clinical application, yet they are still not prevascularized (*30*–*36*). Here, we show that it is possible to even go beyond this approach by undertaking the bioengineering of prevascularized skin grafts that contain a blood and a lymphatic plexus in the dermal compartment. Successful bioengineering of lumen-forming lymphatic capillaries is owed to the coculture of fibroblasts with the endothelium because hLECs alone did not develop into lymphatic capillaries. Fibroblasts are known to rapidly migrate into wound sites to establish an extracellular matrix that supports dermal vascular repair. Thus, we speculate that, in our system, fibroblasts supported the formation of microvessels by creating a physiological environment by matrix remodeling and by production and deposition of nonsoluble factors; however,

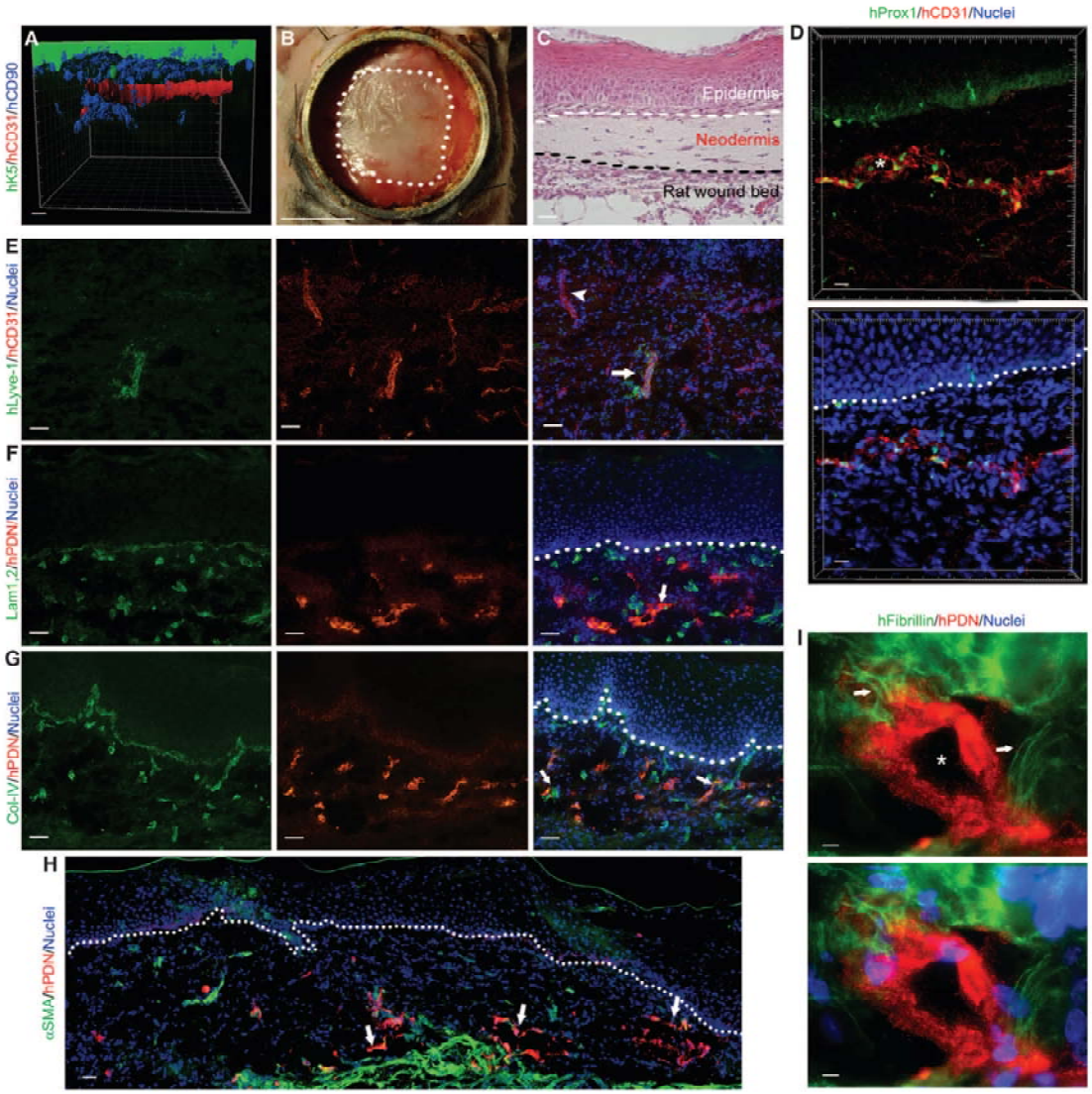

Fig. 6. Blood and lymphatic capillaries are stably maintained in bioengineered human dermo-epidermal skin grafts. Grafts were transplanted onto six rats. (**A**) Hydrogel-based prevascularized dermo-epidermal skin grafts were generated using $CD31^+$ HDMECs that form capillaries, $CD90^+$ human dermal fibroblasts, and human $K5^+$ keratinocytes (Z-stack confocal caption; digital surfacing; grid defines the 3D space). Scale bar, 50 μm. (**B**) The grafts were transplanted onto the backs of immunoincompetent *nu/nu* rats using a graft-protecting chamber. The dimensions of the bioengineered human skin are outlined in white. Scale bar, 1 cm. (**C**) After 2 weeks, hematoxylin and eosin staining revealed the presence of a stratified epidermis and a vascularized neodermis. Scale bar, 50 μm. (**D**) Immunofluorescence analysis of the transplants for human CD31 and Prox1 reveals the presence of a typical lymphatic capillary in the dermis. Asterisk denotes lumen. Cell nuclei were stained with DAPI, shown in bottom image (blue). Scale bars, 25 μm. (**E**) In contrast to the blood capillaries (expressing CD31 only, arrowhead), the lymphatic vessels expressed both human Lyve-1 and CD31 (costaining indicated by arrow). A vessel that expressed CD31 only is denoted by an arrowhead. (**F**) Expression of laminin (Lam1,2) was not detected on human podoplanin$^+$ ($hPDN^+$) lymphatic vessels (arrow). (**G**) The presence of an incomplete basement membrane on the $hPDN^+$ lymphatic capillaries was revealed by staining for collagen type IV (Col-IV, arrows). Scale bars, 100 μm (E to G). (**H**) αSMA-expressing mural cells were not found around the $hPDN^+$ lymphatic capillaries (arrows). Cell nuclei are stained with DAPI (blue). Dashed line indicates the dermo-epidermal junction. Scale bar, 50 μm. (**I**) Immunofluorescence analysis for human fibrillin shows the presence of anchoring filaments (arrows) on the $hPDN^+$ lymphatic capillaries. Asterisks indicate lumen. Scale bar, 10 μm.

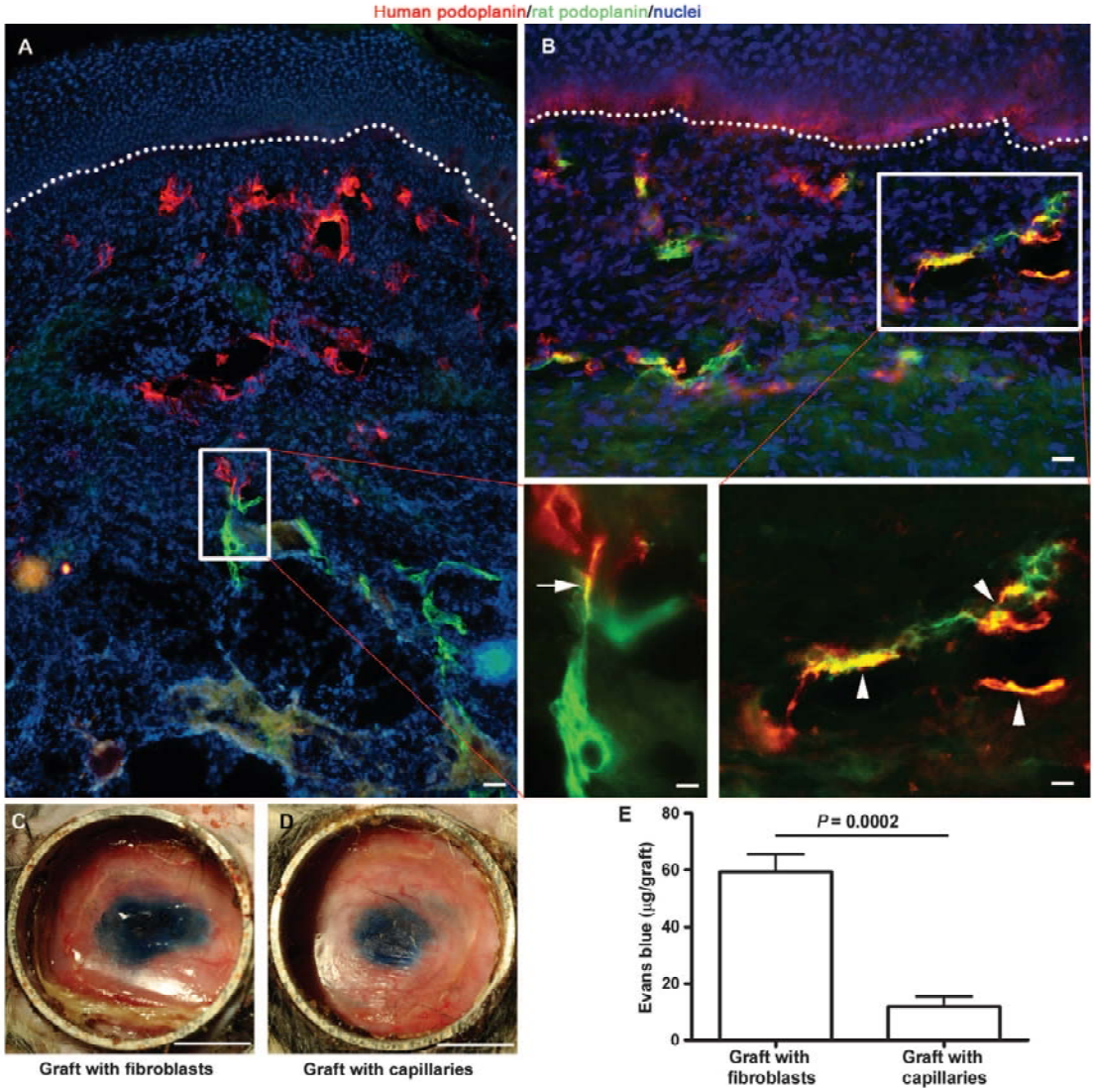

Fig. 7. Bioengineered human lymphatic capillaries anastomose to the recipient animal's lymphatic vasculature and drain fluid. Hydrogel-based, prevascularized dermo-epidermal skin grafts were transplanted onto the backs of immunoincompetent rats as in Fig. 6B. (**A** and **B**) As early as 14 days after transplantation, anastomosis occurred either as a "direct connection" [arrow in inset of (A)] or as a "wrapping connection" [arrowheads in inset of (B)]. Dashed lines indicate the dermo-epidermal junction. Nuclei are stained with DAPI (blue). Confocal images are representative of $n = 6$ animals. Scale bars, 100 μm (A) (magnified view, 35 μm) and 50 μm (B) (magnified view, 25 μm). (**C** to **E**) Fifteen days after transplantation, Evans blue dye was intradermally injected into grafts of four animals containing either only fibroblasts (C) or bioengineered human capillaries (D) and imaged and quantified (E) after 30 minutes. *P* value was determined by Student's *t* test. Scale bars, 1 cm (C and D).

this has not been demonstrated yet. This dermal environment modulation by fibroblasts might explain why, in our 3D hydrogel system, capillary formation occurred in both fibrin and collagen type I hydrogels.

The lymphatic nature of the generated capillaries was confirmed by the expression of lineage-specific markers, as well as by morphology and function. Expression of Prox1—the most specific marker for lymphatic endothelium (*15*, *16*)—Lyve-1, and podoplanin was detected in vitro and in vivo (*37*). The presence of fibrillin-containing anchoring filaments was detected on the human lymphatics, suggesting that the bioengineered capillaries might react to interstitial pressure variations in vivo. Finally, Evans blue dye uptake and drainage assay preliminarily confirmed that the bioengineered lymphatic capillaries were functional in vitro and in vivo, respectively. The lymphangiogenic factors VEGF-C and VEGF-A increased the lymphatic vessel density, whereas

the addition of the lymphangiogenesis inhibitors TGF-β1 and SU5614 resulted in decreased capillary formation. These modulatory induction/inhibition data, in addition to the possibility to retrieve the single cells from the hydrogels after vessel formation had occurred, qualify the 3D hydrogel system as a valuable in vitro model system and screening tool, well suited to identify signaling pathways, chemicals, and compounds involved in, or interfering with, human lymphatic vessel formation. In contrast to our system, most standard human lymphangiogenesis in vitro assays (*38*), such as the tube formation (*39*) or spheroid assays (*40*), are based on the evaluation of simple cord-like structures that only vaguely resemble the real morphology of bona fide lumen-forming human lymphatic capillaries.

When seeded in hydrogels, HDMECs, which consist of a mixture of hBECs and hLECs, spontaneously generated both a blood and a lymphatic vascular network, developing separately, yet adjacently in the same extracellular matrix. Although anastomoses between the two types of human vessels were never observed (*8*), the bioengineered human lymphatic capillaries were found to anastomose to the recipient rat's lymphatic plexus as early as 14 days after in vivo grafting. Human/rat lymphatic anastomosis occurred in either a direct connection or a wrapping connection manner. The "wrapping" anastomosis has been already described for blood vessels: The process includes matrix remodeling, pericyte removal, formation of a double-layered endothelium, and final maturation (*41*). Because the bioengineered lymphatic capillaries exhibited an incomplete basement membrane and no mural cell coverage, and because our immunofluorescence analyses revealed an overlapping of human/rat signals on microvessels, we suggest that the anastomosis of lymphatic microvessels by the wrapping mechanism could be brought about by the generation of a double-layered endothelium before maturation.

Clearly, the effects of the incorporation of a lymphatic plexus into a dermo-epidermal graft on its regeneration after transplantation will have to be further investigated. To satisfy regulatory and safety aspects of translation, leading to approval of this advanced technology for clinical use, these grafts will need to be preclinically tested on an immunocompetent animal model, such as the pig, to investigate on safety, toxicology, and efficacy.

With respect to skin, it is possible to generate complex human skin grafts, encompassing a dermal and an epidermal equivalent (*31*), a melanocyte compartment (*42*), and a plexus of blood and lymphatic capillaries (this study), whereas sweat glands, hair follicles, and neuronal innervation (*43*) have not yet been realized. Now, our study proposes a straightforward approach to engineer fully functional bona fide human lymphatic capillaries in hydrogel-based grafts, thus contributing to this broad spectrum of new possibilities in skin tissue engineering.

MATERIALS AND METHODS

Study design

The objective of this project was to engineer prevascularized dermo-epidermal human skin grafts containing human blood and lymphatic capillaries. First, hLECs were cocultured with human dermal fibroblasts within 3D hydrogels to investigate the capacity of LECs to develop into lumen-forming bona fide lymphatic capillaries. HDMECs—rather than LECs—were then used to engineer prevascularized dermo-epidermal skin substitutes. HDMECs were chosen because they are a mixture of dermal blood and LECs; hence, these cells have the potential to give rise to both types of capillaries. Prevascularized skin grafts were engineered using either collagen type I or fibrin hydrogels, demonstrating that, principally, both types of biomatrices can be successfully used. However, we mainly used fibrin hydrogels because those present higher mechanical stability than collagen hydrogels. Collagen hydrogels were used for the cell reisolation experiments because they are more easily digested than fibrin hydrogels. The morphology and functionality of the lymphatic microvessels were characterized and analyzed both in vitro and in vivo with immunofluorescence, FACS, histology, and Evans blue dye injection.

Statisticians at the University of Zurich were consulted regarding sample size. Briefly, sample size calculations were performed with a confidence level of 95% and a statistical power of 70 to 80%. In vitro, the experimental end point was chosen at 21 days, when most of the engineered capillaries had formed a lumen. In vivo, the experimental end point was 15 days, when epidermal stratification was completed and a basal lamina was deposited. Physical damage of the hydrogels or premature death of the animals resulted in the exclusion from the study. No outlier was encountered in the quantitative analyses. Animals or hydrogels were always assigned randomly to the experimental groups. The experiments were not blinded, with the exception of experiments evaluating the response of the engineered capillaries to anti-lymphangiogenic stimuli (Fig. 3). Three sample images were analyzed for each sample. All experiments were performed in triplicate.

Culture of hLECs

hLECs were purchased from ScienceCell. Cells were cultured in endothelial basal medium (Cambrex) supplemented with 20% fetal bovine serum (Gibco), L-glutamine (2 mM, Fluka), hydrocortisone (10 μg/ml, Fluka), and *N*-6,2′-odibutyryladenosine-3′,5′-cyclic monophosphate sodium salt (cAMP; 25 μg/ml, Fluka) for up to five passages. Cells were grown in a humidified atmosphere at 37°C and 5% CO_2. For the preparation of hydrogel matrices, cAMP was no longer added to the cultured medium, and endothelial cell supporting supplements (Cambrex) were added.

Isolation and culture of human dermal fibroblasts

Dermal fibroblasts were isolated from human foreskins obtained from the University Children's Hospital of Zurich after routine circumcisions and stored in Dulbecco's modified Eagle's medium supplemented with gentamicin, penicillin-streptomycin, and fungizone (Invitrogen). All patients (n = 6) (and/or their parents) gave their written consent for this study in accordance with the Ethics Commission of the Kanton Zurich (notification no. StV-12=06).

Human foreskin biopsies were digested for 15 to 18 hours at 4°C in dispase (12 U/ml) in Hanks' balanced salt solution containing gentamicin (5 mg/ml). Thereafter, the epidermis and the dermis were mechanically separated. After collagenase treatment of the dermis, a total of 4×10^6 dermal cells per 10-cm dish were grown in Dulbecco's modified Eagle's medium (DMEM) supplemented with 10% fetal calf serum, 4 mM L-alanyl-L-glutamine, 1 mM sodium pyruvate, and gentamicin (5 mg/ml). Collagenase was from Sigma-Aldrich, and all other compounds were from Invitrogen.

Isolation and culture of HDMECs and dermal fibroblasts

HDMECs and human dermal fibroblasts were co-isolated from foreskins (n = 8) obtained from the University Children's Hospital of Zurich after routine circumcisions (Ethics Commission notification no. StV-12=06). Foreskins were processed as described earlier (*7*). Isolated HDMECs

and fibroblasts were cocultured on 0.1% gelatin–coated dishes (Sigma-Aldrich) in endothelial cell growth medium-2 (EBM-2 MV with endothelial supplements; Lonza). Every day, fibroblasts were removed by mechanical scratching. FACS analysis for CD90 (Dianova) and CD31 (DakoCytomation) was used to calculate the number of fibroblasts and HDMEC (their ratio was 1:1 in all experiments). The cells were used at passage 1 in all experiments.

Generation of capillaries in hydrogels

Fibrin or collagen hydrogels were produced with a Transwell system (*7*) consisting of six-well culture inserts with membranes with 3-μm pores (BD Falcon). Briefly, for fibrin hydrogels, fibrinogen from bovine plasma (Sigma-Aldrich) was reconstituted in NaCl to a final concentration of 10 mg/ml, and then 11 μl of thrombin (Sigma-Aldrich, 100 U/ml) was added. For collagen hydrogels, membranes were covered with rat tail collagen type I hydrogels (3.2 to 3.4 mg/ml, BD Biosciences). The collagen matrix was prepared as described (*7*, *44*). To 1 ml of hydrogel solution, either 60,000 hLECs in combination with 40,000 human dermal fibroblasts or 100,000 human dermal cells (HDMECs/fibroblasts, 1:1) were added and transferred into an insert for six-well plates. After clotting at room temperature, the preparations were incubated at 37°C for 35 min in a humidified incubator containing 5% CO_2 to ensure polymerization. At the end of the incubation period, culture medium was added to the upper and lower chambers [endothelial cell growth medium-2 (EBM-2 MV with endothelial supplements; Lonza)], and hydrogels were incubated for up to 3 weeks. Medium was changed every second day.

The role of fibroblasts in lymphatic vessel formation

Fibrin hydrogels were produced as described above and cultured for 3 weeks in vitro. The hydrogels with 0 fibroblasts/100,000 LECs were cultured either in culture medium, in culture medium plus VEGF-A (40 ng/ml, Chemicon), in culture medium plus VEGF-C (100 ng/ml, R&D Systems), or in fibroblast-conditioned culture medium. The hydrogels with 10,000 fibroblasts/90,000 LECs or 40,000 fibroblasts/60,000 LECs were grown in culture medium. For the Transwell assay, 100,000 fibroblasts were seeded on the underside of the Transwell, whereas hydrogels with 100,000 LECs were cultured on top. The migration of a little number of fibroblasts was observed from the underside of the insert through the porous membrane intro the hydrogel. Culture medium was changed every day.

Validation of the lymphatic vessel formation in vitro assay

Hydrogels were prepared as described above. At day 0, VEGF-A (40 ng/ml) (Chemicon), VEGF-C (100 ng/ml) (R&D Systems), TGF-β1 (10 ng/ml) (R&D Systems), 10 μM dimethyl sulfoxide (Sigma), and 1,3-dihydro-3-[(3,5-dimethyl-1*H*-pyrrol-2-yl)methylene]-2*H*-indol-2-one (SU5416, Sigma) were added to the culture medium. The medium was changed every second day. After 3 weeks, gels were fixed in 4% paraformaldehyde (PFA) and processed for whole-mount immunostainings. Control culture medium was composed of endothelial basal medium (Cambrex) supplemented with 20% fetal bovine serum (Gibco), L-glutamine (2 mM, Fluka), and hydrocortisone (10 μg/ml, Fluka).

Isolation of single-cell suspensions from hydrogels containing lymphatic capillaries

At day 21, collagen type I hydrogels were incubated in a solution of collagenase type 2/DMEM (35 U/ml, Worthington Lakewood) for 1 hour at 37°C. After the incubation, single cells were collected by the use of cell strainers (0.40 μm, BD Pharmingen), centrifuged, counted, and prepared for FACS sorting (FACSAria III cell sorter, BD Biosciences). $CD31^+/CD90^-$ hLECs and $CD31^-/CD90^+$ human fibroblasts were sorted. The antibodies used were the following: mouse anti-human prelabeled CD31-phycoerythrin (DakoCytomation, 1:50) and monoclonal mouse anti-human prelabeled CD90–fluorescein isothiocyanate (Dianova, 1:10). Finally, the two cell populations were submerged again in gelifying collagen type I to test for the capability to develop into lymphatic capillaries.

Preparation of prevascularized skin grafts

After 2 weeks of culture, 1 million human keratinocytes, isolated as described (*31*), were seeded on top of the prevascularized fibrin hydrogels. One week thereafter, transplantation or whole-mount immunostaining was performed.

2D tube formation assay

Tube formation assays were performed as previously described (*45*). Briefly, a confluent hLEC monolayer was overlaid with collagen type I hydrogels (1 mg/ml; Cohesion). Tube-like structure formation was evaluated after 20 hours.

Evans blue fluid uptake in vitro assay

A solution of Evans blue (25 mg/ml) (Sigma-Aldrich) was prepared in phosphate-buffered saline (PBS). A total of 20 to 80 μl (focal injections of 20 μl) of this solution was laterally injected into a hydrogel with an insulin syringe (0.30 × 12 mm^2). After 20 min, hydrogels were analyzed under bright light. To remove excess dye, one washing step with PBS/0.3% Triton X overnight at room temperature and constant shaking were performed before the whole-mount immunofluorescence staining.

Grafting bioengineered skin grafts onto immunoincompetent *nu/nu* rats

Animal studies were performed with the approval of the Institutional Animal Care of the University of Zurich following the guidelines of the National Institutes of Health. Immunoincompetent female *nu/nu* rats (Elevage Janvier) (n = 12) were anesthetized by inhalation of 5% isoflurane (Baxter) and narcosis maintained by inhalation of 2.5% isoflurane via mask. Before the operation, buprenorphine (0.5 mg/kg) (Temgesic) for analgesia and retinol cream (Vitamin A "Blache"; Bausch & Lomb) for eye protection were applied. To prevent wound closure from the side and overgrowth of the human transplant by rat tissue, a special polypropylene ring (modified Fusenig chamber), 2.6 cm in diameter, was designed in our laboratory. The rings were sutured to full-thickness skin defects created on the back of the rats with nonabsorbable polyester sutures (Ethibond; Ethicon). Cultured prevascularized dermo-epidermal skin grafts were placed into the polypropylene rings and covered with a silicon foil (Silon-SES; Bio Med Sciences) and polyurethane sponges (Ligasano; Ligamed). Rats were sacrificed at 15 days after surgery. At sacrifice, dressings and sutures were removed, and multiple graft biopsies (n = 12) were collected for different analyses.

In vivo lymphatic drainage assessment with Evans blue dye

Fifteen days after transplantation on the rats, 25 μl of Evans blue dye (10 mg/ml in PBS, Sigma-Aldrich) was injected with a Hamilton syringe into hydrogel-based grafts. Thirty minutes later, pictures of the

grafts were taken. Subsequently, animals were sacrificed, and the Evans blue dye was extracted from the graft by incubation for 3 days in formamide (Fluka) at room temperature. The background-subtracted absorbance was measured on an Epoch microplate reader (Bio-Tek) by measuring the wavelength at 620 and 740 nm. The concentration of dye in the extracts was calculated with a standard curve of Evans blue in formamide.

Immunofluorescence stainings and quantifications

Hydrogel matrices were collected and fixed in 4% PFA for 6 hours at room temperature and processed for either whole-mount immunostainings or paraffin/cryo embedding and cutting.

For whole-mount immunostainings, samples were blocked with 10% bovine serum albumin (Sigma-Aldrich) and 0.3% Triton X (Sigma-Aldrich) in PBS. Primary and secondary antibodies were applied overnight at room temperature. Washing steps were performed with PBS and 0.3% Triton X. For paraffin preparations, samples were dehydrated and mounted in paraffin wax. For cryosections, samples were frozen in OCT compound (Tissue-Tek). Cross-sections (10 or 40 μm) were cut and mounted on glass slides. For all immunofluorescence procedures, the following primary antibodies were used: rabbit anti-human Prox1 (Reliatech; 1:300), monoclonal mouse anti-human CD31 (DakoCytomation; 1:50), monoclonal mouse anti-human CD90 (Dianova; 1:10), rabbit anti-human Lyve-1 (Abcam; 1:100), mouse anti-human podoplanin (Santa Cruz Biotechnology, 1:50), mouse anti-human αSMA (DakoCytomation), mouse anti-rat podoplanin (Reliatech), mouse anti-human collagen IV (Abcam), mouse anti-human fibrillin (Millipore), and mouse anti-human laminin 1+2 (Abcam). Corresponding secondary antibodies were labeled with Alexa Fluor 488 or 594 (Molecular Probes). Cell nuclei were counterstained with Hoechst bisbenzimide (Sigma-Aldrich). Stained specimens were examined with a Nikon Eclipse TE-2000-U confocal microscope. Adobe Photoshop CS3 (Adobe Systems) was used for image overlay. The Imaris software (Bitplane AG) was used to create 3D pictures (Z-stack) and digital surface images of confocal data. Computer-assisted morphometric vessel analyses were performed with Adobe Photoshop CS3. The average vessel area and vessel number per group were calculated, and statistical analysis was performed with GraphPad Prism (GraphPad Software Inc.).

Statistical analysis

The statistical analysis was carried out with the software GraphPad Prism. Student's t test, paired, two-tailed, with 95% confidence interval, without adjustments to α levels, was used for all comparisons. $P < 0.05$ was considered significant. Data are shown as means ± SEM.

REFERENCES AND NOTES

1. A. Atala, F. K. Kasper, A. G. Mikos, Engineering complex tissues. *Sci. Transl. Med.* **4**, 160rv12 (2012).
2. S. Böttcher-Haberzeth, T. Biedermann, E. Reichmann, Tissue engineering of skin. *Burns* **36**, 450–460 (2010).
3. H. Bae, A. S. Puranik, R. Gauvin, F. Edalat, B. Carrillo-Conde, N. A. Peppas, A. Khademhosseini, Building vascular networks. *Sci. Transl. Med.* **4**, 160ps23 (2012).
4. A. F. Black, F. Berthod, N. L'Heureux, L. Germain, F. A. Auger, In vitro reconstruction of a human capillary-like network in a tissue-engineered skin equivalent. *FASEB J.* **12**, 1331–1340 (1998).
5. L. Gibot, T. Galbraith, J. Huot, F. A. Auger, A preexisting microvascular network benefits in vivo revascularization of a microvascularized tissue-engineered skin substitute. *Tissue Eng. Part A* **16**, 3199–3206 (2010).
6. D. M. Supp, K. Wilson-Landy, S. T. Boyce, Human dermal microvascular endothelial cells form vascular analogs in cultured skin substitutes after grafting to athymic mice. *FASEB J.* **16**, 797–804 (2002).
7. I. Montaño, C. Schiestl, J. Schneider, L. Pontiggia, J. Luginbühl, T. Biedermann, S. Böttcher-Haberzeth, E. Braziulis, M. Meuli, E. Reichmann, Formation of human capillaries in vitro: The engineering of prevascularized matrices. *Tissue Eng. Part A* **16**, 269–282 (2010).
8. M. Skobe, M. Detmar, Structure, function, and molecular control of the skin lymphatic system. *J. Investig. Dermatol. Symp. Proc.* **5**, 14–19 (2000).
9. R. Gerli, R. Solito, E. Weber, M. Agliano, Specific adhesion molecules bind anchoring filaments and endothelial cells in human skin initial lymphatics. *Lymphology* **33**, 148–157 (2000).
10. A. Henno, S. Blacher, C. Lambert, A. Colige, L. Seidel, A. Noël, C. Lapière, M. de la Brassinne, B. V. Nusgens, Altered expression of angiogenesis and lymphangiogenesis markers in the uninvolved skin of plaque-type psoriasis. *Br. J. Dermatol.* **160**, 581–590 (2009).
11. R. Kunstfeld, S. Hirakawa, Y. K. Hong, V. Schacht, B. Lange-Asschenfeldt, P. Velasco, C. Lin, F. Fiebiger, X. Wei, Y. Wu, D. Hicklin, P. Bohlen, M. Detmar, Induction of cutaneous delayed-type hypersensitivity reactions in VEGF-A transgenic mice results in chronic skin inflammation associated with persistent lymphatic hyperplasia. *Blood* **104**, 1048–1057 (2004).
12. F. Pedica, C. Ligorio, P. Tonelli, S. Bartolini, P. Baccarini, Lymphangiogenesis in Crohn's disease: An immunohistochemical study using monoclonal antibody D2-40. *Virchows Arch.* **452**, 57–63 (2008).
13. A. Saaristo, T. Tammela, A. Farkkilä, M. Kärkkäinen, E. Suominen, S. Yla-Herttuala, K. Alitalo, Vascular endothelial growth factor-C accelerates diabetic wound healing. *Am. J. Pathol.* **169**, 1080–1087 (2006).
14. E. Kriehuber, S. Breiteneder-Geleff, M. Groeger, A. Soleiman, S. F. Schoppmann, G. Stingl, D. Kerjaschki, D. Maurer, Isolation and characterization of dermal lymphatic and blood endothelial cells reveal stable and functionally specialized cell lineages. *J. Exp. Med.* **194**, 797–808 (2001).
15. Y. K. Hong, N. Harvey, Y. H. Noh, V. Schacht, S. Hirakawa, M. Detmar, G. Oliver, Prox1 is a master control gene in the program specifying lymphatic endothelial cell fate. *Dev. Dyn.* **225**, 351–357 (2002).
16. J. T. Wigle, N. Harvey, M. Detmar, I. Lagutina, G. Grosveld, M. D. Gunn, D. G. Jackson, G. Oliver, An essential role for *Prox1* in the induction of the lymphatic endothelial cell phenotype. *EMBO J.* **21**, 1505–1513 (2002).
17. K. Hida, Y. Hida, D. N. Amin, A. F. Flint, D. Panigrahy, C. C. Morton, M. Klagsbrun, Tumor-associated endothelial cells with cytogenetic abnormalities. *Cancer Res.* **64**, 8249–8255 (2004).
18. T. A. Fong, L. K. Shawver, L. Sun, C. Tang, H. App, T. J. Powell, Y. H. Kim, R. Schreck, X. Wang, W. Risau, A. Ullrich, K. P. Hirth, G. McMahon, SU5416 is a potent and selective inhibitor of the vascular endothelial growth factor receptor (Flk-1/KDR) that inhibits tyrosine kinase catalysis, tumor vascularization, and growth of multiple tumor types. *Cancer Res.* **59**, 99–106 (1999).
19. S. Levenberg, J. Rouwkema, M. Macdonald, E. S. Garfein, D. S. Kohane, D. C. Darland, R. Marini, C. A. van Blitterswijk, R. C. Mulligan, P. A. D'Amore, R. Langer, Engineering vascularized skeletal muscle tissue. *Nat. Biotechnol.* **23**, 879–884 (2005).
20. N. C. Rivron, J. J. Liu, J. Rouwkema, J. de Boer, C. A. van Blitterswijk, Engineering vascularised tissues in vitro. *Eur. Cell. Mater.* **15**, 27–40 (2008).
21. S. Gupta, Optimal use of negative pressure wound therapy for skin grafts. *Int. Wound J.* **9** (Suppl. 1), 40–47 (2012).
22. L. Jewell, R. Guerrero, A. R. Quesada, L. S. Chan, W. L. Garner, Rate of healing in skin-grafted burn wounds. *Plast. Reconstr. Surg.* **120**, 451–456 (2007).
23. T. Hitchcock, L. Niklason, Lymphatic tissue engineering: Progress and prospects. *Ann. N. Y. Acad. Sci.* **1131**, 44–49 (2008).
24. L. E. Niklason, J. Koh, A. Solan, Tissue engineering of the lymphatic system. *Ann. N. Y. Acad. Sci.* **979**, 27–34; discussion 35–38 (2002).
25. C. L. Helm, A. Zisch, M. A. Swartz, Engineered blood and lymphatic capillaries in 3-D VEGF-fibrin-collagen matrices with interstitial flow. *Biotechnol. Bioeng.* **96**, 167–176 (2007).
26. C. P. Ng, C. L. Helm, M. A. Swartz, Interstitial flow differentially stimulates blood and lymphatic endothelial cell morphogenesis in vitro. *Microvasc. Res.* **68**, 258–264 (2004).
27. C. L. Helm, M. E. Fleury, A. H. Zisch, F. Boschetti, M. A. Swartz, Synergy between interstitial flow and VEGF directs capillary morphogenesis in vitro through a gradient amplification mechanism. *Proc. Natl. Acad. Sci. U.S.A.* **102**, 15779–15784 (2005).
28. Tt. Dai, Zh. Jiang, Sl. Li, Gd. Zhou, J. D. Kretlow, Wg. Cao, W. Liu, Yl. Cao, Reconstruction of lymph vessel by lymphatic endothelial cells combined with polyglycolic acid scaffolds: A pilot study. *J. Biotechnol.* **150**, 182–189 (2010).
29. K. N. Margaris, R. A. Black, Modelling the lymphatic system: Challenges and opportunities. *J. R. Soc. Interface* **9**, 601–612 (2012).
30. E. Braziulis, T. Biedermann, F. Hartmann-Fritsch, C. Schiestl, L. Pontiggia, S. Böttcher-Haberzeth, E. Reichmann, M. Meuli, Skingineering I: Engineering porcine dermo-epidermal skin analogues for autologous transplantation in a large animal model. *Pediatr. Surg. Int.* **27**, 241–247 (2011).

31. E. Braziulis, M. Diezi, T. Biedermann, L. Pontiggia, M. Schmucki, F. Hartmann-Fritsch, J. Luginbühl, C. Schiestl, M. Meuli, E. Reichmann, Modified plastic compression of collagen hydrogels provides an ideal matrix for clinically applicable skin substitutes. *Tissue Eng. Part C Methods* **18**, 464–474 (2012).
32. E. Reichmann, EuroSkinGraft: Novel generation of skin substitutes to clinically treat a broad spectrum of severe skin defects, FP7/2007-2013 grant agreement no. 279024; http://www.euroskingraft.eu.
33. C. Schiestl, T. Biedermann, E. Braziulis, F. Hartmann-Fritsch, S. Böttcher-Haberzeth, M. Arras, N. Cesarovic, F. Nicolls, C. Linti, E. Reichmann, M. Meuli, Skingineering II: Transplantation of large-scale laboratory-grown skin analogues in a new pig model. *Pediatr. Surg. Int.* **27**, 249–254 (2010).
34. R. V. Shevchenko, S. L. James, S. E. James, A review of tissue-engineered skin bioconstructs available for skin reconstruction. *J. R. Soc. Interface* **7**, 229–258 (2010).
35. Regenicin, Permaderm; http://www.regenicin.com/about/about-permaderm.html.
36. A. Feuerstein, FDA did not approve Regenicin skin graft; http://www.thestreet.com/story/11579041/1/fda-did-not-approve-regenicin-skin-graft.html.
37. A. Alajati, A. M. Laib, H. Weber, A. M. Boos, A. Bartol, K. Ikenberg, T. Korff, H. Zentgraf, C. Obodozie, R. Graeser, S. Christian, G. Finkenzeller, G. B. Stark, M. Hérault, H. G. Augustin, Spheroid-based engineering of a human vasculature in mice. *Nat. Methods* **5**, 439–445 (2008).
38. F. Bruyère, A. Noël, Lymphangiogenesis: In vitro and in vivo models. *FASEB J.* **24**, 8–21 (2010).
39. V. Schacht, M. I. Ramirez, Y. K. Hong, S. Hirakawa, D. Feng, N. Harvey, M. Williams, A. M. Dvorak, H. F. Dvorak, G. Oliver, M. Detmar, T1α/podoplanin deficiency disrupts normal lymphatic vasculature formation and causes lymphedema. *EMBO J.* **22**, 3546–3556 (2003).
40. Y. Xu, L. Yuan, J. Mak, L. Pardanaud, M. Caunt, I. Kasman, B. Larrivée, R. Del Toro, S. Suchting, A. Medvinsky, J. Silva, J. Yang, J. L. Thomas, A. W. Koch, K. Alitalo, A. Eichmann, A. Bagri, Neuropilin-2 mediates VEGF-C–induced lymphatic sprouting together with VEGFR3. *J. Cell Biol.* **188**, 115–130 (2010).
41. G. Cheng, S. Liao, H. Kit Wong, D. A. Lacorre, E. di Tomaso, P. Au, D. Fukumura, R. K. Jain, L. L. Munn, Engineered blood vessel networks connect to host vasculature via wrapping-and-tapping anastomosis. *Blood* **118**, 4740–4749 (2011).
42. S. Böttcher-Haberzeth, A. S. Klar, T. Biedermann, C. Schiestl, C. Meuli-Simmen, E. Reichmann, M. Meuli, "Trooping the color": Restoring the original donor skin color by addition of melanocytes to bioengineered skin analogs. *Pediatr. Surg. Int.* **29**, 239–247 (2013).
43. T. Biedermann, S. Böttcher-Haberzeth, A. S. Klar, L. Pontiggia, C. Schiestl, C. Meuli-Simmen, E. Reichmann, M. Meuli, Rebuild, restore, reinnervate: Do human tissue engineered dermo-epidermal skin analogs attract host nerve fibers for innervation? *Pediatr. Surg. Int.* **29**, 71–78 (2013).
44. D. E. Costea, L. L. Loro, E. A. Dimba, O. K. Vintermyr, A. C. Johannessen, Crucial effects of fibroblasts and keratinocyte growth factor on morphogenesis of reconstituted human oral epithelium. *J. Invest. Dermatol.* **121**, 1479–1486 (2003).
45. K. Kajiya, S. Hirakawa, B. Ma, I. Drinnenberg, M. Detmar, Hepatocyte growth factor promotes lymphatic vessel formation and function. *EMBO J.* **24**, 2885–2895 (2005).

Acknowledgments: We are grateful to E. Manuel for helping with the human skin sample collection. **Funding:** This work was supported by two grants from the European Union (EuroSTEC: LSHB-CT-2006-037409 and EuroSkinGraft: FP7/2007-2013 grant agreement no. 279024) and the Clinical Research Priority Programs of the Faculty of Medicine of the University of Zurich. We are particularly grateful to the Foundation Gaydoul and the sponsors of "DonaTissue" (T. Meier and R. Zingg) for their financial support and their interest in our work. **Author contributions:** D.M. designed the study, performed the experiments, analyzed the data, and wrote and reviewed the manuscript. J.L. designed the study, performed the experiments, analyzed the data, and reviewed the manuscript. S.S. performed the experiments. M.M. discussed the data and reviewed the manuscript. E.R. designed the study, discussed the data, and wrote and reviewed the manuscript. **Competing interests:** The authors declare that they have no competing interests. **Data and materials availability:** A materials transfer agreement is required for transfer of materials.

Submitted 26 June 2013
Accepted 8 January 2014
Published 29 January 2014
10.1126/scitranslmed.3006894

Citation: D. Marino, J. Luginbühl, S. Scola, M. Meuli, E. Reichmann, Bioengineering dermo-epidermal skin grafts with blood and lymphatic capillaries. *Sci. Transl. Med.* **6**, 221ra14 (2014).

2.2 RAPID PERFUSION DIRECTS THE HEALING OF PREVASCULARIZED DERMO-EPIDERMAL SKIN SUBSTITUTES FROM SCAR FORMATION TOWARDS REGENERATION

Joachim Luginbühl[1], Daniela Marino[1], Fabienne Hartmann-Fritsch[1], Agnieszka S. Klar[1], Simonetta Scola[1], Martin Meuli[2] and Ernst Reichmann[1]

[1]Tissue Biology Research Unit, Department of Surgery,

University Children's Hospital, Zurich, Switzerland

[2]Pediatric Burn Center, Plastic and Reconstructive Surgery,

University Children's Hospital, Zurich, Switzerland

Address correspondence to:

Prof. Dr. Ernst Reichmann

Tissue Biology Research Unit, Department of Surgery

University Children's Hospital

August Forel-Strasse 7

CH-8008 Zurich, Switzerland

Phone +41 44 634 89 11

Fax +41 44 634 89 18

E-mail: ernst.reichmann@kispi.uzh.ch

Short title: Rapid perfusion promotes skin healing

Abbreviations

PDESS	Prevascularized dermo-epidermal skin substitute
dai	Days after integration
dpT	Days post transplantation
NPDESS	Non-prevascularized dermo-epidermal skin substitute
HDMEC	Human dermal microvascular endothelial cells
FACS	Fluorescence activated cell sorting

2.2.1 ABSTRACT

Rapid re-establishment of a functional vascularization is a precondition for the proper healing of tissues. We found that bioengineered human dermo-epidermal skin substitutes, if non-prevascularized, undergo a crisis after transplantation onto recipient immunocompromised Nu/Nu rats. This crisis resulted in significantly reduced survival of transplanted cells, which acted towards graft shrinkage. In addition, a scar-like arrangement of dermal collagen bundles was initiated. Here, we bioengineered dermo-epidermal skin substitutes containing a composite vascular plexus consisting of physiologically distinct, pericyte-covered blood capillaries and pericyte-free lymphatic capillaries, and analyzed the effects of prevascularization on the healing of the transplant *in vivo*. The bioengineered capillaries connected to the recipient's blood and lymphatic vascular system and accelerated rat blood and lymphatic angiogenesis. Rapid perfusion of the bioengineered blood capillary plexus avoided the above mentioned crisis by exerting several beneficial effects on the healing of the skin substitute. Importantly, the early generation of a non-scar texture of mature collagen bundles was observed, which was accompanied by the development of rete ridge-like structures and capillary loops, essential structures in human skin. Our results indicate that rapid graft perfusion unlocks latent regenerative processes that shift the healing of dermo-epidermal skin substitutes from a scar-like organization towards real tissue renewal.

2.2.2 INTRODUCTION

Cultured autologous skin substitutes represent a promising alternative to autologous split-thickness skin grafts for the treatment of large skin injuries[166,226]. Since rapid and tight attachment of the epidermal and dermal layers is crucial for a successful outcome of skin transplantations[166], dermo-epidermal skin substitutes (DESS) in which the epidermal and dermal layers are combined before transplantation bear a great potential. However, if containing only keratinocytes and fibroblasts, DESS exhibit structural and functional deficiencies when compared to full-thickness skin. A major limitation of DESS is the lack of blood and lymphatic capillaries[182,227]. It has been shown that the early nourishment of full-thickness skin grafts occurs by rapid connection (anastomosis) of pre-existing blood capillaries with the recipient's vasculature[228]. Without pre-existing capillaries, re-vascularization needs to occur by the slow *de novo* formation of capillaries rather than by rapid anastomosis. This exposes DESS to a period of oxygen and nutrient deprivation early after transplantation, with potentially harmful effects on skin healing[229,230]. Accordingly, promotion of angiogenesis has been shown to support wound healing[231-234], whereas inhibition of angiogenesis can impair the same[235,236].

An effective strategy to promote angiogenesis is to provide the skin substitute with bioengineered capillaries prior to transplantation (prevascularization). Similar to the pre-existing capillaries in full-thickness skin grafts, these bioengineered capillaries can rapidly anastomose with the recipient's vasculature early after transplantation and accelerate perfusion. We and others have previously established that the generation of functional blood capillaries in different tissue substitutes is achievable[182,207,237-239]. Additionally, since the importance of the lymphatic vascular system for cutaneous wound healing is increasingly recognized[240,241], we have demonstrated in a very recent study that both blood and lymphatic capillaries of human origin can be simultaneously bioengineered within DESS and that the lymphatic capillaries improve the drainage of fluid from the transplant *in vivo*[227]. However, the biological effects of prevascularizing bioengineered DESS with both blood and lymphatic capillaries on their remodeling after transplantation have not been determined yet.

In the present study, we sought to further characterize and optimize the prevascularization process to generate a dense network of physiologically distinct blood and lymphatic capillaries in DESS. In a second step, we explored the biological effects of

prevascularization of DESS after they had been transplanted onto immuno-compromized nu/nu rats. We found that during prevascularization, fibroblasts differentiated into pericytes and specifically covered blood capillaries, while they hardly associated with lymphatic capillaries, demonstrating development of a physiological dermal microvasculature [240]. After transplantation, the engineered capillaries anastomosed with the recipient's vasculatures and accelerated the host blood and lymphatic angiogenic response. Importantly, the rapid anastomosis of the blood capillaries prevented a post-transplantational crisis which accompanies the early healing of non-prevascularized DESS (NPDESS). Prevention of this crisis significantly increased the survival of transplanted cells and reduced shrinkage. Furthermore, the healing of PDESS, in contrast to NPDESS, was accompanied by the generation of capillary loops in the dermal equivalent and the de novo formation of rete ridges in the epidermis, structures that provide skin with resistance to mechanical sheer stress and optimize blood supply from the dermis to the epidermis.

2.2.3 RESULTS

The bioengineering of human dermal blood and lymphatic capillaries

We have previously defined environmental conditions that enable the bioengineering of networks of human blood and lymphatic capillaries by integration of HDMEC and human dermal fibroblasts into fibrin hydrogels[227]. Here, to optimize capillary formation, we integrated fibrin hydrogels with different HDMEC:fibroblast ratios (9:1, 4:1, 7:3, 3:2, 1:1, 2:3, 3:7, 100000cells/ml) and quantified the capillary area, the branch point density and the mean capillary diameter 21 days after integration (21dai) using wholemount immunofluorescence stainings for human-specific CD31 (hCD31) (Fig. S1). The HDMEC:fibroblast ratio of 1:1 maximized capillary formation, resulting in a dense vascular plexus (Fig. 1a). We analyzed the composition of blood and lymphatic capillaries by immunofluorescence for the lymphatic marker hProx1 in combination with hCD31 (Fig. 1b). Fibrin hydrogels integrated with a HDMEC:fibroblast ratio of 1:1 contained 75% (±6.1%) blood capillaries and 25% (±4.8) lymphatic capillaries. Consistent with previous reports[207,242], we found that the extent of capillary formation correlated with the degree by which the capillaries were covered with hCD90+ fibroblasts (Fig. 1c and Fig. S1). High magnification confocal microscopy revealed that these fibroblasts tightly wrapped around the abluminal side of the capillaires in a periendothelial position (Fig. 1d). Accordingly, immunofluorescence stainings for smooth muscle a-actin (α-SMA) and hNG2-proteoglycan (hNG2), two established pericyte markers[243], revealed that capillary-associated fibroblasts expressed α-SMA and hNG2, exhibiting a pericyte phenotype (Fig. 1e). Quantitative analysis of these stainings showed that pericyte coverage was maximized in fibrin hydrogels with a HDMEC:fibroblast ratio of 1:1, and thus, in fibrin hydrogels showing the highest extent of capillary morphogenesis (Fig. 1e and Fig. S1). It has been shown that pericytes have more stringent growth requirements in culture than fibroblasts[244]. In line with this study, fluorescence-activated cell sorting (FACS) and immunofluorescence stainings for α-SMA and hNG2 on fibroblast cultures at passage 0 (p0) and p4 revealed an almost complete loss of α-SMA-positive cells after prolonged time in culture (Fig. S2a and b). In contrast, the number of hNG2-expressing fibroblasts increased from ~60% at p0 to ~98% at p4. Additionally, FACS analysis of HDMEC cultures at p0 indicated that these cultures may contain a small number of contaminating pericytes (Fig. S2a). Thus, to determine whether the pericytes identified in

prevascularized fibrin hydrogels 21dai were derived from the fibroblast rather than from the HDMEC cultures, we integrated unlabelled HDMEC together with GFP-labelled fibroblasts into fibrin hydrogels. These GFP-labelled fibroblasts (p4) showed up-regulation of hNG2 expression and lack of α-SMA expression upon extended culture on plastic, similar to non-labelled fibroblasts (Fig. S2c). At 21dai, hNG2/α-SMA-positive pericytes associating with capillaries consistently expressed GFP (Fig. S2d). Furthermore, we found that GFP-positive fibroblasts not associated with capillaries expressed α-SMA, but lost hNG2 expression. Thus, these results revealed that during *in vitro* prevascularization, fibroblasts differentiate into hNG2/α-SMA-positive pericytes and stabilize capillaries, corroborating an earlier study[245]. In contrast, fibroblast not-associated with capillaries expressed α-SMA, but lacked hNG2 expression, indicating differentiation into myofibroblasts-like cells[246]. Since lymphatic capillaries are only marginally covered by pericytes *in vivo*[240], we quantified pericyte coverage of blood and lymphatic capillaries using triple immunofluorescent stainings for hCD31, the lymphatic marker Lyve-1 and hNG2 on sections of prevascularized fibrin hydrogels 21dai (Fig. 1f). Notably, only 4% of lymphatic capillaries were covered by hNG2-positive pericytes, whereas 84% of blood capillaries exhibited pericyte coverage.

Prevascularization of DESS accelerates blood and lymphatic vascular regeneration *in vivo*

To investigate the effects of prevascularization on the development of bioengineered DESS *in vivo*, we generated PDESS and transplanted them onto the backs of immunocompromized Nu/Nu rats employing a modified Fusenig chamber (Fig. S3). 14 days post-transplantation (14dpT), PDESS were excised and the human and rat capillary plexuses were analyzed by immunofluorescence staining for hCD31 and rat/hCD31 on thick (50μm) sections, respectively (Fig. 2a, upper panel). This staining revealed a pattern of long, uni-directional rat capillaries projecting perpendicular towards the human epidermis and establishing short-cut connections between the rat capillaries in the wound bed and the human capillary network in the PDESS. Confocal microscopy revealed stretches of anastomosed rat-human blood capillaries (Fig. 2a, inserts). When parallel sections of the same PDESS were stained with antibodies against podoplanin, a lymphatic marker, anastomosis between rat and human lymphatic capillaries at 14dpT was observed only at a few spots (Fig. 2a, lower panel). Next, we generated PDESS and non-

prevascularized DESS and compared the kinetics of overall rat capillary ingrowth by immunofluorescence staining for hCD31 and rat/hCD31 at 4, 9 and 14dpT (Fig. S4a). In accordance with a previous study[238], the ingrowth of rat capillaries, as measured by determination of the distance of the uppermost rat capillary to the basement membrane at each time-point, was markedly accelerated in PDESS (Fig. 2b). Furthermore, we specifically quantified the rate of rat lymphatic ingrowth at 4, 9 and 14dpT using human and rat-specific podoplanin antibodies (Fig. S4b). In contrast to rat blood capillaries, rat lymphatic capillaries had not yet invaded the dermal compartment of both, NPDESS and PDESS at 9dpT. However, at 14dpT, rat lymphatic ingrowth was clearly more advanced in PDESS than in NPDESS (Fig. 2c).

As shown previously, lymphatic capillaries bioengineered by our method were functional and promoted fluid drainage *in vivo*[227]. To determine whether the bioengineered blood capillaries were functional and connected to the recipient's (rat) capillaries, we analyzed sections of NPDESS and PDESS between 2 and 9dpT for the presence of blood perfused human capillaries (Fig. 2d). Notably, at 4dpT, PDESS contained numerous blood-perfused capillaries that were distributed throughout the transplant, whereas yet no perfused capillaries were found within NPDESS. Immunofluorescence on paraffin sections for hCD31 in combination with the green autofluorescence of rat erythrocytes revealed that the perfused capillaries within PDESS at 4dpT were exclusively of human origin (Fig. 2e), confirming successful anastomosis of the engineered blood capillary plexus. Thus, these results identified an early post-transplantational period (between 4 and 9dpT) during which PDESS, in contrast to NPDESS, were supported by a functional blood vasculature consisting of anastomosed human blood capillaries and ingrowing rat blood capillaries. Lymphatic vascular regeneration, although being accelerated in PDESS at later stages, was not observed between 4 and 9dpT in both, NPDESS and PDESS.

Rapid anastomosis of bioengineered blood capillaries prevents an early post-transplantational tissue crisis

Adequate blood supply to provide sufficient tissue oxygenation, nutrition and growth factor supply is crucial during wound healing and graft remodeling[229,230]. Therefore, we determined the ratio of proliferative human cells to the total number of human cells in NPDESS and PDESS at 4 and 9dpT using Ki-67 and hCD90 antibodies (Fig. S4c). We found a 3.4-fold increase in the proliferation of human fibroblasts and a 2-fold increase in

the proliferation of human keratinocytes in PDESS at 4dpT (Fig. 3a). At 9dpT, fibroblast and keratinocyte proliferation in PDESS was increased by 8.7-fold and 2.7-fold, respectively. Conversely, no significant variation in proliferation was observed *in vitro* (24dai). Assessment of the ratio of apoptotic human cells to the total number of human cells using caspase-8 and hCD90 antibodies revealed a 2.7-fold decreased fibroblast apoptosis in PDESS at 4dpT and a 5.8-fold decreased fibroblast apoptosis at 9dpT (Fig. 3a and S4d). Notably, keratinocytes hardly expressed caspase-8 *in vivo* and *in vitro*, while caspase-8 expression in fibroblasts *in vitro* appeared to be slightly decreased in PDESS (1.4-fold). Additionally, we quantified the total number of keratinocytes (PanCK+) and fibroblasts (hCD90+) in NPDESS and PDESS *in vitro* (24dai; Fig. 3b) and at 4, 9 and 14dpT (Fig. 3c). There was no significant difference in the number of human cells between NPDESS and PDESS before transplantation. After transplantation, however, we found a continuous increase in the number of human cells in PDESS, which at 14dpT reached a 3.2-fold increase in fibroblast numbers and a 2.3-fold increase in keratinocyte numbers compared to NPDESS. In NPDESS, the number of fibroblasts decreased between 9 and 14dpT and the keratinocyte number stagnated between 4 and 9dpT, indicating a phase of crisis. Accordingly, prevascularization significantly reduced shrinkage of the transplant, as assessed by quantification of the epithelialized area in NPDESS and PDESS 21dpT (Fig. 3d). Analysis of the kinetics of epidermal stratification, keratinocyte differentiation and the establishment of epidermal homeostasis using 3 different pairs of epidermal markers (K15+K19/Involucrin+Loricrin/Laminin5α3+K1) revealed that the observed increase in proliferation in PDESS did not interfere with the normal time-course of epidermal development (Fig. S5).

Prevascularization induces the formation of rete ridges and capillary loops

Already simple histological comparisons of transplanted PDESS and NPDESS by H&E stainings showed clear differences in the structure of the dermo-epidermal junction (Fig. 4a). At 4dpT, the neo-epidermis in NPDESS was hardly interlocked with the underlying dermis and exhibited an entirely even and plane basal morphology. The weak dermo-epidermal adherence was underlined by the fact that the two tissues readily separated upon sectioning. At 14dpT and at 21dpT, the neo-epidermis of NPDESS showed better attachment to the dermis, but still consistently exhibited a plane basal morphology lacking any rete ridge-like protrusions. In marked contrast, the neo-epidermis of PDESS 4dpT was

considerably better interlocked with the dermis trough developing rete ridge-like protrusions projecting into the dermis. These protrusions progressively increased in size over time and eventually developed into rete ridges-like structures by 21dpT. Quantifications of the rete ridge ratios of NPDESS and PDESS 21dpT corroborated these findings (Fig. 4a).

There is evidence that certain markers such as melanoma chondroitin sulfate proteoglycan (MCSP) are distributed in a clustered pattern in human epidermis[247]. In line with these studies, analysis of normal human foreskin revealed hMCSP expression to be confined to basal keratinocytes located in the "tip" of dermal papillae (Fig. 4b). To exclude that the protrusions observed in PDESS were artefacts of tissue preparation, we analyzed NPDESS and PDESS for MCSP expression at 21dpT. We found a complete absence of MCSP expression along the entire epidermis in NPDESS. In PDESS, MCSP was expressed in regions containing rete ridges, but absent in areas without rete ridges (Fig. 4b). Moreover, MCSP expression in PDESS was predominantly confined to the tips of dermal papillae and thus, highly reminiscent of the natural pattern of MCSP expression in human skin, underlining the bona fide identity of the developing rete ridges.

As shown in Fig. 4c, normal human skin contains dermal capillaries forming capillary loops that project between two adjacent rete ridges towards the tip of each dermal papilla. Visualization of rat and human capillaries in both NPDESS and PDESS revealed that despite the appearance of rat capillaries near the dermo-epidermal junction in NPDESS 14dpT, capillary loop formation was not initiated until 21dpT. In contrast, in PDESS, invading rat capillaries projected into the developing rete ridges and formed typical capillary loops, which was confirmed by confocal analysis (Fig. 4d). To determine whether the sole presence of HDMEC had an inductive effect on skin reconstitution and morphogenesis, we analyzed NPDESS and PDESS *in vitro,* after both skin substitutes had been raised to the air liquid phase to induce epidermal stratification (Fig. S6). Both types of skin substitutes equally developed a differentiated and stratified epidermis within 2 weeks *in vitro*, as evidenced by H&E staining and immunofluorescence for panCK (Fig. S6a). Detection of hCD31 confirmed the presence of endothelial structures underneath the epidermis in PDESS and their absence in NPDESS. We determined the Ki-67+ cell to total cell ratio, the caspase-8+ cell to total cell ratio and the rete ridge ratio in *in vitro* stratified NPDESS and PDESS. The sole presence of endothelial structures did neither alter proliferation or apoptosis, nor did it induce rete ridge formation (Fig. S6b and c).

Indeed, when we analyzed PDESS at very early time-points after transplantation (2-4dpT), we found a striking correlation between the number of perfused blood capillaries situated immediately underneath the epidermis and the extent of beginning rete ridge formation (Fig. S6d), indicating that rapid perfusion of the bioengineered capillaries is a pre-condition for the induction of rete ridge (and capillary loop) formation.

Prevascularization accelerates dermal remodeling and decreases scar formation

Since prevascularization of DESS induced the formation of rete ridges and capillary loops, hence supported the development of normal physiological skin structures in the transplanted PDESS, we set out to determine whether prevascularization had an impact on dermal remodeling and scar formation[248]. We first analyzed the remodeling of fibrin into collagen-1 *in vivo* by quantification of the fibrin-positive and collagen-1-positive areas on sections of NPDESS and PDESS at 4, 9 and 14dpT. We found that both, fibrin degradation (Fig. 5a and Fig. S7a) as well as collagen-1 deposition (Fig. 5b and Fig. S7b) were significantly accelerated in transplanted PDESS at 9dpT (1.9-fold and 3.8-fold, respectively) and at 14dpT (2.3-fold and 1.2-fold, respectively). No significant differences were found at 4dpT. Next, we assessed collagen maturity and bundle orientation at 21dpT by picrosirius red staining (Fig. 5c). Normal human skin and human scar tissue served as controls. Microscopical analysis under polarized light revealed that in normal human skin, collagen bundles are arranged in a crosshatch motif with a randomized orientation, which yields a strong birefringent signal under polarized light. In human scars, collagen bundles are oriented in parallel to the epidermis, which dramatically reduces the birefringent signal. A scar-like collagen matrix was observed in transplanted NPDESS. Intriguingly, in transplanted PDESS, the same reconstituted dermal tissue showed a randomized collagen bundle orientation exhibiting a strong birefringent signal. Hence, the collagen phenotype in PDESS (21dpT) was highly reminiscent of the collagen phenotype of normal human skin.

Given the central role of myofibroblasts in scar formation[249], we additionally analyzed the clearance of myofibroblasts in NPDESS and PDESS by immunofluorescent staining for α-SMA to mark myofibroblasts (and pericytes), either hCD31 or rat+hCD31 to mark human and rat capillaries and hCD90 to identify the borders of the human transplant at 4 and 9dpT (Fig. 5d). At 4dpT, the human dermis of PDESS contained a high number of myofibroblasts (a-SMA-positive fibroblasts not associated with capillaries), whereas they

were yet completely absent within the human dermis in NPDESS (Fig. S7c). Notably, at 9dpT, α-SMA-positive cells in PDESS within the human dermis were already confined to capillaries, suggesting a progressed stage of myofibroblast clearance (Fig. 5d). In contrast, in NPDESS at 9dpT, myofibroblasts were still present at high numbers.

2.2.4 DISCUSSION

Clinical application of bioengineered DESS to date may be the best possible solution for patients with large full-thickness skin defects[166,182,184,240,248,250,251]. However, although on the forefront of tissue engineering and plastic and burn surgery, when applied on a living organism, these DESS seem to develop into just a "very good scar". A central finding of this study is that a small skin biopsy is sufficient to allow for the generation of prevascularized dermo epidermal skin substitutes (PDESS) containing networks of both, blood and lymphatic capillaries. We found that during the process of prevascularization, fibroblasts differentiate into pericytes which specifically cover blood capillaries, but do not associate with lymphatic capillaries, hence creating a physiological dermal microvasculature[240]. Notably, when HDMEC and fibroblasts were mixed at a ratio of 1:1, this resulted in optimal numbers of blood and lymphatic capillaries as well as in a physiological degree of pericyte coverage of the blood capillaries. These findings indicate that differentiation of fibroblasts into pericytes is an essential precondition for successful *in vitro* prevascularization. After transplantation, the engineered blood and lymphatic capillaries connected to the recipient's blood and lymphatic vasculatures and accelerated rat blood and lymphatic re-vascularization. Intriguingly, anastomosis occurred by long and unbranched rat capillaries that directly projected from the rat wound bed towards the graft. These "short-cut" connections achieved prompt perfusion of the bio-engineered plexus, hence rapid nourishment of the graft's dermis and epidermis was accomplished. We hypothesize that here a chemotactic mechanism, initiated by the bio-engineered capillary plexus was responsible.

The very rapid perfusion of the bioengineered blood capillaries prevented a crisis induced by undernutrition and severe hypoxia, which commonly occurs after transplantation of npDESS. This crisis inhibits proliferation and triggers apoptosis; hence leading to shrinkage of the skin substitute. In PDESS, shrinkage was decreased and dermal collagen fibers did no longer arrange into scar-like, parallel and condensed bundles, but rather exhibited a non-scar, antiparallel distribution of mature collagen fibers. As collagen-1 deposition by dermal fibroblasts is strictly oxygen-dependent, collagen synthesis and the arrangement of mature collagen fibers in a non-scar fashion may be explained by this rapid and efficient perfusion. We consider this close-to-normal dermal collagen structure as one of the most important findings of this study. Along these lines, we observed the

formation of capillary loops and the development of rete ridges in transplanted PDESS, which massively strengthen the functiononality of the dermo-epidermal junction[27,252]. As rete ridges and capillary loops do not develop within human scars[248], this finding further substantiates the notion that rapid perfusion of PDESS triggers the organotypic (non-scar) remodeling of these types of skin grafts. Rather than turning into a very good scar, the perfused PDESS activates developmental processes that act towards normal skin structures and against scarring. Since most effects of graft remodelling occurred long before lymphatic regeneration took place, our findings suggest that it is the rapid perfusion of the bio-engineered blood plexus that largely avoids deposition of a scar-like dermal architecture within the healing DESS. Future experiments will have to determine whether and how complete tissue-fluid homeostasis can be achieved by the lymphatic type of the here bio-engineered micro vessels. These may well avoid the initiation of seromas, hence further contribute to a rapid and successful take of this new generation of skin grafts.

2.2.5 MATERIALS AND METHODS

Study design

Statisticians at the University of Zurich were consulted regarding sample size. Briefly, sample size calculations were performed with a confidence level of 95% and a statistical power of 70-80%. For *in vitro* analysis of prevascularized fibrin hydrogels, the experimental end point was chosen at 21 days, when the majority of the engineered capillaries had formed a lumen.

For determination of the optimal HDMEC/fibroblast ratio for *in vitro* capillary formation, HDMEC cultures were analyzed for the number of contaminating fibroblasts by FACS, after which donor-matched fibroblasts were added to obtain the desired ratio. 21dai, the hydrogels were embedded in Tissue Tek and completely sectioned. Thereafter, 3-4 random sections were selected and 3 sample images were analyzed for each sample.

For *in vivo* comparison of NPDESS and PDESS, both skin substitutes were generated using donor-matched fibroblasts and keratinocytes. For the assembly of NPDESS, 50000 fibroblasts/ml fibrin were integrated. For the assembly of PDESS, a 1:1 mixture of HDMEC (50000cells/ml fibrin) and fibroblasts (50000cells/ml fibrin) isolated from the same skin biopsy was added. 21dai, the skin substutes were overlaid with a suspension of keratinocytes (750000keratinocytes/hydrogel) and incubated for another 4 days under submerged conditions. PDESS and NPDESS that did not show a closed layer of keratinocytes 4 days after application, as analyzed by Fluorescein diacetate staining (FdA, see below), were excluded from the study. At different time-points after transplantation, NPDESS and DPESS were excised and half of the transplant was embedded in Tissue Tek, the other half in paraffin. After completed sectioning and analysis, 3-4 random sections were selected and 3 sample images were analyzed for each sample. All experiments were performed in triplicates and the hydrogels and animals were always assigned randomely to the experimental groups. The total number independent experiments is indicated in the figure legends (n).

Cell isolation

For HDMEC isolation, foreskins were cut into approximately 1 cm^2 pieces and incubated with 75U/mL collagenase type II (Worthington, Lakewood, NY) at 37°C for 1 h. HDMECs were harvested by scraping the dermal side with the back of a scalpel blade.

The cell suspension was centrifuged at 170 g for 10 min and the cell pellet was resuspended in microvascular endothelial cell growth medium-2 (EBM-2 MV; Lonza, Basel, Switzerland) with supplements (Lonza, CC-4147). HDMECs were grown on 1% gelatine-coated culture dishes in 5% CO2 at 37°C. Overgrowth of endothelial cell cultures was prevented by repeatedly scratching the contaminating fibroblasts off the culture dish with a sterile gauge needle. The medium was changed three times a week. HDMEC were used at passage 0 in all experiments.

For keratinocyte and fibroblast isolation, skin biopsies were further digested for 15–18 hours at 4°C in 12U/ml dispase in Hank's buffered salt solution containing 5 $mg*ml^{-1}$ gentamycin. Thereafter, the epidermis and the dermis could be separated using forceps. The epidermis was further digested in 1% trypsin, 5mM EDTA for maximal 3 minutes at 37 °C. The dermal tissue was digested in $2mgml^{-1}$ collagenase for approximately 60 minutes at 37 °C. Epidermal cells were resuspended in serum-free keratinocyte medium containing 25 $mg*ml^{-1}$ bovine pituitary extract, 0.2 $ng*ml^{-1}$ EGF, and 5 mg/ml gentamycin. A total of $4*10^6$ dermal cells per Ø10cm dish were grown in DMEM supplemented with 10% fetal calf serum, 4mM L-alanyl-L-glutamine, 1mM sodium pyruvate, and 5 mg/ml gentamycin. Collagenase was from Sigma (Buchs, Switzerland), all other compounds were from Invitrogen (Basel, Switzerland).

Assembly of fibrin-based NPDESS and PDESS

Prior to integration into fibrin hydrogels, we routinely determined the number of contaminating fibroblasts in HDMEC cultures using FACS. Fibrinogen from bovine plasma (Sigma-Aldrich, Buchs, Switzerland) was reconstituted in NaCl according to the instructions of the provider to a final concentration of 10 mg/ml. For the analysis of prevascularized fibrin hydrogels *in vitro*, HDMEC and fibroblasts were submerged in 3ml of fibrinogen solution in defined ratios (100000cells/ml). For the generation of PDESS (50000 HDMEC/ml + 50000 fibroblasts/ml) and NPDESS (50000 fibroblasts/ml), donor-matched fibroblasts were used and the cells were integrated into 3ml of fibrinogen solution. 33 µl thrombin (Sigma-Aldrich, 100U/mL) were added and the solution was transferred into six-well plates. After clotting at room temperature, the preparations were incubated at 37°C for 30min in a humidified incubator containing 5% CO2 to ensure polymerization of fibrin. Afterwards, EBM-2MV (Lonza, Basel, Switzerland) was added to the upper and lower chambers, and fibrin hydrogels were cultured for 21 days.

Thereafter, $7.5*10^5$ keratinocytes in RGM were seeded on top of each skin substitute and the gels were incubated for another 3-4 days under submerged conditions until transplantation.

Transplantation

Animal studies were performed with the approval of the Institutional Animal Care of the University of Zurich following the guidelines of the National Institutes of Health. Immunoincompetent female Nu=Nu rats (Elevage Janvier) were anaesthetized by inhalation of 5% isofluran (Baxter, Volketswil, Switzerland) and narcosis maintained by inhalation of 2.5% isofluran via mask. Before the operation, 0.5mg/kg buprenorphin (Temgesic_; Essex, Luzern, Switzerland) for analgesia and retinol cream (Vitamin A ‘‘Blache’’_; Bausch & Lomb, Berlin, Germany) for eye protection were applied. To prevent wound closure from the side and overgrowth of the human transplant by rat tissue, a special polypropylene ring (modified fusenig chamber), 2.6 cm in diameter, was designed in our laboratory. The rings were sutured to full-thickness skin defects created on the back of the rats using nonabsorbable polyester sutures (Ethibond_; Ethicon, Norderstedt, Germany). Cultured NPDESS and pDESS were placed into the polypropylene rings and covered with a silicon foil (Silon-SES; BMS) and polyurethane sponges (Ligasano_; Ligamed, adolzbufe, Germany). Rats were sacrificed at 2, 4, 9, 14 and 21 days after surgery. At sacrifice, dressings and sutures were removed and multiple graft biopsies were collected for different analyses.

Histology and Immunofluorescence

Biopsies were embedded in Tissue Tek and/or paraffin blocks. Cryosections (12µm for thin sections and 50µm for thick sections) were fixed for 5 min in acetone–methanol at -20°C and stained with the following antibodies: From Dako (Baar, Switzerland): mouse anti-human CD31 (1:100), mouse anti-human/rat panCK (1:100), mouse anti-human α-SMA (1:100), mouse anti-human panCK (1:100), mouse anti-human cytokeratin 19 (1:100), rabbit anti-mouse Fluoresceinisothiocyanat (FITC)-conjugated (1:100), rabbit anti-mouse Tetramethylrhodamine-5-isothiocyanat (TRITC)-conjugated (1:200), swine anti-rabbit FITC (1:50). From Santa Cruz (Labforce AG, Nunningen, Switzerland): mouse anti-podoplanin (1:100), mouse anti-human lam5α3 (1:100), mouse anti-rat HIS48 (1:50), goat anti-rabbit TRITC (1:200). From Reliatech (Wolfenbüttel, Germany): rabbit anti-

human Prox-1 (1:300 – 1:500). From Abcam (Cambridge, United Kingdom): rabbit anti-human/rat Lyve-1 (1:50), rabbit anti-human/rat Laminin1+2 (1:100), mouse anti-human/rat collagen-1 (1:100), rabbit anti-human caspase-8 (1:50), rabbit anti-human loricrin (1:500). From Biolegend (San Diego, CA): mouse anti-human CD90/Thy1 (Biolegend; 1:20). From R&D Systems (Abingdon, United Kingdom): phycoerythrin-conjugated mouse anti-human NG2/MCSP (1:20). From Pro Gen (Heidelberg, Germany): guinea pig anti-human cytokeratin 5 (1:100). From BD Pharmingen (Allschwil, Switzerland): mouse anti-rat/human CD31 (1:50), mouse anti-human Ki67 (1:100). From Genetex (Irvine, CA): mouse anti-human fibrin (1:50). From Novus Biologicals (Cambridge, United Kingdom): mouse anti-human cytokeratin 1 (1:200). From Spring Bioscience (Pleasanton, CA): mouse anti-human/rat cytokeratin 15 (1:50). From Neomarkers (Fremont, CA): mouse anti-human involucrin (1:100). All antibodies were incubated at room temperature for 1 h. Nuclei were counterstained with Hoechst. All slides were mounted with fluorescent mounting medium (Dako, Baar, Switzerland). Specificity of human cell markers was routinely confirmed by absence of any signal in the animal tissue. In addition, omission of the first antibody was used as a negative control.

Fluorescent-activated cell sorting (FACS)

FACS was performed to analyze HDMEC cultures for the number of contaminating fibroblasts and to analyze fibroblast cultures for the presence of α-SMA/NG2-positive pericytes. The cell cultures were trypsinized, centrifuged and resuspended in 200µl 2% BSA solution. For the detection of intracellular α-SMA, the cells were treated with 10% saponine for 5-10min.

Fibroblast transduction

Dermal fibroblasts were grow to a confluence of approximately 70% in 24-well plates. The medium was reduced to 300µl, 3µl of Hexadimethrine bromide was added to enhance transduction and the plate was incubated for 60min at 37° in a humidified incubator in an atmosphere of 5-7% CO2. MISSION® pLKO.1-puro-UbC-TurboGFP™ Transduction Particles were added to each well and the plate incubated for 18-20 hours at 37°. On the next day, the medium was changed and puromycin at a concentration of 8µg/ml was added to kill untransduced fibroblasts. Fresh puromycin was added for 4-5 days after

which resistant colonies could be identified and expanded. All compounds were from Invitrogen, Basel, Switzerland).

In vitro stratification

NPDESS and PDESS were assembled as described above. After culture for 21days at 37° in a humidified incubator in an atmosphere of 5-7% CO2, NPDESS and PDESS were overlaid with a suspension of keratinocytes (750000cells/ml) and incubated for another 3-4 days under submerged conditions. Thereafter, the medium was removed, 2ml of Rheinwald&Green medium was added to the lower chamber and the skin substitutes were lifted to air-liquid phase to induce epidermal stratification. 14 days after onset of *in vitro* stratification, NPDESS and PDESS were embedded and analyzed.

Sirius Red staining

Sirius red (Direct Red 80; Sigma, St. Louis, MO) staining was performed to evaluate collagen bundle orientation in the specimens according to the manufactures protocol. Briefly, paraffin sections were de-waxed and re-hydrated. Nuclei were stained with Weigert's haematoxylin. Subsequently, sections were stained in picro-sirius red for one hour. Afterwards, sections were washed with acidified water, dehydrated and mounted in mounting media. Birefringence pattern was evaluated using polarized light microscopy to determine collagen maturity and bundle orientation.

Fluorescein diacetate (FdA) vital cell staining

Fluorescein diacetate (FdA) staining was performed to determine keratinocyte confluency as published and proven to be suitable for the determination of cell viability in tissue-engineered skin [253]. In short, cell culture medium was replaced for 2 min with the equal volume of 5 lM FdA in PBS, freshly prepared from a stock solution of 5 mM FdA in acetone. The FdA was removed by washing twice in PBS before fresh culture medium was applied. Fluorescein fluorescence was evaluated using microscopy (Nikon SMZ1500 fluorescent stereo microscope, FITC filter, Nikon DXM1200F camera).

Statistical analysis

In vivo data for quantifications were collected from 5 distinct rounds of experiments with 3 replicates each. Transplants were completely sectioned and 4 random sections were

chosen for immunofluorescent stainings and subsequent quantifications. Statistical analysis was performed using GraphPad Prism 4.02 (GraphPad Software Inc., La Jolla, CA). T-tests were performed to determine significance using GraphPad Prism 4.02. Significance levels were determined using post-tests, and were set at *$p<0.05$, **$p<0.01$, and ***$p<0.001$.

2.2.6 FIGURES AND FIGURE LEGENDS

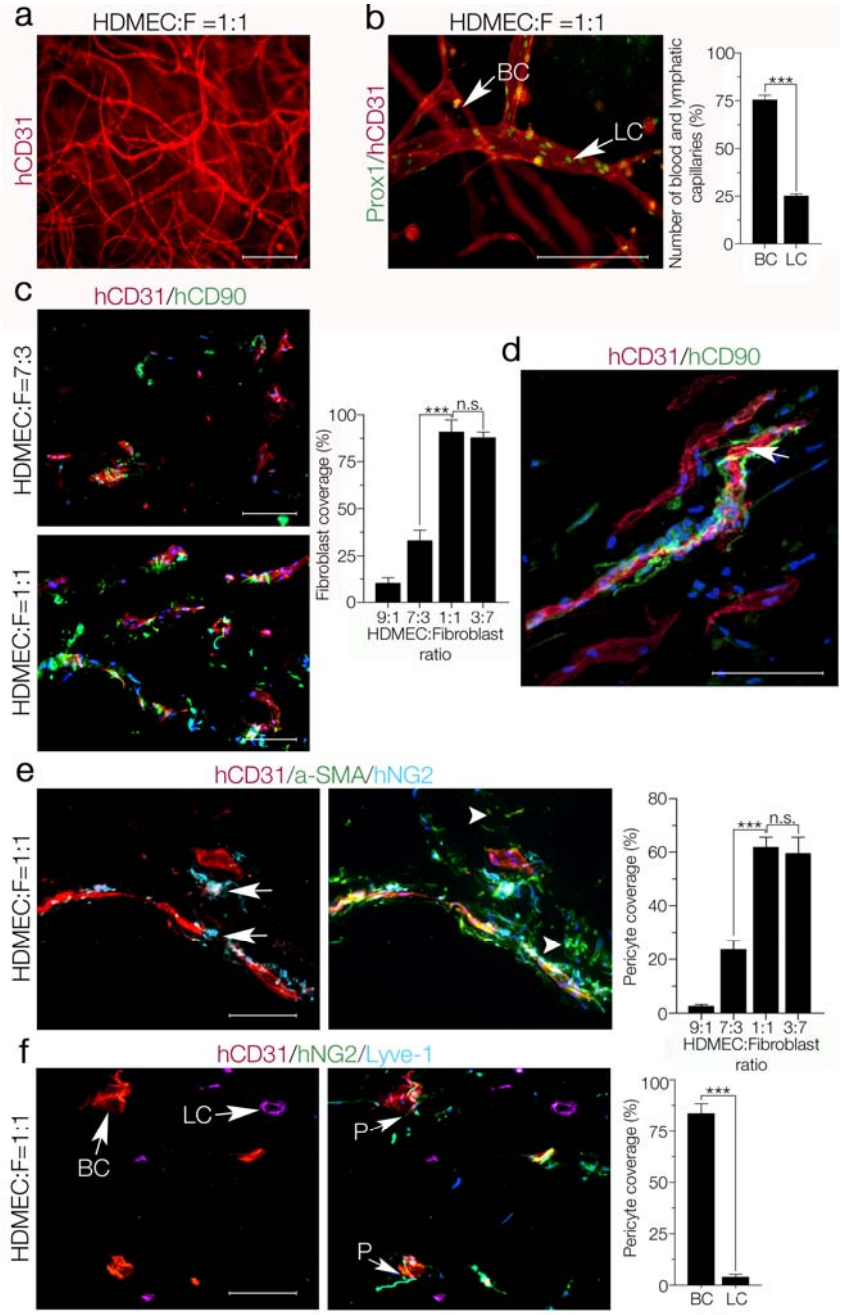

Figure 1. The bioengineering of human blood and lymphatic capillaries *in vitro*. (**a**) Wholemount hCD31 immunofluorescence staining of fibrin hydrogels (HDMEC:fibroblast=1:1) 21dai. (**b**) Quantification of blood and lymphatic capillary numbers by wholemount immunofluorescence stainings for hCD31 and Prox-1 21dai (n=5). BC: blood capillary, LC: lymphatic capillary. (**c**) Assessment of the percentage of fibroblast (CD90+)-covered capillaries in fibrin hydrogels integrated with different HDMEC:fibroblast ratios 21dai (n=5). (**d**) Confocal microscopy of immunofluorescence staining for hCD31 and hCD90 21dai. Arrow: capillary lumen. (**e**) Pericyte coverage was determined by immunofluorescence stainings for hCD31, a-SMA and hNG2 21dai (n=6). Arrows: hNG2+/a-SMA+ pericytes. Arrowheads: hNG2-/a-SMA+ (myo)fibroblasts. (**f**) Quantification of immunofluorescence stainings for hCD31, hNG2 and Lyve-1 21dai (n=5). BC: blood capillary, LC: lymphatic capillary, P: pericyte. Cell nuclei in C-F: blue. b, c, e and f: mean ± SEM. Scale bars: 100 µm.

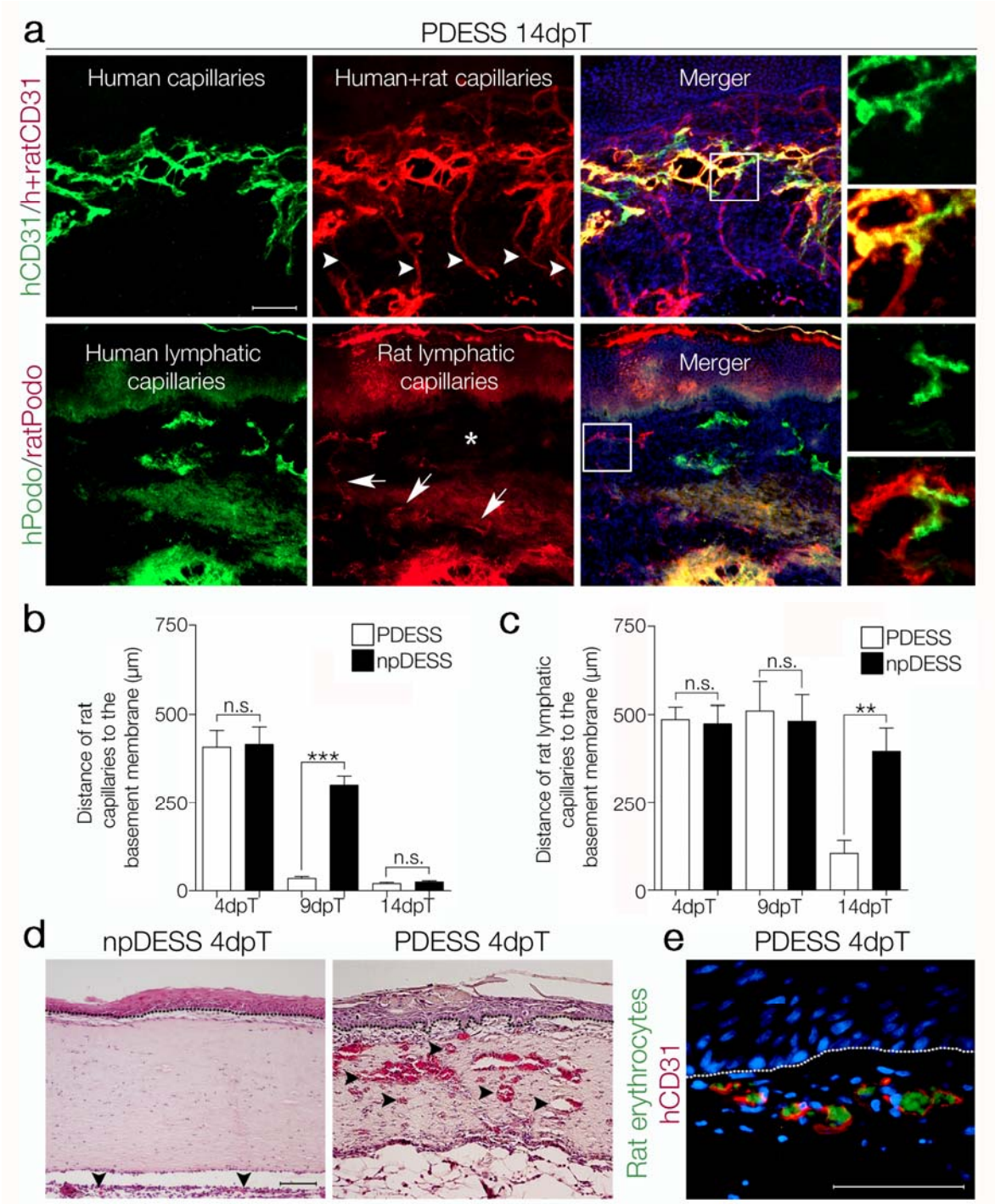

Figure 2. Prevascularization accelerates blood and lymphatic vascular regeneration *in vivo*. (**a**) Immunofluorescence staining for hCD31 and rat/hCD31 (upper panel), or for hPodoplanin and ratPodoplanin (bottom panel) on parallel sections of a PDESS 14dpT. Inserts: points of anastomosis. Arrowheads: rat "short-cut" capillaries. Arrows: rat lymphatic capillaries. (**b** and **c**) Quantifications of the distance of the uppermost rat blood (b) and lymphatic (c) capillary to the basement membrane in NPDESS and PDESS at 4, 9 and 14dpT (n=5). (**d**) Representative H&E-stainings on sections of NPDESS and PDESS excised 4dpT. Arrowheads: perfused blood capillaries. (**e**) Rat blood perfused capillaries within PDESS at 4dpT were exclusively of human origin (n=5). Autofluorescent rat erythrocytes in green. Cell nuclei in a and e: blue. d and e: black and white dotted lines mark the dermo-epidermal junction. b and c: mean ± SEM. Scale bars: 100 µm.

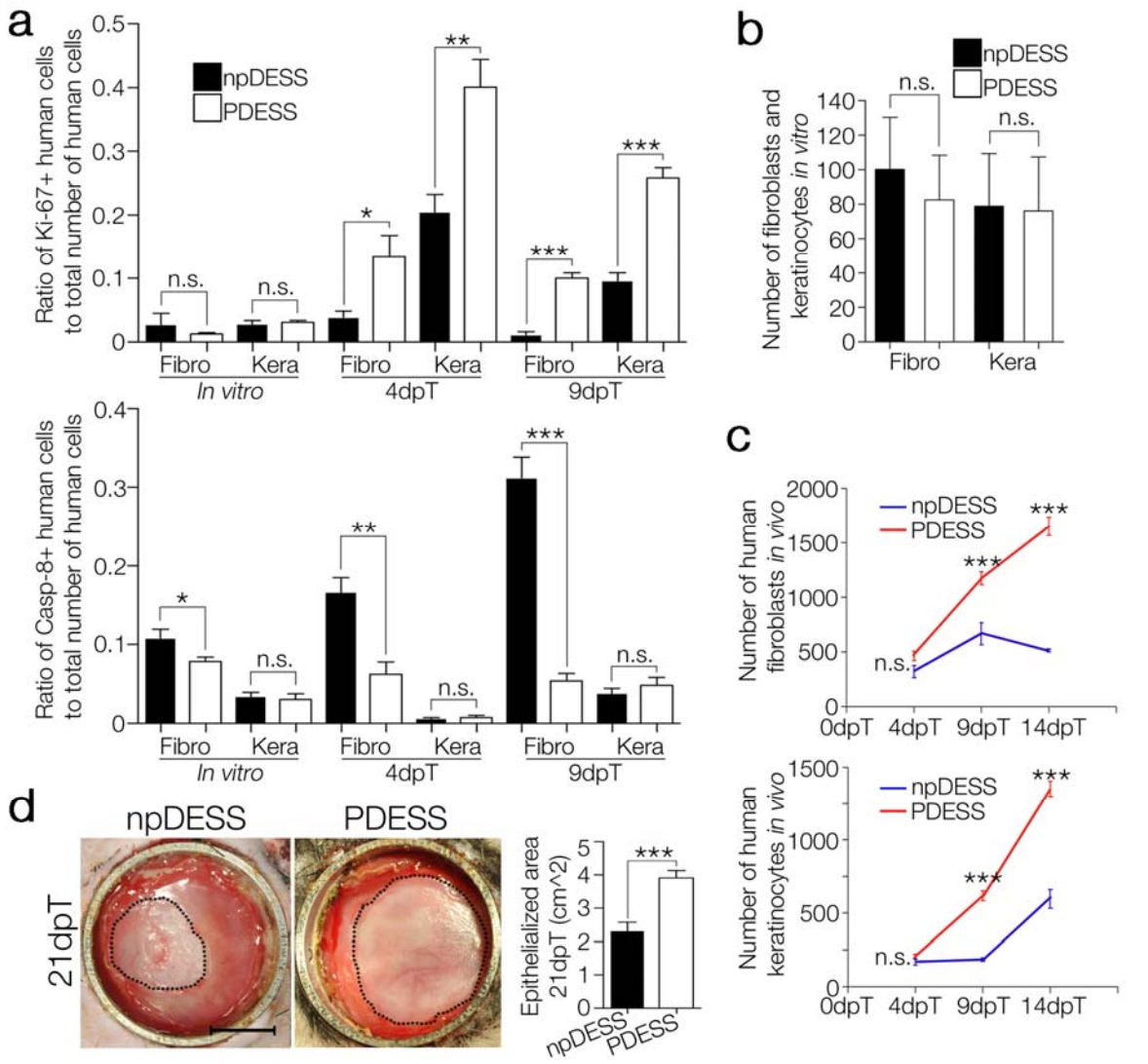

Figure 3. Rapid blood perfusion promotes proliferation, reduces apoptosis and decreases graft shrinkage. (**a**) Proliferation (upper panel) and apoptosis (down panel) were analyzed by quantifications of the ratio of Ki-67+ human cells to total human cells or caspase-8+ human cells to total human cells, respectively, on sections of NPDESS and PDESS *in vitro* (24dai) and at 4 and 9dpT (n=6). (**b**) No difference in the number of fibroblast and keratinocytes between NPDESS and PDESS *in vitro* (24dpS) (n=5). (**c**) Quantifications of the number of human keratinocytes and fibroblasts in NPDESS and PDESS at 4, 9 and 14dpT (n=5). (**d**) Shrinkage of the transplant was analyzed by quantification of the epithelialized area 21dpT (black dotted line) (n=4). a-d: mean ± SEM. Scale bar: 1cm.

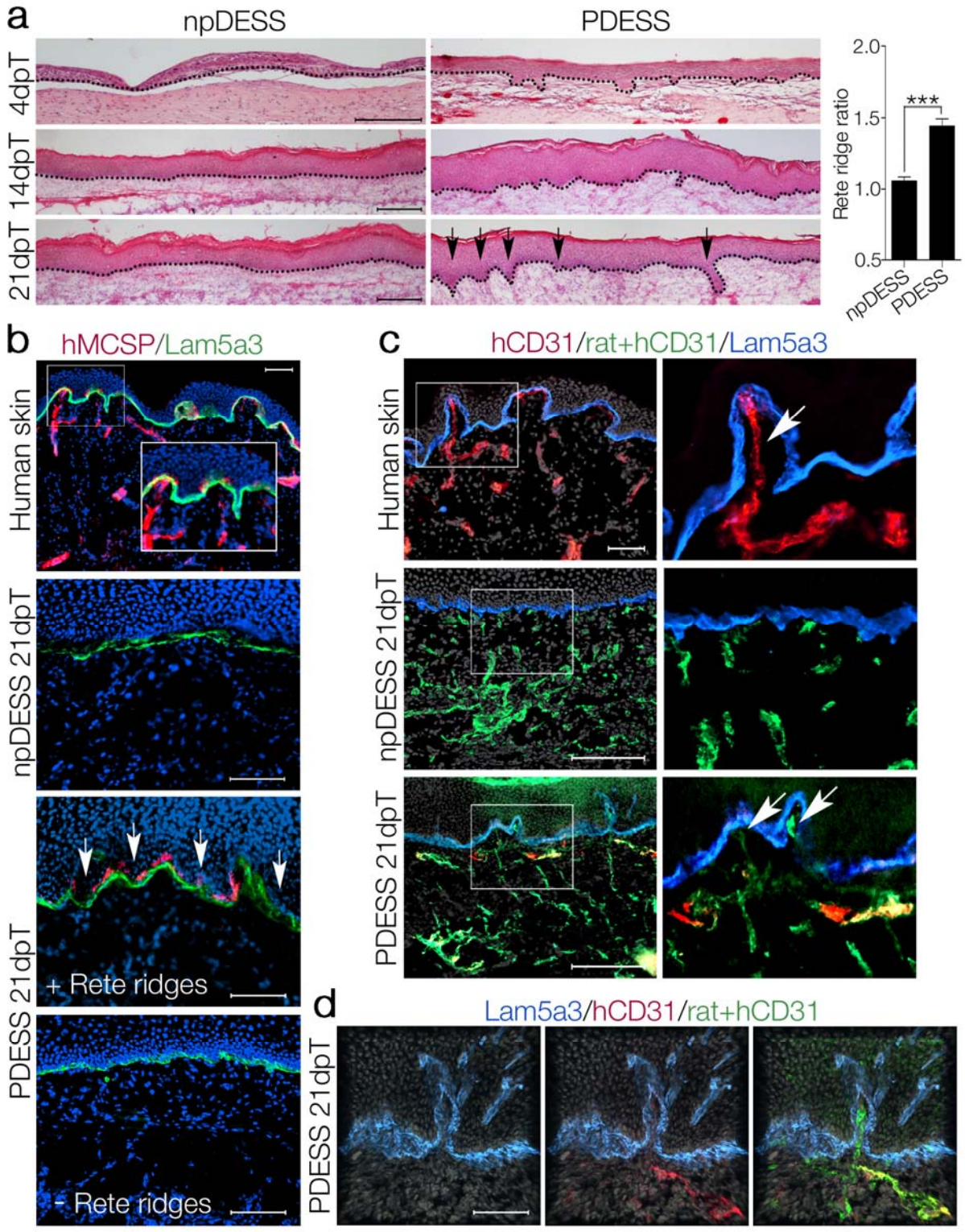

Figure 4. Prevascularization induces the organotypic remodeling of the dermo-epidermal junction (**a**) Representative H&E stainings on paraffin sections of NPDESS and PDESS at 9, 14 and 21dpT and quantification of the rete ridge ratio (length of the superficial epidermis divided by the length of the dermo-epidermal junction) (n=5). Black dotted line: dermo-epidermal junction. Arrows: rete ridges. (**b**) Immunofluorescence staining for hMCSP and Lam5a3 on sections of normal human skin and NPDESS/PDESS at 14dpT. Arrows: rete ridges. (**c**) Immunofluorescence staining for hCD31, rat/hCD31 and Lam5a3 on sections of normal human skin, and NPDESS and PDESS 21dpT. Arrows: capillary loops in human skin and PDESS. (**d**) Confocal microscopy of a capillary loop in PDESS 14dpT stained by immunofluorescence for hCD31, rat/hCD31 and Lam5a3. Cell nuclei in b: blue. Cell nuclei in c and d: grey. a: mean ± SEM. Scale bars: 100µm.

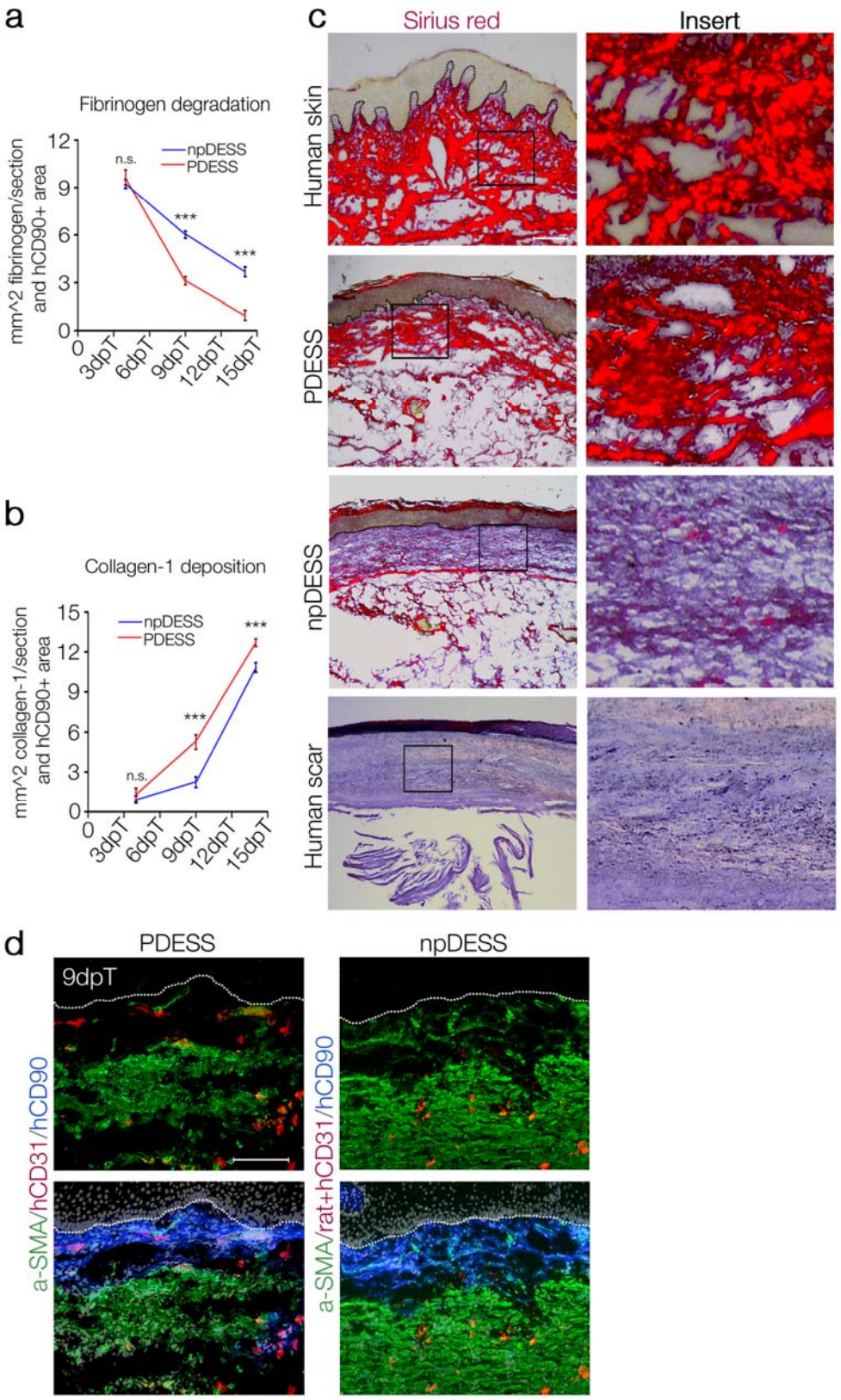

Figure 5. Prevascularization induces the regenerative remodeling of DESS. (**a**) Quantification of the fibrin-positive area on sections of NPDESS and PDESS at 4, 9 and 14dpT (n=5). (**b**) Quantification of collagen-1-positive area in NPDESS and PDESS at 4, 9 and 14dpT (n=5). (**c**) Representative analysis of normal human skin, human scar tissue, and NPDESS/PDESS for collagen bundle maturity and orientation using picrosirius red staining and polarized light 21dpT (n=5). (**d**) Immunofluorescence staining for α-SMA and hCD31 (PDESS) or rat+hCD31 and hCD90 (NPDESS) on sections of NPDESS and PDESS at 9dpT. c and d: black and white dotted lines mark the dermo-epidermal junction. Cell nuclei in e: grey. a, b: mean ± SEM. Scale bars: 100µm.

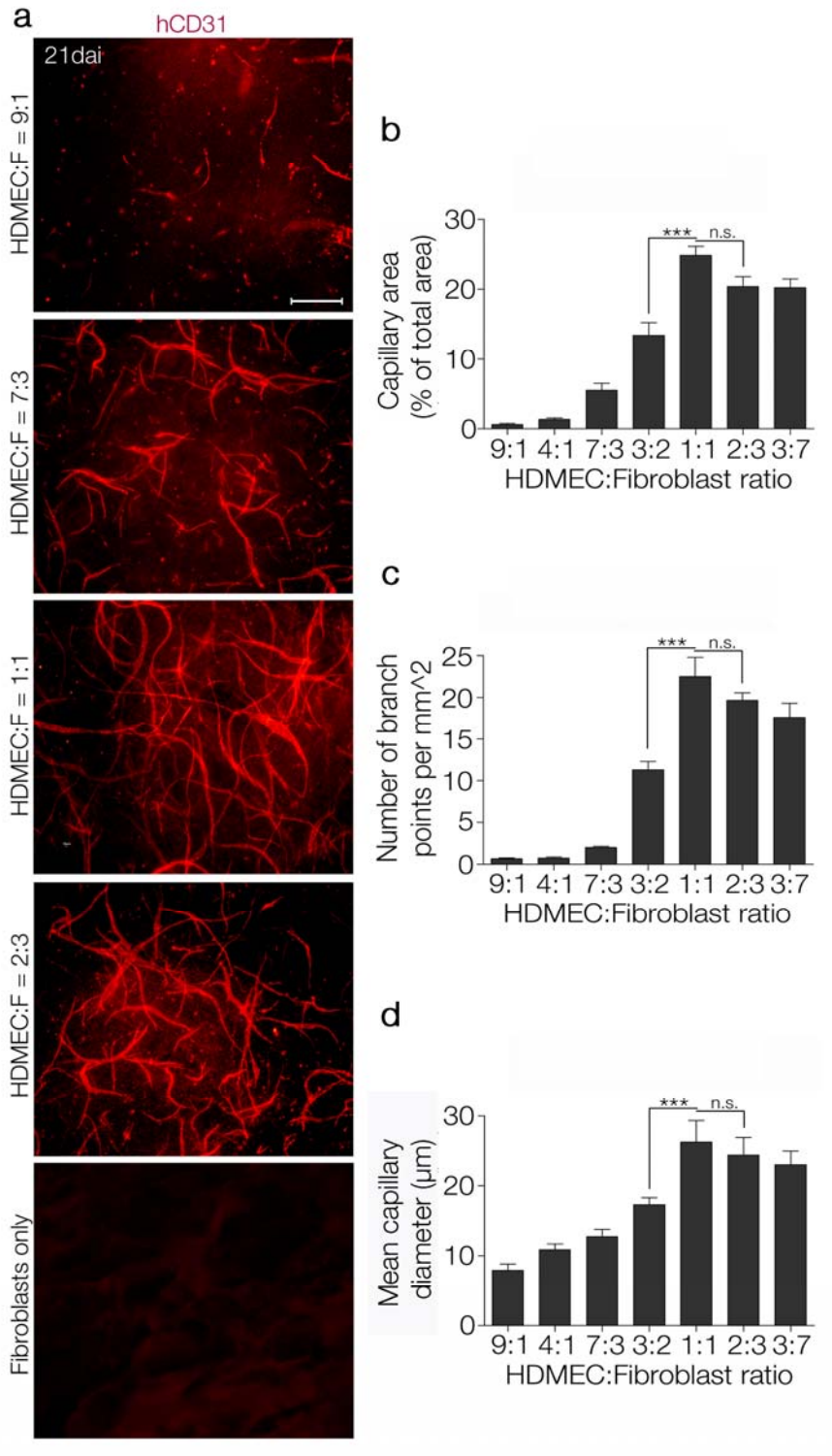

Figure S1. Determination of the optimal HDMEC/fibroblast ratio for *in vitro* capillary formation. (**a**) HDMEC and fibroblasts were integrated into fibrin hydrogels at different ratios and analyzed for capillary formation by wholemount immunofluorescence stainings for hCD31 21dai. (**b-d**) Quantification of the capillary area (b), the branch point density (c) and the mean capillary diameter (d) in fibrin hydrogels integrated with different HDMEC/fibroblast ratios (n=5). b-d: mean ± SEM. Scale bar: 100µm.

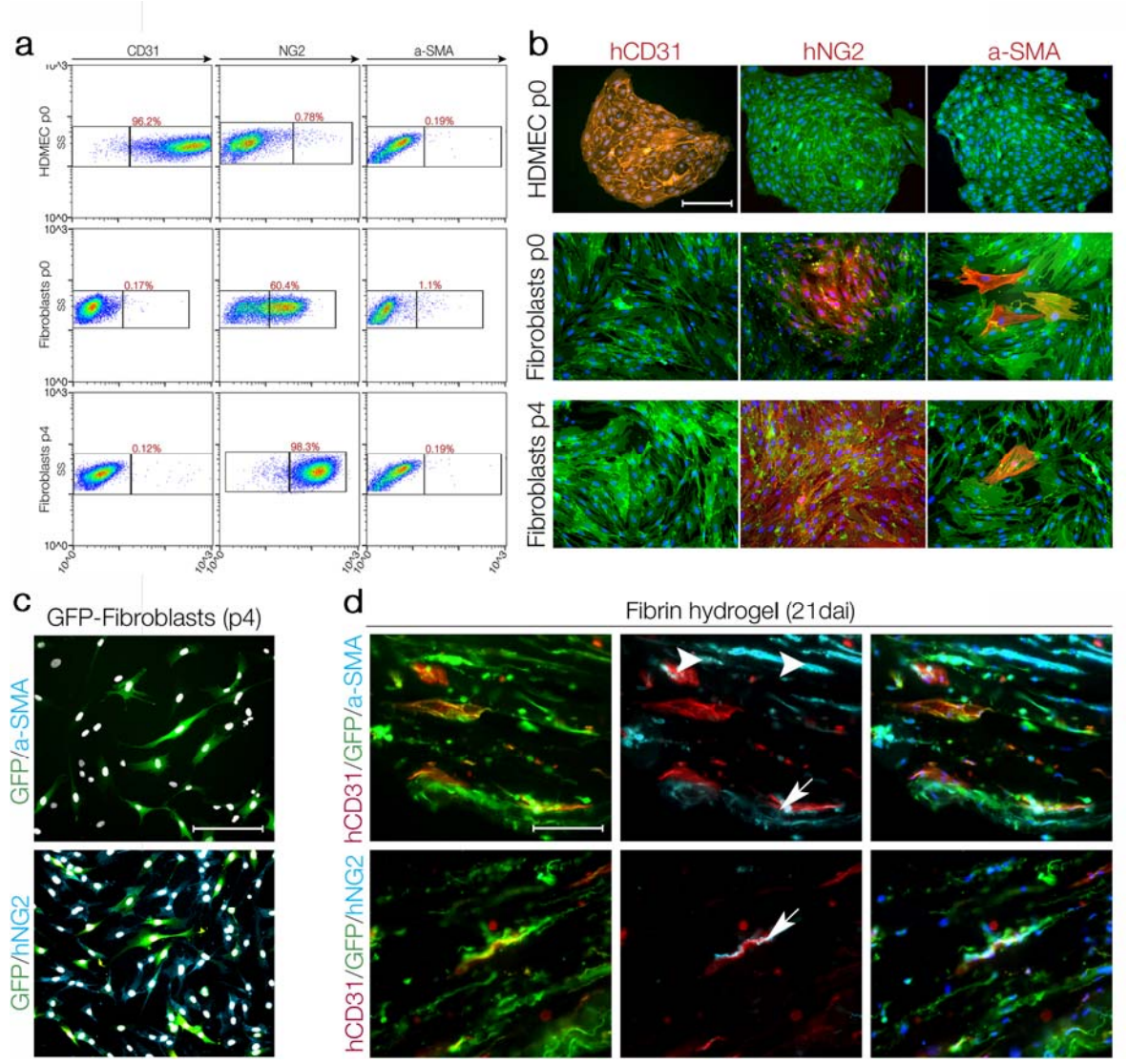

Figure S2. Fibroblasts differentiate into pericytes during *in vitro* prevascularization. (**a**) FACS analysis and representative immunofluorescent stainings using hCD31, hNG2 and a-SMA antibodies on HDMEC cultures at p0 and on fibroblast cultures on p0 and p4. (**b**) Representative immunofluorescence stainings for α-SMA and hNG2 of cultured GFP-transduced fibroblasts at p5. (**c**) After integration, GFP-transduced fibroblast gave rise to α-SMA+/NG2+ pericytes associated with capillaries (arrows) and α-SMA+/NG2- fibroblasts not associated with capillaries (arrowheads). Cell nuclei in a and c: blue. Cell nuclei in b: white. Scale bars: 100μm.

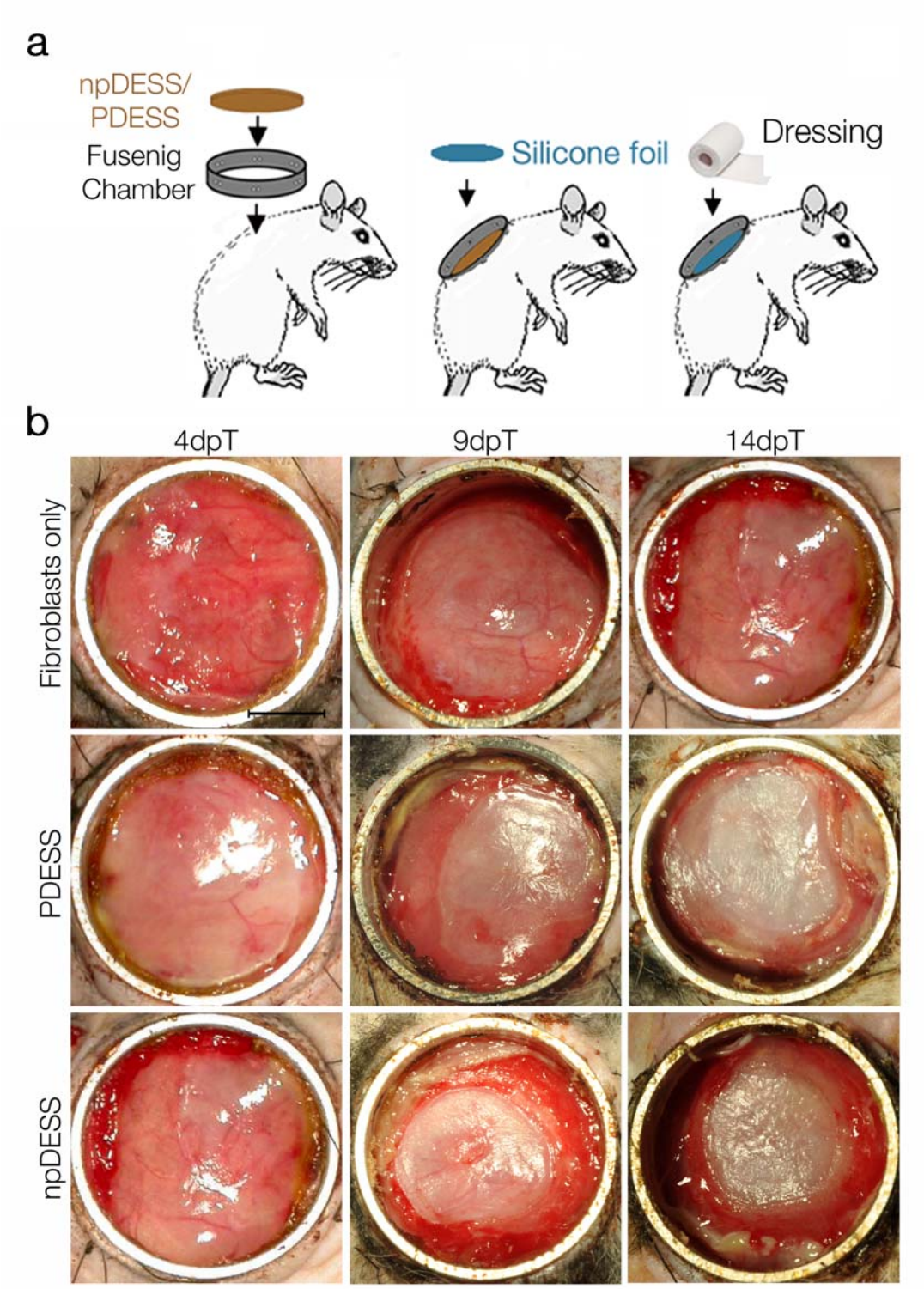

Figure S3. Transplantation procedure using the modified Fusenig chamber. (**a**) The transplant was sheltered from rat tissue overgrowth by a polypropylene ring sutured on the back of the rat. Drying of the transplant was prevented by overlying it with a silicone foil. (**b**) Representative macroscopic views on transplanted NPDESS and PDESS as well as fibrin gels integrated with fibroblasts only, at 4, 9 and 14dpT. Scale bar: 10mm.

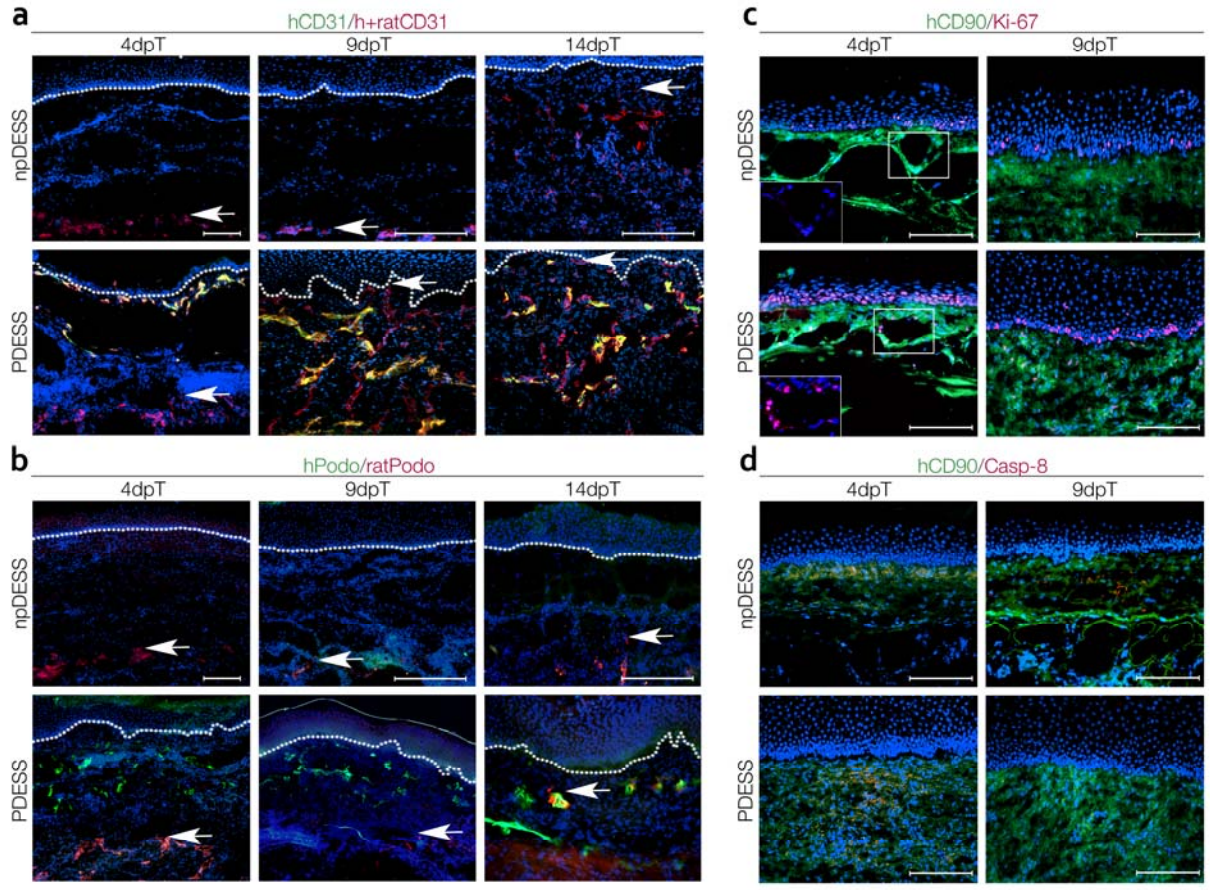

Figure S4. Delay of revascularization of NPDESS correlates with an early tissue crisis. The kinetics of rat blood and lymphatic revascularization were analyzed by immunofluorescent stainings of hCD31/rat+hCD31 (blood and lymphatic capillaries; **a**) and hPodoplanin/ratPodoplanin (lymphatic capillaries; **b**) on sections of NPDESS and PDESS at 4, 9 and 14dpT. For quantitative analysis, the distance of the uppermost rat blood/lymphatic capillary (arrows) to the dermo-epidermal junction (white dashed lines) was measured. (**c**) Representative immunofluorescence stainings for Ki-67 and hCD90 on sections of NPDESS and PDESS at 4 and 9dpT. Insert reveals a high number of Ki-67+ human dermal fibroblasts in PDESS 4dpT, whereas in NPDESS, human fibroblasts hardly expressed Ki-67 (n=6). (**d**) Representative immunofluorescence stainings for Casp-8 and hCD90 on sections of NPDESS and PDESS at 4 and 9dpT (n=6). Cell nuclei in a-d: blue. Scale bars: 100µm.

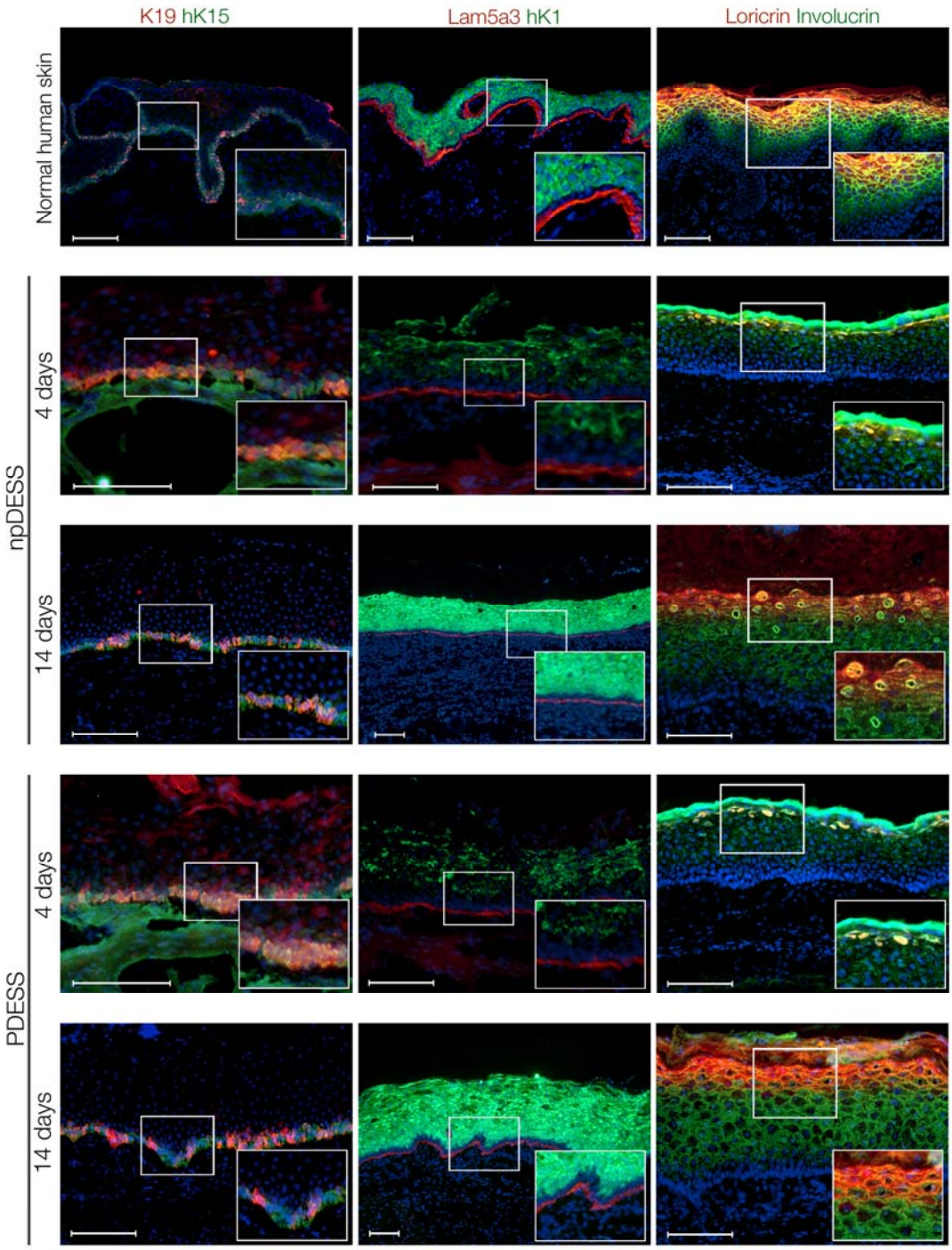

Figure S5. Analysis of epidermal homeostasis and differentiation in NPDESS and PDESS. NPDESS and PDESS were analyzed for differences in epidermal homeostasis and differentiation at 4 and 14dpT using the following marker pairs: K19/K15, K1/Lam5a3, Involucrin/Loricrin. No difference in the kinetics of the establishment of epidermal homeostasis and differentiation was found between NPDESS and PDESS. Cell nuclei are blue. Scale bars: 100µm.

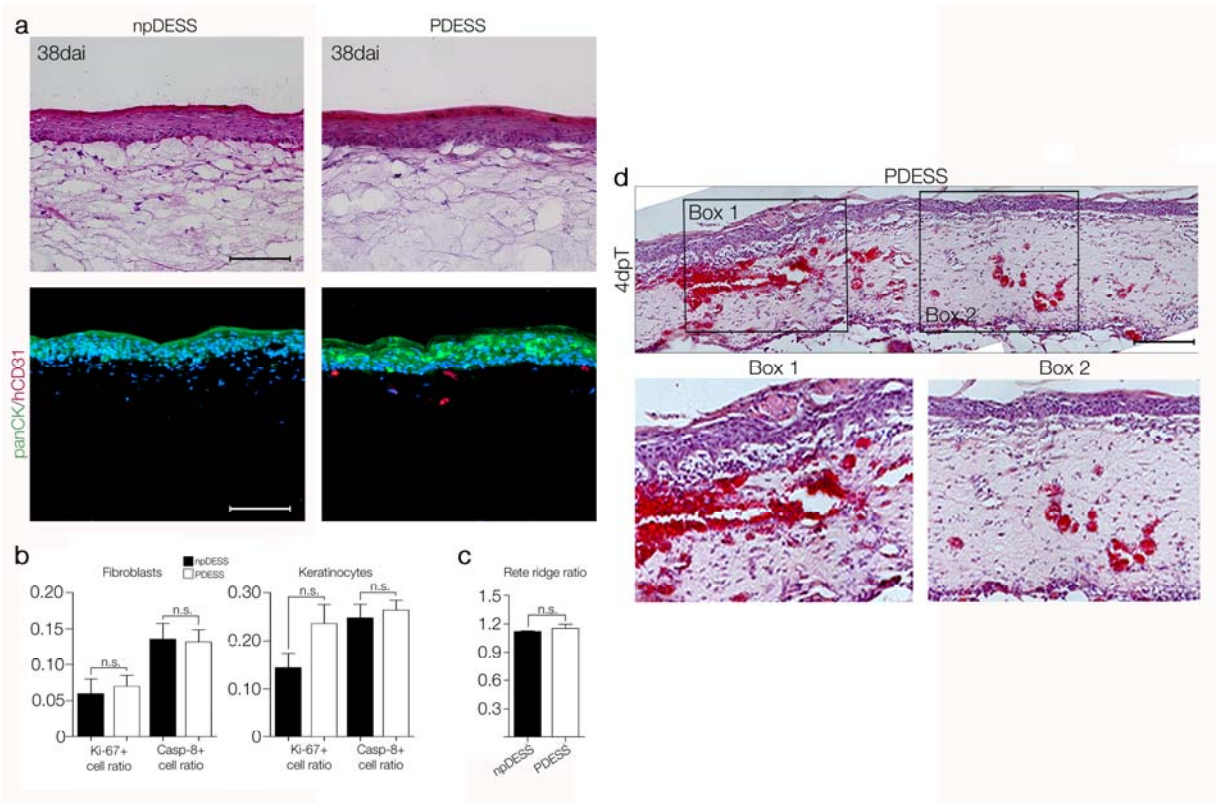

Figure S6. Endothelial structures alone are not sufficient to induce the effects of prevascularization. (**a**) Analysis of NPDESS and PDESS after air-liquid phase exposure 38dai, and of epidermal stratification, as demonstrated by H&E stainings (upper panel) or immunofluorescence stainings for hCD31 and panCK (bottom panel). (**b**) Similar proliferation and apoptosis of fibroblasts and keratinocytes of NPDESS and PDESS after *in vitro* stratification (n=4). (**c**) Similar rete-ridge ratio of NPDESS and PDESS after *in vitro* stratification (n=4). (**d**) Early after transplantation (4dpT), the density of perfused capillaries underneath the epidermis correlated with the development of epidermal protrusions (rete ridges). Box1 highlights a region with a high number of perfused capillaries and epidermal protrusions, Box2 highlights a region with a low number of perfused capillaries and epidermal protrusions. Cell nuclei in a: blue. b and c: mean ± SEM. Scale bars: 100µm.

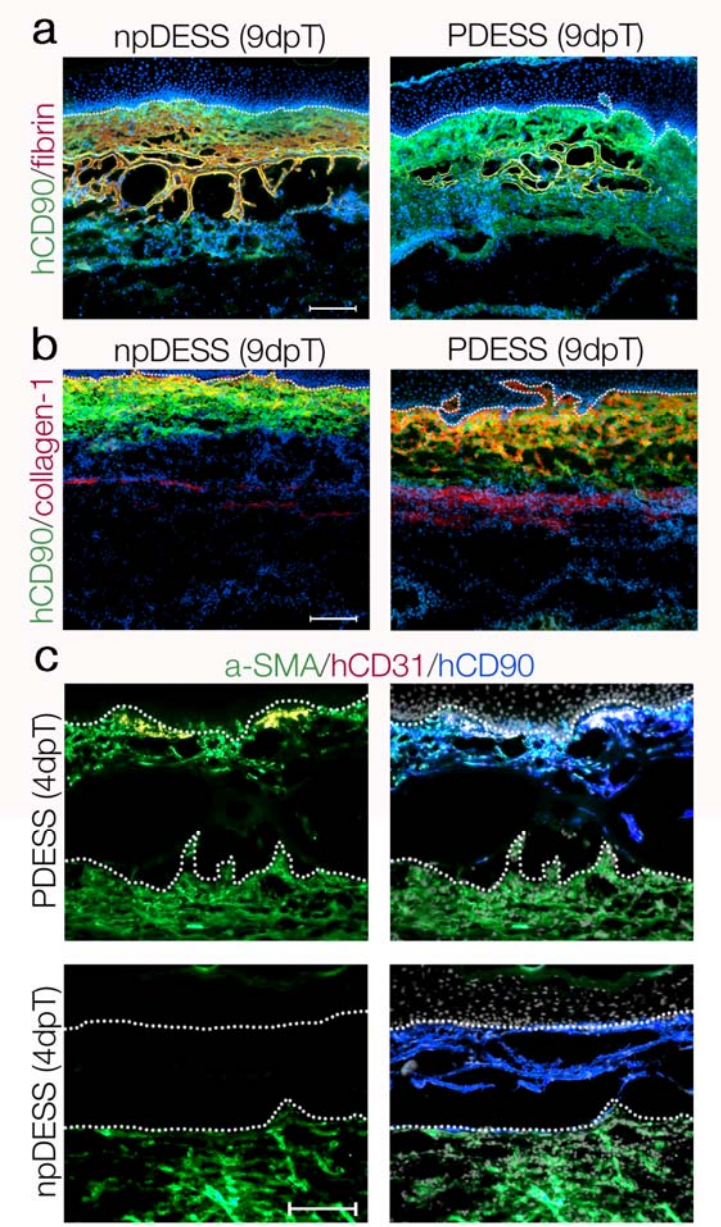

Figure S7. Prevascularization accelerates dermal remodelling and myofibroblast clearance. (**a**) Representative immunofluorescence staining for hCD90 and fibrin on sections of NPDESS and PDESS at 9dpT. (**b**) Representative immunofluorescence staining for hCD90 and collagen-1 on sections of NPDESS and PDESS at 9dpT. (**c**) Representative immunofluorescence staining of a-SMA, hCD31 and hCD90 on sections of NPDESS and PDESS at 4dpT. Cell nuclei are blue. White dashed line in a, b and d marks the dermo-epidermal junction. Scale bars: 100μm.

3 CONCLUSIONS

The aim of my thesis was to bioengineer human dermo-epidermal skin substitutes (DESS) containing both functional blood and lymphatic capillaries, and to analyze the biological effects of prevascularization on DESS reconstitution *in vivo*. Despite the increasing recognition of the critical importance of the lymphatic system in the human body, the publications presented in this work represent the first reports about the simultaneous generation of functional blood and lymphatic capillaries within an artificial organ like the skin.

To achieve the simultaneous bioengineering of blood and lymphatic capillaries, I took advantage of the heterogeneity of human dermal microvascular endothelial cells (HDMEC) which are known to consist of blood and lymphatic endothelial cells[254] and therefore provide the building blocks for the development of these two distinc capillary types. After integration into fibrin hydrogels, the HDMEC spontaneously developed into lumenized blood and lymphatic capillaries that could be distinguished by the expression of lymph-specific markers as well as by the lymph-specific ability to uptake fluid *in vitro* and *in vivo*[255]. Interestingly, the only reports about the bioengineering of lymphatic capillaries so far included the use of a technically demanding bioreactor and constant interstitial flow[256-258]. However, these studies did not analyze the bioengineered lymphatic capillaries after their transplantation *in vivo*. I found that the lymphatic capillaries bioengineered by our method physiologically responded to lymphangiogenic and anti-lymphangiogenic stimuli. Furthermore, in contrast to the blood capillaries, the lymphatic capillaries were not covered by pericytes. *In vivo*, the lymphatic capillaries anastomosed with the recipient lymphatic vasculature at around 14 days after transplantation, hence triggering the drainage of fluids from the graft. Likewise, the bioengineered blood capillaries anastomosed with the rat blood capillaries, and blood anastomosis clearly preceeded lymphatic anastomosis. These data provide evidence that the simultaneous bioengineering of functionally distinct blood and lymphatic capillaries by integration of HDMEC into fibrin hydrogels is possible. However, the prevascularized fibrin hydrogels presented in this work qualify not only as an optimally and physiologically vascularized dermal template for the generation of DESS, but also as a valuable *in vitro* model system

and screening tool to identify signalling pathways, chemicals and compounds involved in human blood and lymphatic vessel formation.

Analysis of the survival and integration of the bioengineered blood capillaries revealed that in addition to the rapid anastomosis of the blood capillaries at 4 days after transplantation, prevascularization promoted the ingrowth of rat blood capillaries into the graft. These results corroborate an earlier study showing that a preexisting microvascular network benefits *in vivo* revascularization of a microvascularized tissue-engineered skin substitute[238]. Intriguingly, we found the rat lymphatic ingrowth also was speeded up in PDESS, even though at a later stage than blood capillary ingrowth. Therefore, prevascularization with blood and lymphatic capillaries accelerated blood and lymphatic vascular regeneration by two discinct mechanisms: anastomosis and promotion of rat capillary ingrowth.

To analyze the effects of prevascularization on DESS reconstitution, I compared the healing of PDESS and NPDESS after transplantation, focussing on several central aspects of cutaneous healing cascade including cell proliferation, cell apoptosis, graft shrinkage, dermal remodelling, collagen deposition and myofibroblast clearance. Intriguingly, I found that prevascularization improved not only healing processes that are known to be strictly dependent on oxygen (cell proliferation and apoptosis, collagen deposition, myofibroblast differentiation), but additionally shifted the reconstitution of PDESS from scar formation towards regeneration. This shift was accompanied by the deposition of randomly organized collagen bundles in a non-scar fashion as well as by the *de novo* formation of rete ridges and capillary loops. Even though a detailed mechanistic insight into the molecular and cellular pathways underlying the observed beneficial effects of prevascularization on skin reconstitution was beyond the scope of this work, my results suggest a combination of different factors that could have acted in concert: First, oxygen is required for multiple processes of the normal cutaneous healing cascade, including the production of energy equivalents like ATP, the production of reactive oxygen species (ROS) necessary for inflammatory processes, collagen production, re-epithelialization, growth factor secretion and the differentiation of fibroblasts into myofibroblasts[144,146,238]. Therefore, prevascularization of DESS is likely to promote skin regeneration simply by accelerating the delivery of oxygen to the energetically demanding tissue during healing.

Secondly, I showed that the incorporation of pre-existing lymphatic capillaries into DESS improves the drainage of fluids after transplantation. Even though lymphatic anastomosis

occurred after blood anastomosis, it is tempting to speculate that the improved fluid drainage could have further contributed to the improved healing of PDESS at a later stage, for example by decreasing the risk of edema/seroma formation - accumulations of exessive interstitial tissue fluids - which have been shown to be detrimental for the wound healing process[240]. Furthermore, the increased delivery of fluids from the bioengineered blood capillaries to the healing tissue is likely to impose the need for increased drainage of these fluids by lymphatic capillaries.

And thirdly, there is a growing body of evidence indicating that endothelial cells provide inductive signals during the development of different organs independent of their blood and serum transporting role[3,208,209,211]. Performing *in vitro* stratification experiments, I found that the development of rete ridges and capillary loops, which were observed exclusively after the transplantation of PDESS, was not initiated simply by the presence of BEC and LEC-derived capillary structures. Likewise, the changes in the proliferation and apoptosis of human fibroblasts and keratinocytes between NPDESS and PDESS did not occur *in vitro*. Therefore, my data collectively suggest that it was the rapid perfusion of the bioengineered blood capillary network that unlocked latent regenerative processes and shifted the healing of PDESS from scar formation towards regeneration.

Finally, a great deal of work was attributed to the analysis of conditions that improve the generation of blood and lymphatic capillaries. Endothelial cells have been shown to require the presence of mesenchymal cells for *in vitro* capillary formation[207]. Therefore, I analyzed the effect of seeding different HDMEC : fibroblast ratios into fibrin hydrogels. Interestingly, HDMEC : fibroblast ratios that showed most extensive capillary formation also maximized the clustering of pericytes around the capillaries, underlining the essential function of pericytes for *in vitro* angiogenesis[207]. The pericytes were derived from the fibroblasts and specifically targeted the blood capillaries, whereas they hardly associated with lymphatic capillaries. In experiments using pure LECs, LEC required the physical presence of fibroblasts for capillary formation similar to BEC. Clearly, the function of fibroblasts during lymphatic capillary formation *in vitro* is not to stabilize the developing capillaries as pericytes. Other functions could be the secretion of non-soluble lymphangiogenic factors or extracellular matrix proteinases that degrade and prepare the fibrin hydrogel for lymphatic capillary morphgenesis.

Further studies now will have to unravel the exact contribution of the bioengineered blood and lymphatic capillaries to the observed effects and to analyze the underlying molecular pathways. Also, it will be important to reduce the production time of PDESS to a time frame that is compatible with the needs of a given patient. Presently, we need 20 days to produce a PDESS of human origin that gets perfused within 3-4 days after transplantation. Consequently, these grafts would not be applicable as an initial surgical treatment of patients suffering from acute skin injuries. However, we may be able to shorten the time frame of production, once we have systematically optimized the GMP production process of generating PDESS. A patient suffering from severe skin injury may then profit from these grafts at about two weeks after the start of his surgical treatment. In any case, PDESS can be applied to a broad spectrum of elective cases, such as patients suffering from congenital nevi, disfiguring scars or tumors.

4 REFERENCES

1. Albrecht, R. & Zeth, K. Structural basis of outer membrane protein biogenesis in bacteria. *The Journal of biological chemistry* **286**, 27792-27803.
2. Proksch, E., Brandner, J.M. & Jensen, J.M. The skin: an indispensable barrier. *Experimental dermatology* **17**, 1063-1072 (2008).
3. Yamaguchi, Y.*, et al.* Human skin responses to UV radiation: pigment in the upper epidermis protects against DNA damage in the lower epidermis and facilitates apoptosis. *Faseb J* **20**, 1486-1488 (2006).
4. Elias, P.M. & Menon, G.K. Structural and lipid biochemical correlates of the epidermal permeability barrier. *Advances in lipid research* **24**, 1-26 (1991).
5. Schafer, M. & Werner, S. The cornified envelope: a first line of defense against reactive oxygen species. *The Journal of investigative dermatology* **131**, 1409-1411.
6. Bayat, A., McGrouther, D.A. & Ferguson, M.W. Skin scarring. *BMJ (Clinical research ed* **326**, 88-92 (2003).
7. Kershaw, E.E. & Flier, J.S. Adipose tissue as an endocrine organ. *The Journal of clinical endocrinology and metabolism* **89**, 2548-2556 (2004).
8. Wajchenberg, B.L. Subcutaneous and visceral adipose tissue: their relation to the metabolic syndrome. *Endocrine reviews* **21**, 697-738 (2000).
9. Blanpain, C. & Fuchs, E. Epidermal stem cells of the skin. *Annual review of cell and developmental biology* **22**, 339-373 (2006).
10. Jones, P. & Simons, B.D. Epidermal homeostasis: do committed progenitors work while stem cells sleep? *Nature reviews* **9**, 82-88 (2008).
11. Andreadis, S.T., Hamoen, K.E., Yarmush, M.L. & Morgan, J.R. Keratinocyte growth factor induces hyperproliferation and delays differentiation in a skin equivalent model system. *Faseb J* **15**, 898-906 (2001).
12. Rochat, A., Kobayashi, K. & Barrandon, Y. Location of stem cells of human hair follicles by clonal analysis. *Cell* **76**, 1063-1073 (1994).
13. Mihic-Probst, D.*, et al.* Tumor cell plasticity and angiogenesis in human melanomas. *PloS one* **7**, e33571.
14. Polakovicova, S., Seidenberg, H., Mikusova, R., Polak, S. & Pospisilova, V. Merkel cells--review on developmental, functional and clinical aspects. *Bratislavske lekarske listy* **112**, 80-87.
15. Amagai, M. Adhesion molecules. I: Keratinocyte-keratinocyte interactions; cadherins and pemphigus. *The Journal of investigative dermatology* **104**, 146-152 (1995).
16. Kim, D.K. & Holbrook, K.A. The appearance, density, and distribution of Merkel cells in human embryonic and fetal skin: their relation to sweat gland and hair follicle development. *The Journal of investigative dermatology* **104**, 411-416 (1995).
17. Jimbow, K., Quevedo, W.C., Jr., Fitzpatrick, T.B. & Szabo, G. Some aspects of melanin biology: 1950-1975. *The Journal of investigative dermatology* **67**, 72-89 (1976).
18. Wasmeier, C., Hume, A.N., Bolasco, G. & Seabra, M.C. Melanosomes at a glance. *Journal of cell science* **121**, 3995-3999 (2008).
19. Katz, S.I., Tamaki, K. & Sachs, D.H. Epidermal Langerhans cells are derived from cells originating in bone marrow. *Nature* **282**, 324-326 (1979).
20. Holbrook, K.A. Biologic structure and function: perspectives on morphologic approaches to the study of the granular layer keratinocyte. *The Journal of investigative dermatology* **92**, 84S-104S (1989).
21. Hohl, D. [A new star in the heavens of epidermal proteins: loricrin--what is it?]. *Der Hautarzt; Zeitschrift fur Dermatologie, Venerologie, und verwandte Gebiete* **41**, 299-301 (1990).
22. Bragulla, H.H. & Homberger, D.G. Structure and functions of keratin proteins in simple, stratified, keratinized and cornified epithelia. *Journal of anatomy* **214**, 516-559 (2009).
23. Briggaman, R.A. & Wheeler, C.E., Jr. The epidermal-dermal junction. *The Journal of investigative dermatology* **65**, 71-84 (1975).
24. Haass, N.K. & Herlyn, M. Normal human melanocyte homeostasis as a paradigm for understanding melanoma. *The journal of investigative dermatology. Symposium proceedings / the Society for Investigative Dermatology, Inc* **10**, 153-163 (2005).

25. Koch, S., Kohl, K., Klein, E., von Bubnoff, D. & Bieber, T. Skin homing of Langerhans cell precursors: adhesion, chemotaxis, and migration. *The Journal of allergy and clinical immunology* **117**, 163-168 (2006).
26. Deane, J.A. & Hickey, M.J. Molecular mechanisms of leukocyte trafficking in T-cell-mediated skin inflammation: insights from intravital imaging. *Expert reviews in molecular medicine* **11**, e25 (2009).
27. Draheim, K.M. & Lyle, S. Epithelial stem cells. *Methods in molecular biology (Clifton, N.J* **750**, 261-274.
28. Ross, F.P. & Christiano, A.M. Nothing but skin and bone. *The Journal of clinical investigation* **116**, 1140-1149 (2006).
29. Raghunath, M.*, et al.* Cross-linking of the dermo-epidermal junction of skin regenerating from keratinocyte autografts. Anchoring fibrils are a target for tissue transglutaminase. *The Journal of clinical investigation* **98**, 1174-1184 (1996).
30. Gupta, R., Woodley, D.T. & Chen, M. Epidermolysis bullosa acquisita. *Clinics in dermatology* **30**, 60-69.
31. Gurtner, G.C., Werner, S., Barrandon, Y. & Longaker, M.T. Wound repair and regeneration. *Nature* **453**, 314-321 (2008).
32. Ghahary, A. & Ghaffari, A. Role of keratinocyte-fibroblast cross-talk in development of hypertrophic scar. *Wound Repair Regen* **15 Suppl 1**, S46-53 (2007).
33. Frayn, K.N., Arner, P. & Yki-Jarvinen, H. Fatty acid metabolism in adipose tissue, muscle and liver in health and disease. *Essays in biochemistry* **42**, 89-103 (2006).
34. Kipling, D., Davis, T., Ostler, E.L. & Faragher, R.G. What can progeroid syndromes tell us about human aging? *Science (New York, N.Y* **305**, 1426-1431 (2004).
35. De Val, S. & Black, B.L. Transcriptional control of endothelial cell development. *Developmental cell* **16**, 180-195 (2009).
36. Larrivee, B., Freitas, C., Suchting, S., Brunet, I. & Eichmann, A. Guidance of vascular development: lessons from the nervous system. *Circulation research* **104**, 428-441 (2009).
37. Rhoades R., P.R. *Human Physiology 4th Edition*, (2003).
38. Adams, R.H. & Alitalo, K. Molecular regulation of angiogenesis and lymphangiogenesis. *Nature reviews* **8**, 464-478 (2007).
39. Braverman, I.M. The cutaneous microcirculation: ultrastructure and microanatomical organization. *Microcirculation* **4**, 329-340 (1997).
40. Meyer, W., Kacza, J., Zschemisch, N.H., Godynicki, S. & Seeger, J. Observations on the actual structural conditions in the stratum superficiale dermidis of porcine ear skin, with special reference to its use as model for human skin. *Ann Anat* **189**, 143-156 (2007).
41. Podjasek, J.O., Wetter, D.A., Pittelkow, M.R. & Wada, D.A. Cutaneous small-vessel vasculitis associated with solid organ malignancies: the Mayo Clinic experience, 1996 to 2009. *Journal of the American Academy of Dermatology* **66**, e55-65.
42. Kosaka, M., Kato, T. & Kawana, S. Cutaneous small vessel vasculitis accompanied by pustulosis palmaris et plantaris. *Case reports in dermatology* **4**, 66-71.
43. Bergers, G. & Song, S. The role of pericytes in blood-vessel formation and maintenance. *Neuro-oncology* **7**, 452-464 (2005).
44. Mottaz, J.H., Zelickson, A.S., Thorne, E.G. & Wachs, G. Blood vessel changes in psoriatic skin. *Acta dermato-venereologica* **53**, 195-198 (1973).
45. Choi, K., Kennedy, M., Kazarov, A., Papadimitriou, J.C. & Keller, G. A common precursor for hematopoietic and endothelial cells. *Development (Cambridge, England)* **125**, 725-732 (1998).
46. Chung, Y.S.*, et al.* Lineage analysis of the hemangioblast as defined by FLK1 and SCL expression. *Development (Cambridge, England)* **129**, 5511-5520 (2002).
47. Coultas, L., Chawengsaksophak, K. & Rossant, J. Endothelial cells and VEGF in vascular development. *Nature* **438**, 937-945 (2005).
48. Armstrong, E.J. & Bischoff, J. Heart valve development: endothelial cell signaling and differentiation. *Circulation research* **95**, 459-470 (2004).
49. Lin, F., Wang, N. & Zhang, T.C. The role of endothelial-mesenchymal transition in development and pathological process. *IUBMB life* **64**, 717-723.
50. Risau, W. Differentiation of endothelium. *Faseb J* **9**, 926-933 (1995).
51. Risau, W. & Flamme, I. Vasculogenesis. *Annual review of cell and developmental biology* **11**, 73-91 (1995).
52. Asahara, T.*, et al.* Bone marrow origin of endothelial progenitor cells responsible for postnatal vasculogenesis in physiological and pathological neovascularization. *Circulation research* **85**, 221-228 (1999).
53. Asahara, T.*, et al.* Isolation of putative progenitor endothelial cells for angiogenesis. *Science (New York, N.Y* **275**, 964-967 (1997).

54. Asahara, T.*, et al.* VEGF contributes to postnatal neovascularization by mobilizing bone marrow-derived endothelial progenitor cells. *Embo J* **18**, 3964-3972 (1999).
55. Schatteman, G.C. Adult bone marrow-derived hemangioblasts, endothelial cell progenitors, and EPCs. *Current topics in developmental biology* **64**, 141-180 (2004).
56. Urbich, C. & Dimmeler, S. Endothelial progenitor cells: characterization and role in vascular biology. *Circulation research* **95**, 343-353 (2004).
57. Takahashi, T.*, et al.* Ischemia- and cytokine-induced mobilization of bone marrow-derived endothelial progenitor cells for neovascularization. *Nature medicine* **5**, 434-438 (1999).
58. Reyes, M.*, et al.* Origin of endothelial progenitors in human postnatal bone marrow. *The Journal of clinical investigation* **109**, 337-346 (2002).
59. Schmeisser, A.*, et al.* Monocytes coexpress endothelial and macrophagocytic lineage markers and form cord-like structures in Matrigel under angiogenic conditions. *Cardiovascular research* **49**, 671-680 (2001).
60. Beltrami, A.P.*, et al.* Adult cardiac stem cells are multipotent and support myocardial regeneration. *Cell* **114**, 763-776 (2003).
61. Miranville, A.*, et al.* Improvement of postnatal neovascularization by human adipose tissue-derived stem cells. *Circulation* **110**, 349-355 (2004).
62. Wurmser, A.E.*, et al.* Cell fusion-independent differentiation of neural stem cells to the endothelial lineage. *Nature* **430**, 350-356 (2004).
63. Vokes, S.A.*, et al.* Hedgehog signaling is essential for endothelial tube formation during vasculogenesis. *Development (Cambridge, England)* **131**, 4371-4380 (2004).
64. Carmeliet, P.*, et al.* Abnormal blood vessel development and lethality in embryos lacking a single VEGF allele. *Nature* **380**, 435-439 (1996).
65. Shalaby, F.*, et al.* Failure of blood-island formation and vasculogenesis in Flk-1-deficient mice. *Nature* **376**, 62-66 (1995).
66. Carmeliet, P. Angiogenesis in health and disease. *Nature medicine* **9**, 653-660 (2003).
67. Thurston, G. Role of Angiopoietins and Tie receptor tyrosine kinases in angiogenesis and lymphangiogenesis. *Cell and tissue research* **314**, 61-68 (2003).
68. Sacchi, G., Weber, E., Agliano, M., Raffaelli, N. & Comparini, L. The structure of superficial lymphatics in the human thigh: precollectors. *The Anatomical record* **247**, 53-62 (1997).
69. Casley-Smith, J.R. The fine structure and functioning of tissue channels and lymphatics. *Lymphology* **13**, 177-183 (1980).
70. Jurisic, G. & Detmar, M. Lymphatic endothelium in health and disease. *Cell and tissue research* **335**, 97-108 (2009).
71. Gerli, R., Solito, R., Weber, E. & Agliano, M. Specific adhesion molecules bind anchoring filaments and endothelial cells in human skin initial lymphatics. *Lymphology* **33**, 148-157 (2000).
72. Danussi, C.*, et al.* Emilin1 deficiency causes structural and functional defects of lymphatic vasculature. *Molecular and cellular biology* **28**, 4026-4039 (2008).
73. Bridenbaugh, E.A., Gashev, A.A. & Zawieja, D.C. Lymphatic muscle: a review of contractile function. *Lymphatic research and biology* **1**, 147-158 (2003).
74. Trzewik, J., Mallipattu, S.K., Artmann, G.M., Delano, F.A. & Schmid-Schonbein, G.W. Evidence for a second valve system in lymphatics: endothelial microvalves. *Faseb J* **15**, 1711-1717 (2001).
75. Schmid-Schonbein, G.W. The second valve system in lymphatics. *Lymphatic research and biology* **1**, 25-29; discussion 29-31 (2003).
76. Cueni, L.N. & Detmar, M. The lymphatic system in health and disease. *Lymphatic research and biology* **6**, 109-122 (2008).
77. Machnik, A.*, et al.* Macrophages regulate salt-dependent volume and blood pressure by a vascular endothelial growth factor-C-dependent buffering mechanism. *Nature medicine* **15**, 545-552 (2009).
78. Ryan, T.J. Structure and function of lymphatics. *The Journal of investigative dermatology* **93**, 18S-24S (1989).
79. Braverman, I.M. & Keh-Yen, A. Ultrastructure of the human dermal microcirculation. III. The vessels in the mid- and lower dermis and subcutaneous fat. *The Journal of investigative dermatology* **77**, 297-304 (1981).
80. Oka, M.*, et al.* Inhibition of endogenous TGF-beta signaling enhances lymphangiogenesis. *Blood* **111**, 4571-4579 (2008).
81. Oliver, G. & Harvey, N. A stepwise model of the development of lymphatic vasculature. *Ann N Y Acad Sci* **979**, 159-165; discussion 188-196 (2002).
82. Srinivasan, R.S.*, et al.* Lineage tracing demonstrates the venous origin of the mammalian lymphatic vasculature. *Genes & development* **21**, 2422-2432 (2007).

83. Francois, M.*, et al.* Sox18 induces development of the lymphatic vasculature in mice. *Nature* **456**, 643-647 (2008).
84. Johnson, N.C.*, et al.* Lymphatic endothelial cell identity is reversible and its maintenance requires Prox1 activity. *Genes & development* **22**, 3282-3291 (2008).
85. Kriehuber, E.*, et al.* Isolation and characterization of dermal lymphatic and blood endothelial cells reveal stable and functionally specialized cell lineages. *The Journal of experimental medicine* **194**, 797-808 (2001).
86. Petrova, T.V.*, et al.* Lymphatic endothelial reprogramming of vascular endothelial cells by the Prox-1 homeobox transcription factor. *Embo J* **21**, 4593-4599 (2002).
87. Marino, D. Identification of molecular mechanisms controlling lymphatic vessel formation by use of the embryonic stem-cell derived embryoid body assay. *DISS. ETH Nr. 18687* (2009).
88. Gerhardt, H. & Betsholtz, C. Endothelial-pericyte interactions in angiogenesis. *Cell and tissue research* **314**, 15-23 (2003).
89. Armulik, A., Abramsson, A. & Betsholtz, C. Endothelial/pericyte interactions. *Circulation research* **97**, 512-523 (2005).
90. Sims, D.E. Recent advances in pericyte biology--implications for health and disease. *The Canadian journal of cardiology* **7**, 431-443 (1991).
91. Yamanishi, H., Fujiwara, S. & Soma, T. Perivascular localization of dermal stem cells in human scalp. *Experimental dermatology* **21**, 78-80.
92. Baluk, P., Hashizume, H. & McDonald, D.M. Cellular abnormalities of blood vessels as targets in cancer. *Current opinion in genetics & development* **15**, 102-111 (2005).
93. Berger, M., Bergers, G., Arnold, B., Hammerling, G.J. & Ganss, R. Regulator of G-protein signaling-5 induction in pericytes coincides with active vessel remodeling during neovascularization. *Blood* **105**, 1094-1101 (2005).
94. Hughes, S. & Chan-Ling, T. Characterization of smooth muscle cell and pericyte differentiation in the rat retina in vivo. *Investigative ophthalmology & visual science* **45**, 2795-2806 (2004).
95. Collett, G.D. & Canfield, A.E. Angiogenesis and pericytes in the initiation of ectopic calcification. *Circulation research* **96**, 930-938 (2005).
96. Sundberg, C., Ivarsson, M., Gerdin, B. & Rubin, K. Pericytes as collagen-producing cells in excessive dermal scarring. *Laboratory investigation; a journal of technical methods and pathology* **74**, 452-466 (1996).
97. Leveen, P.*, et al.* Mice deficient for PDGF B show renal, cardiovascular, and hematological abnormalities. *Genes & development* **8**, 1875-1887 (1994).
98. Lindahl, P., Johansson, B.R., Leveen, P. & Betsholtz, C. Pericyte loss and microaneurysm formation in PDGF-B-deficient mice. *Science (New York, N.Y* **277**, 242-245 (1997).
99. Hellstrom, M., Kalen, M., Lindahl, P., Abramsson, A. & Betsholtz, C. Role of PDGF-B and PDGFR-beta in recruitment of vascular smooth muscle cells and pericytes during embryonic blood vessel formation in the mouse. *Development (Cambridge, England)* **126**, 3047-3055 (1999).
100. Heldin, C.H. & Westermark, B. Mechanism of action and in vivo role of platelet-derived growth factor. *Physiological reviews* **79**, 1283-1316 (1999).
101. Nurden, A.T. Platelets, inflammation and tissue regeneration. *Thrombosis and haemostasis* **105 Suppl 1**, S13-33.
102. Martin, P. Wound healing--aiming for perfect skin regeneration. *Science (New York, N.Y* **276**, 75-81 (1997).
103. Brown, E.J. Phagocytosis. *Bioessays* **17**, 109-117 (1995).
104. Rappolee, D.A., Mark, D., Banda, M.J. & Werb, Z. Wound macrophages express TGF-alpha and other growth factors in vivo: analysis by mRNA phenotyping. *Science (New York, N.Y* **241**, 708-712 (1988).
105. Leibovich, S.J. & Ross, R. The role of the macrophage in wound repair. A study with hydrocortisone and antimacrophage serum. *The American journal of pathology* **78**, 71-100 (1975).
106. Martin, P. & Leibovich, S.J. Inflammatory cells during wound repair: the good, the bad and the ugly. *Trends in cell biology* **15**, 599-607 (2005).
107. Martin, P.*, et al.* Wound healing in the PU.1 null mouse--tissue repair is not dependent on inflammatory cells. *Curr Biol* **13**, 1122-1128 (2003).
108. Kariya, Y. & Gu, J. N-glycosylation of ss4 integrin controls the adhesion and motility of keratinocytes. *PloS one* **6**, e27084.
109. Larjava, H., Salo, T., Haapasalmi, K., Kramer, R.H. & Heino, J. Expression of integrins and basement membrane components by wound keratinocytes. *The Journal of clinical investigation* **92**, 1425-1435 (1993).

110. Clark, R.A., Ashcroft, G.S., Spencer, M.J., Larjava, H. & Ferguson, M.W. Re-epithelialization of normal human excisional wounds is associated with a switch from alpha v beta 5 to alpha v beta 6 integrins. *The British journal of dermatology* **135**, 46-51 (1996).
111. Paladini, R.D., Takahashi, K., Bravo, N.S. & Coulombe, P.A. Onset of re-epithelialization after skin injury correlates with a reorganization of keratin filaments in wound edge keratinocytes: defining a potential role for keratin 16. *The Journal of cell biology* **132**, 381-397 (1996).
112. Werner, S.*, et al.* The function of KGF in morphogenesis of epithelium and reepithelialization of wounds. *Science (New York, N.Y* **266**, 819-822 (1994).
113. Nanney, L.B.*, et al.* Novel approaches for understanding the mechanisms of wound repair. *The journal of investigative dermatology. Symposium proceedings / the Society for Investigative Dermatology, Inc* **11**, 132-139 (2006).
114. Greiling, D. & Clark, R.A. Fibronectin provides a conduit for fibroblast transmigration from collagenous stroma into fibrin clot provisional matrix. *Journal of cell science* **110 (Pt 7)**, 861-870 (1997).
115. Manon-Jensen, T., Itoh, Y. & Couchman, J.R. Proteoglycans in health and disease: the multiple roles of syndecan shedding. *The FEBS journal* **277**, 3876-3889.
116. Olczyk, P., Komosinska-Vassev, K., Winsz-Szczotka, K., Kuznik-Trocha, K. & Olczyk, K. [Hyaluronan: structure, metabolism, functions, and role in wound healing]. *Postepy higieny i medycyny doswiadczalnej (Online)* **62**, 651-659 (2008).
117. Tonnesen, M.G., Feng, X. & Clark, R.A. Angiogenesis in wound healing. *The journal of investigative dermatology. Symposium proceedings / the Society for Investigative Dermatology, Inc* **5**, 40-46 (2000).
118. Folkman, J. & D'Amore, P.A. Blood vessel formation: what is its molecular basis? *Cell* **87**, 1153-1155 (1996).
119. Risau, W. Mechanisms of angiogenesis. *Nature* **386**, 671-674 (1997).
120. Detmar, M.*, et al.* Hypoxia regulates the expression of vascular permeability factor/vascular endothelial growth factor (VPF/VEGF) and its receptors in human skin. *The Journal of investigative dermatology* **108**, 263-268 (1997).
121. Clark, R.A.*, et al.* Fibronectin is produced by blood vessels in response to injury. *The Journal of experimental medicine* **156**, 646-651 (1982).
122. Brooks, P.C., Clark, R.A. & Cheresh, D.A. Requirement of vascular integrin alpha v beta 3 for angiogenesis. *Science (New York, N.Y* **264**, 569-571 (1994).
123. Ilan, N., Mahooti, S. & Madri, J.A. Distinct signal transduction pathways are utilized during the tube formation and survival phases of in vitro angiogenesis. *Journal of cell science* **111 (Pt 24)**, 3621-3631 (1998).
124. Beanes, S.R., Dang, C., Soo, C. & Ting, K. Skin repair and scar formation: the central role of TGF-beta. *Expert reviews in molecular medicine* **5**, 1-22 (2003).
125. Lovvorn, H.N., 3rd*, et al.* Relative distribution and crosslinking of collagen distinguish fetal from adult sheep wound repair. *Journal of pediatric surgery* **34**, 218-223 (1999).
126. Juckett, G. & Hartman-Adams, H. Management of keloids and hypertrophic scars. *American family physician* **80**, 253-260 (2009).
127. Longaker, M.T. & Adzick, N.S. The biology of fetal wound healing: a review. *Plastic and reconstructive surgery* **87**, 788-798 (1991).
128. Roy, S. & Levesque, M. Limb regeneration in axolotl: is it superhealing? *TheScientificWorldJournal* **6 Suppl 1**, 12-25 (2006).
129. Whitby, D.J. & Ferguson, M.W. The extracellular matrix of lip wounds in fetal, neonatal and adult mice. *Development (Cambridge, England)* **112**, 651-668 (1991).
130. Hsu, M., Peled, Z.M., Chin, G.S., Liu, W. & Longaker, M.T. Ontogeny of expression of transforming growth factor-beta 1 (TGF-beta 1), TGF-beta 3, and TGF-beta receptors I and II in fetal rat fibroblasts and skin. *Plastic and reconstructive surgery* **107**, 1787-1794; discussion 1795-1786 (2001).
131. Rolfe, K.J.*, et al.* A role for TGF-beta1-induced cellular responses during wound healing of the non-scarring early human fetus? *The Journal of investigative dermatology* **127**, 2656-2667 (2007).
132. Scheid, A.*, et al.* Physiologically low oxygen concentrations in fetal skin regulate hypoxia-inducible factor 1 and transforming growth factor-beta3. *Faseb J* **16**, 411-413 (2002).
133. Longaker, M.T.*, et al.* Studies in fetal wound healing, VI. Second and early third trimester fetal wounds demonstrate rapid collagen deposition without scar formation. *Journal of pediatric surgery* **25**, 63-68; discussion 68-69 (1990).
134. Liechty, K.W., Adzick, N.S. & Crombleholme, T.M. Diminished interleukin 6 (IL-6) production during scarless human fetal wound repair. *Cytokine* **12**, 671-676 (2000).

135. Jain, K., Sykes, V., Kordula, T. & Lanning, D. Homeobox genes Hoxd3 and Hoxd8 are differentially expressed in fetal mouse excisional wounds. *The Journal of surgical research* **148**, 45-48 (2008).
136. Saaristo, A.*, et al.* Vascular endothelial growth factor-C accelerates diabetic wound healing. *Am J Pathol* **169**, 1080-1087 (2006).
137. Falanga, V. Wound healing and its impairment in the diabetic foot. *Lancet* **366**, 1736-1743 (2005).
138. Stone, H.B., Coleman, C.N., Anscher, M.S. & McBride, W.H. Effects of radiation on normal tissue: consequences and mechanisms. *The lancet oncology* **4**, 529-536 (2003).
139. Gabriel, V. Hypertrophic scar. *Physical medicine and rehabilitation clinics of North America* **22**, 301-310, vi.
140. Chalmers, R.L. The evidence for the role of transforming growth factor-beta in the formation of abnormal scarring. *International wound journal* **8**, 218-223.
141. Namazi, M.R., Fallahzadeh, M.K. & Schwartz, R.A. Strategies for prevention of scars: what can we learn from fetal skin? *International journal of dermatology* **50**, 85-93.
142. Bedogni, B.*, et al.* The hypoxic microenvironment of the skin contributes to Akt-mediated melanocyte transformation. *Cancer cell* **8**, 443-454 (2005).
143. Evans, S.M., Schrlau, A.E., Chalian, A.A., Zhang, P. & Koch, C.J. Oxygen levels in normal and previously irradiated human skin as assessed by EF5 binding. *The Journal of investigative dermatology* **126**, 2596-2606 (2006).
144. Schreml, S.*, et al.* Oxygen in acute and chronic wound healing. *The British journal of dermatology* **163**, 257-268.
145. Izadi, K. & Ganchi, P. Chronic wounds. *Clinics in plastic surgery* **32**, 209-222 (2005).
146. Gordillo, G.M. & Sen, C.K. Revisiting the essential role of oxygen in wound healing. *American journal of surgery* **186**, 259-263 (2003).
147. Sen, C.K. The general case for redox control of wound repair. *Wound Repair Regen* **11**, 431-438 (2003).
148. Allen, D.B.*, et al.* Wound hypoxia and acidosis limit neutrophil bacterial killing mechanisms. *Arch Surg* **132**, 991-996 (1997).
149. Myllyla, R., Tuderman, L. & Kivirikko, K.I. Mechanism of the prolyl hydroxylase reaction. 2. Kinetic analysis of the reaction sequence. *European journal of biochemistry / FEBS* **80**, 349-357 (1977).
150. Roy, S.*, et al.* Oxygen sensing by primary cardiac fibroblasts: a key role of p21(Waf1/Cip1/Sdi1). *Circulation research* **92**, 264-271 (2003).
151. McIntire, L.V. World technology panel report on tissue engineering. *Annals of biomedical engineering* **30**, 1216-1220 (2002).
152. Stock, U.A. & Vacanti, J.P. Tissue engineering: current state and prospects. *Annual review of medicine* **52**, 443-451 (2001).
153. Murphy, S.V. & Atala, A. Organ engineering - combining stem cells, biomaterials, and bioreactors to produce bioengineered organs for transplantation. *Bioessays*.
154. Takahashi, K. & Yamanaka, S. Induction of pluripotent stem cells from mouse embryonic and adult fibroblast cultures by defined factors. *Cell* **126**, 663-676 (2006).
155. Robinton, D.A. & Daley, G.Q. The promise of induced pluripotent stem cells in research and therapy. *Nature* **481**, 295-305.
156. Kawamura, M.*, et al.* Enhanced survival of transplanted human induced pluripotent stem cell-derived cardiomyocytes by the combination of cell sheets with the pedicled omental flap technique in a porcine heart. *Circulation* **128**, S87-94.
157. Nam, Y.J.*, et al.* Reprogramming of human fibroblasts toward a cardiac fate. *Proceedings of the National Academy of Sciences of the United States of America* **110**, 5588-5593.
158. Priori, S.G., Napolitano, C., Di Pasquale, E. & Condorelli, G. Induced pluripotent stem cell-derived cardiomyocytes in studies of inherited arrhythmias. *The Journal of clinical investigation* **123**, 84-91.
159. Wernig, M.*, et al.* Neurons derived from reprogrammed fibroblasts functionally integrate into the fetal brain and improve symptoms of rats with Parkinson's disease. *Proceedings of the National Academy of Sciences of the United States of America* **105**, 5856-5861 (2008).
160. Chin, M.H.*, et al.* Induced pluripotent stem cells and embryonic stem cells are distinguished by gene expression signatures. *Cell stem cell* **5**, 111-123 (2009).
161. Deng, J.*, et al.* Targeted bisulfite sequencing reveals changes in DNA methylation associated with nuclear reprogramming. *Nature biotechnology* **27**, 353-360 (2009).
162. Guenther, M.G.*, et al.* Chromatin structure and gene expression programs of human embryonic and induced pluripotent stem cells. *Cell stem cell* **7**, 249-257.

163. Bock, C.*, et al.* Reference Maps of human ES and iPS cell variation enable high-throughput characterization of pluripotent cell lines. *Cell* **144**, 439-452.
164. Berman, B., Viera, M.H., Amini, S., Huo, R. & Jones, I.S. Prevention and management of hypertrophic scars and keloids after burns in children. *The Journal of craniofacial surgery* **19**, 989-1006 (2008).
165. Falanga, V. Chronic wounds: pathophysiologic and experimental considerations. *The Journal of investigative dermatology* **100**, 721-725 (1993).
166. MacNeil, S. Progress and opportunities for tissue-engineered skin. *Nature* **445**, 874-880 (2007).
167. Nie, X.*, et al.* Successful application of tissue-engineered skin to refractory ulcers. *Clinical and experimental dermatology* **32**, 699-701 (2007).
168. Billingham RE., M.P. Technique of free skin grafting in mammals. *J Exp Biol* **28**, 385-402 (1950).
169. Karasek, M.A. In vitro culture of human skin epithelial cells. *The Journal of investigative dermatology* **47**, 533-540 (1966).
170. Rheinwald, J.G. & Green, H. Serial cultivation of strains of human epidermal keratinocytes: the formation of keratinizing colonies from single cells. *Cell* **6**, 331-343 (1975).
171. Bell, E., Ehrlich, H.P., Buttle, D.J. & Nakatsuji, T. Living tissue formed in vitro and accepted as skin-equivalent tissue of full thickness. *Science (New York, N.Y* **211**, 1052-1054 (1981).
172. Kowalske, K.J. Burn wound care. *Physical medicine and rehabilitation clinics of North America* **22**, 213-227, v.
173. Achauer, B.M. & Martinez, S.E. Burn wound pathophysiology and care. *Critical care clinics* **1**, 47-58 (1985).
174. Quinby, W.C., Jr., Burke, J.F. & Bondoc, C.C. Primary excision and immediate wound closure. *Intensive care medicine* **7**, 71-76 (1981).
175. Boyce, S.T.*, et al.* Cultured skin substitutes reduce donor skin harvesting for closure of excised, full-thickness burns. *Annals of surgery* **235**, 269-279 (2002).
176. Green, H., Kehinde, O. & Thomas, J. Growth of cultured human epidermal cells into multiple epithelia suitable for grafting. *Proceedings of the National Academy of Sciences of the United States of America* **76**, 5665-5668 (1979).
177. Horch, R.E., Bannasch, H. & Stark, G.B. Transplantation of cultured autologous keratinocytes in fibrin sealant biomatrix to resurface chronic wounds. *Transplantation proceedings* **33**, 642-644 (2001).
178. Boyce, S.T. Cultured skin substitutes: a review. *Tissue Eng* **2**, 255-266 (1996).
179. Supp, D.M., Wilson-Landy, K. & Boyce, S.T. Human dermal microvascular endothelial cells form vascular analogs in cultured skin substitutes after grafting to athymic mice. *Faseb J* **16**, 797-804 (2002).
180. Burke, J.F., Yannas, I.V., Quinby, W.C., Jr., Bondoc, C.C. & Jung, W.K. Successful use of a physiologically acceptable artificial skin in the treatment of extensive burn injury. *Annals of surgery* **194**, 413-428 (1981).
181. Phillips, T.J.*, et al.* The longevity of a bilayered skin substitute after application to venous ulcers. *Archives of dermatology* **138**, 1079-1081 (2002).
182. Black, A.F., Berthod, F., L'Heureux, N., Germain, L. & Auger, F.A. In vitro reconstruction of a human capillary-like network in a tissue-engineered skin equivalent. *Faseb J* **12**, 1331-1340 (1998).
183. Shepherd, B.R.*, et al.* Vascularization and engraftment of a human skin substitute using circulating progenitor cell-derived endothelial cells. *Faseb J* **20**, 1739-1741 (2006).
184. Gibot, L., Galbraith, T., Huot, J. & Auger, F.A. A preexisting microvascular network benefits in vivo revascularization of a microvascularized tissue-engineered skin substitute. *Tissue engineering* **16**, 3199-3206.
185. Tremblay, P.L., Hudon, V., Berthod, F., Germain, L. & Auger, F.A. Inosculation of tissue-engineered capillaries with the host's vasculature in a reconstructed skin transplanted on mice. *Am J Transplant* **5**, 1002-1010 (2005).
186. Kaully, T., Kaufman-Francis, K., Lesman, A. & Levenberg, S. Vascularization--the conduit to viable engineered tissues. *Tissue engineering* **15**, 159-169 (2009).
187. Red-Horse, K., Crawford, Y., Shojaei, F. & Ferrara, N. Endothelium-microenvironment interactions in the developing embryo and in the adult. *Developmental cell* **12**, 181-194 (2007).
188. Sun, Q.*, et al.* Sustained vascular endothelial growth factor delivery enhances angiogenesis and perfusion in ischemic hind limb. *Pharmaceutical research* **22**, 1110-1116 (2005).
189. Doi, K.*, et al.* Enhanced angiogenesis by gelatin hydrogels incorporating basic fibroblast growth factor in rabbit model of hind limb ischemia. *Heart and vessels* **22**, 104-108 (2007).

190. Ennett, A.B., Kaigler, D. & Mooney, D.J. Temporally regulated delivery of VEGF in vitro and in vivo. *Journal of biomedical materials research* **79**, 176-184 (2006).
191. Kaigler, D., Wang, Z., Horger, K., Mooney, D.J. & Krebsbach, P.H. VEGF scaffolds enhance angiogenesis and bone regeneration in irradiated osseous defects. *J Bone Miner Res* **21**, 735-744 (2006).
192. Perets, A*., et al.* Enhancing the vascularization of three-dimensional porous alginate scaffolds by incorporating controlled release basic fibroblast growth factor microspheres. *Journal of biomedical materials research* **65**, 489-497 (2003).
193. Laschke, M.W*., et al.* Incorporation of growth factor containing Matrigel promotes vascularization of porous PLGA scaffolds. *Journal of biomedical materials research* **85**, 397-407 (2008).
194. Anderson, S.M., Siegman, S.N. & Segura, T. The effect of vascular endothelial growth factor (VEGF) presentation within fibrin matrices on endothelial cell branching. *Biomaterials* **32**, 7432-7443.
195. Carmeliet, P. & Conway, E.M. Growing better blood vessels. *Nature biotechnology* **19**, 1019-1020 (2001).
196. Richardson, T.P., Peters, M.C., Ennett, A.B. & Mooney, D.J. Polymeric system for dual growth factor delivery. *Nature biotechnology* **19**, 1029-1034 (2001).
197. Nillesen, S.T*., et al.* Increased angiogenesis and blood vessel maturation in acellular collagen-heparin scaffolds containing both FGF2 and VEGF. *Biomaterials* **28**, 1123-1131 (2007).
198. Chung, H.J. & Park, T.G. Surface engineered and drug releasing pre-fabricated scaffolds for tissue engineering. *Advanced drug delivery reviews* **59**, 249-262 (2007).
199. Kirkpatrick, C.J*., et al.* Experimental approaches to study vascularization in tissue engineering and biomaterial applications. *Journal of materials science* **14**, 677-681 (2003).
200. Choi, N.W*., et al.* Microfluidic scaffolds for tissue engineering. *Nature materials* **6**, 908-915 (2007).
201. Nahmias, Y., Schwartz, R.E., Verfaillie, C.M. & Odde, D.J. Laser-guided direct writing for three-dimensional tissue engineering. *Biotechnology and bioengineering* **92**, 129-136 (2005).
202. Wang, G.J., Hsu, Y.F., Hsu, S.H. & Horng, R.H. JSR photolithography based microvessel scaffold fabrication and cell seeding. *Biomedical microdevices* **8**, 17-23 (2006).
203. Ryu, W*., et al.* The construction of three-dimensional micro-fluidic scaffolds of biodegradable polymers by solvent vapor based bonding of micro-molded layers. *Biomaterials* **28**, 1174-1184 (2007).
204. Choi, Y., McClain, M.A., LaPlaca, M.C., Frazier, A.B. & Allen, M.G. Three dimensional MEMS microfluidic perfusion system for thick brain slice cultures. *Biomedical microdevices* **9**, 7-13 (2007).
205. Wang, G.J., Chen, C.L., Hsu, S.H., Chiang, Y.L. . Bio-MEMS fabricated artificial capillaries for tissue engineering. *Microsyst Tech* **12**(2005).
206. Darland, D.C. & D'Amore, P.A. Blood vessel maturation: vascular development comes of age. *The Journal of clinical investigation* **103**, 157-158 (1999).
207. Levenberg, S*., et al.* Engineering vascularized skeletal muscle tissue. *Nature biotechnology* **23**, 879-884 (2005).
208. Stainier, D.Y., Weinstein, B.M., Detrich, H.W., 3rd, Zon, L.I. & Fishman, M.C. Cloche, an early acting zebrafish gene, is required by both the endothelial and hematopoietic lineages. *Development (Cambridge, England)* **121**, 3141-3150 (1995).
209. Matsumoto, K., Yoshitomi, H., Rossant, J. & Zaret, K.S. Liver organogenesis promoted by endothelial cells prior to vascular function. *Science (New York, N.Y* **294**, 559-563 (2001).
210. Alt, B*., et al.* Arteries define the position of the thyroid gland during its developmental relocalisation. *Development (Cambridge, England)* **133**, 3797-3804 (2006).
211. Lammert, E., Cleaver, O. & Melton, D. Induction of pancreatic differentiation by signals from blood vessels. *Science (New York, N.Y* **294**, 564-567 (2001).
212. Lammert, E*., et al.* Role of VEGF-A in vascularization of pancreatic islets. *Curr Biol* **13**, 1070-1074 (2003).
213. Esni, F., Johansson, B.R., Radice, G.L. & Semb, H. Dorsal pancreas agenesis in N-cadherin-deficient mice. *Developmental biology* **238**, 202-212 (2001).
214. Mukouyama, Y.S., Shin, D., Britsch, S., Taniguchi, M. & Anderson, D.J. Sensory nerves determine the pattern of arterial differentiation and blood vessel branching in the skin. *Cell* **109**, 693-705 (2002).
215. Mukouyama, Y.S., Gerber, H.P., Ferrara, N., Gu, C. & Anderson, D.J. Peripheral nerve-derived VEGF promotes arterial differentiation via neuropilin 1-mediated positive feedback. *Development (Cambridge, England)* **132**, 941-952 (2005).

216. Shen, Q.*, et al.* Endothelial cells stimulate self-renewal and expand neurogenesis of neural stem cells. *Science (New York, N.Y* **304**, 1338-1340 (2004).
217. Chen, X.*, et al.* Rapid anastomosis of endothelial progenitor cell-derived vessels with host vasculature is promoted by a high density of cotransplanted fibroblasts. *Tissue Eng Part A* **16**, 585-594.
218. Alajati, A.*, et al.* Spheroid-based engineering of a human vasculature in mice. *Nature methods* **5**, 439-445 (2008).
219. Correa de Sampaio, P.*, et al.* A heterogeneous in vitro three dimensional model of tumour-stroma interactions regulating sprouting angiogenesis. *PloS one* **7**, e30753.
220. Kang, K.T., Allen, P. & Bischoff, J. Bioengineered human vascular networks transplanted into secondary mice reconnect with the host vasculature and re-establish perfusion. *Blood* **118**, 6718-6721.
221. Rouwkema, J., de Boer, J. & Van Blitterswijk, C.A. Endothelial cells assemble into a 3-dimensional prevascular network in a bone tissue engineering construct. *Tissue Eng* **12**, 2685-2693 (2006).
222. Wang, L.*, et al.* Osteogenesis and angiogenesis of tissue-engineered bone constructed by prevascularized beta-tricalcium phosphate scaffold and mesenchymal stem cells. *Biomaterials* **31**, 9452-9461.
223. Mendes, L.F.*, et al.* Perivascular-like cells contribute to the stability of the vascular network of osteogenic tissue formed from cell sheet-based constructs. *PloS one* **7**, e41051.
224. Caspi, O.*, et al.* Tissue engineering of vascularized cardiac muscle from human embryonic stem cells. *Circulation research* **100**, 263-272 (2007).
225. Stevens, K.R.*, et al.* Physiological function and transplantation of scaffold-free and vascularized human cardiac muscle tissue. *Proceedings of the National Academy of Sciences of the United States of America* **106**, 16568-16573 (2009).
226. Bottcher-Haberzeth, S., Biedermann, T. & Reichmann, E. Tissue engineering of skin. *Burns* **36**, 450-460 (2010).
227. Marino, D., Luginbuhl, J., Scola, S., Meuli, M. & Reichmann, E. Bioengineering dermo-epidermal skin grafts with blood and lymphatic capillaries. *Science translational medicine* **6**, 221ra214 (2014).
228. O'Ceallaigh, S., Herrick, S.E., Bluff, J.E., McGrouther, D.A. & Ferguson, M.W. Quantification of total and perfused blood vessels in murine skin autografts using a fluorescent double-labeling technique. *Plastic and reconstructive surgery* **117**, 140-151 (2006).
229. Schreml, S.*, et al.* Oxygen in acute and chronic wound healing. *The British journal of dermatology* **163**, 257-268 (2010).
230. Tandara, A.A. & Mustoe, T.A. Oxygen in wound healing--more than a nutrient. *World journal of surgery* **28**, 294-300 (2004).
231. Romano Di Peppe, S.*, et al.* Adenovirus-mediated VEGF(165) gene transfer enhances wound healing by promoting angiogenesis in CD1 diabetic mice. *Gene therapy* **9**, 1271-1277 (2002).
232. Sun, G.*, et al.* Dextran hydrogel scaffolds enhance angiogenic responses and promote complete skin regeneration during burn wound healing. *Proceedings of the National Academy of Sciences of the United States of America* **108**, 20976-20981 (2011).
233. Hendrickx, B.*, et al.* Integration of blood outgrowth endothelial cells in dermal fibroblast sheets promotes full thickness wound healing. *Stem cells (Dayton, Ohio)* **28**, 1165-1177 (2010).
234. Danner, S.*, et al.* The use of human sweat gland-derived stem cells for enhancing vascularization during dermal regeneration. *The Journal of investigative dermatology* **132**, 1707-1716 (2012).
235. Ekstrand, A.J.*, et al.* Deletion of neuropeptide Y (NPY) 2 receptor in mice results in blockage of NPY-induced angiogenesis and delayed wound healing. *Proceedings of the National Academy of Sciences of the United States of America* **100**, 6033-6038 (2003).
236. Mori, R., Kondo, T., Nishie, T., Ohshima, T. & Asano, M. Impairment of skin wound healing in beta-1,4-galactosyltransferase-deficient mice with reduced leukocyte recruitment. *The American journal of pathology* **164**, 1303-1314 (2004).
237. Dvir, T.*, et al.* Prevascularization of cardiac patch on the omentum improves its therapeutic outcome. *Proceedings of the National Academy of Sciences of the United States of America* **106**, 14990-14995 (2009).
238. Gibot, L., Galbraith, T., Huot, J. & Auger, F.A. A preexisting microvascular network benefits in vivo revascularization of a microvascularized tissue-engineered skin substitute. *Tissue Eng Part A* **16**, 3199-3206 (2010).
239. Montano, I.*, et al.* Formation of human capillaries in vitro: the engineering of prevascularized matrices. *Tissue engineering* **16**, 269-282 (2010).

240. Skobe, M. & Detmar, M. Structure, function, and molecular control of the skin lymphatic system. *The journal of investigative dermatology. Symposium proceedings / the Society for Investigative Dermatology, Inc* **5**, 14-19 (2000).
241. Hong, Y.K.*, et al.* VEGF-A promotes tissue repair-associated lymphatic vessel formation via VEGFR-2 and the alpha1beta1 and alpha2beta1 integrins. *Faseb J* **18**, 1111-1113 (2004).
242. Antonelli-Orlidge, A., Saunders, K.B., Smith, S.R. & D'Amore, P.A. An activated form of transforming growth factor beta is produced by cocultures of endothelial cells and pericytes. *Proceedings of the National Academy of Sciences of the United States of America* **86**, 4544-4548 (1989).
243. Dar, A.*, et al.* Multipotent vasculogenic pericytes from human pluripotent stem cells promote recovery of murine ischemic limb. *Circulation* **125**, 87-99 (2012).
244. Gitlin, J.D. & D'Amore, P.A. Culture of retinal capillary cells using selective growth media. *Microvascular research* **26**, 74-80 (1983).
245. Berthod, F., Symes, J., Tremblay, N., Medin, J.A. & Auger, F.A. Spontaneous fibroblast-derived pericyte recruitment in a human tissue-engineered angiogenesis model in vitro. *Journal of cellular physiology* **227**, 2130-2137 (2012).
246. Vi, L., de Lasa, C., DiGuglielmo, G.M. & Dagnino, L. Integrin-linked kinase is required for TGF-beta1 induction of dermal myofibroblast differentiation. *The Journal of investigative dermatology* **131**, 586-593 (2011).
247. Legg, J., Jensen, U.B., Broad, S., Leigh, I. & Watt, F.M. Role of melanoma chondroitin sulphate proteoglycan in patterning stem cells in human interfollicular epidermis. *Development (Cambridge, England)* **130**, 6049-6063 (2003).
248. Yannas, I.V. Similarities and differences between induced organ regeneration in adults and early foetal regeneration. *Journal of the Royal Society, Interface / the Royal Society* **2**, 403-417 (2005).
249. Werner, S., Krieg, T. & Smola, H. Keratinocyte-fibroblast interactions in wound healing. *The Journal of investigative dermatology* **127**, 998-1008 (2007).
250. Metcalfe, A.D. & Ferguson, M.W. Tissue engineering of replacement skin: the crossroads of biomaterials, wound healing, embryonic development, stem cells and regeneration. *Journal of the Royal Society, Interface / the Royal Society* **4**, 413-437 (2007).
251. Bottcher-Haberzeth, S., Biedermann, T. & Reichmann, E. Tissue engineering of skin. *Burns* **36**, 450-460.
252. Xiong, X., Wu, T. & He, S. Physical forces make rete ridges in oral mucosa. *Medical hypotheses*.
253. Armour, A.D., Powell, H.M. & Boyce, S.T. Fluorescein diacetate for determination of cell viability in tissue-engineered skin. *Tissue engineering* **14**, 89-96 (2008).
254. Sauter, B., Foedinger, D., Sterniczky, B., Wolff, K. & Rappersberger, K. Immunoelectron microscopic characterization of human dermal lymphatic microvascular endothelial cells. Differential expression of CD31, CD34, and type IV collagen with lymphatic endothelial cells vs blood capillary endothelial cells in normal human skin, lymphangioma, and hemangioma in situ. *J Histochem Cytochem* **46**, 165-176 (1998).
255. Marino, D., Luginbuhl, J., Scola, S., Meuli, M. & Reichmann, E. Bioengineering dermo-epidermal skin grafts with blood and lymphatic capillaries. *Science translational medicine* **6**, 221ra214.
256. Ng, C.P., Helm, C.L. & Swartz, M.A. Interstitial flow differentially stimulates blood and lymphatic endothelial cell morphogenesis in vitro. *Microvasc Res* **68**, 258-264 (2004).
257. Helm, C.L., Fleury, M.E., Zisch, A.H., Boschetti, F. & Swartz, M.A. Synergy between interstitial flow and VEGF directs capillary morphogenesis in vitro through a gradient amplification mechanism. *Proceedings of the National Academy of Sciences of the United States of America* **102**, 15779-15784 (2005).
258. Helm, C.L., Zisch, A. & Swartz, M.A. Engineered blood and lymphatic capillaries in 3-D VEGF-fibrin-collagen matrices with interstitial flow. *Biotechnology and bioengineering* **96**, 167-176 (2007).

5 ACKNOWLEDGEMENTS

I would like to thank Prof. Dr. Ernst Reichmann for giving me the opportunity of doing my PhD studies in his group. Thank you for patiently supporting and supervising me throughout these years.

I would like to thank Prof. Dr. Reinhard Dummer for supervising my PhD thesis and Prof. Dr. Max Gassmann for being in my committee.

This work was financially supported by the EU-FP6 project EuroSTEC (soft tissue engineering for congenital birth defects in children: contract: LSHB-CT-2006-037409), and by the University of Zurich. I am particularly grateful to the Fondation Gaydoul for their generous financial support and interest in my work.

Many thanks to Prof. Dr. Martin Meuli and PD Dr. Clemens Schiestl for their support and providing me with insights into the field of fetal surgery, plastic and reconstructive surgery, and the treatment of burn injuries.

I would also like to thank the present and former members of the TBRU for all their support and helpful suggestions during these years. Exceptional thanks go to Daniela Marino, the time with you has been unforgettable, thank you so much for supporting me on so many aspects of science and life in general throughout these years.

And finally, I would like to express my deepest gratefulness to my family and my friends. You have been there for me before and during my PhD and also will be there thereafter. No words can express how much this means to me.

6 CURRICULUM VITAE

Joachim Luginbühl
Höschgasse 36, 8008 Zürich, Switzerland
Phone: +41 78 892 46 49
E-mail: J.Luginbuehl@kispi.uzh.ch

Personal data

Date of birth:	02.12.1981
Place of birth:	St.Gallen, Switzerland
Nationality:	Swiss
Marital status:	Unmarried

Education

10/2008 - present	PhD in the group of Prof. Dr. Ernst Reichmann Tissue biology research unit, Department of surgery – University Children's Hospital, Zurich. FP6 EuroStec PhD program http://www.eurostec.eu/
03/2006 – 05/2008	Master of Science in the group of Prof. Dr. Silvia Arber; Biocenter, Basel Titel of the Master thesis: Unraveling genetic control-mechanisms of motor circuitry in mouse
06/2002 – 01/2006	Study of Biology at the Biocenter in Basel
07/2001	High school graduation, Romanshorn, Switzerland

Work experience

07/2003 – 09/2003	Volunteer at Tortugas, Mexico
07/2002 – 09/2002	Internship at Nestlé Schweiz AG, Quality-control lab Basel. Revision of a new concept documenting laboratory equipment (standard operating procedure), chemical examinations etc.
08/2001 – 12/2001	Internship at Nestlé Schweiz AG, Quality-control lab Basel. Compile approx. 170 instructions that describe the examination of all primary products used in the manufactory: pH, common salt, photospectrometric examination, peroxid-number, free fatty acids, sensory examination etc.

Professional Skills

Cell culture: human, rat, pig and mouse primary cell types; assembly and analysis of human skin substitutes in vitro and in vivo; assembly and analysis of a human dermal microvasculature consisting of blood and lymphatic microvessels; animal surgery (mouse and rat); FACS; immunofluorescence; PCR; cloning; in situ hybridization; confocal microscopy; molecular biology.

Further education and workshops

- Education and training of persons carrying out animal experiments, Basel, Switzerland, 10/2006
- LTK Module 20E: Introductory Course in Laboratory Animal Science, Zürich, Switzerland, 05/2009
- Weiterbildung: Das Zürcher Schweinemodell, Bern, Switzerland, 08/2011
- Novartis Topik basic information security training, Basel, Switzerland, 11/2006

Conferences with oral presentations

ESAO	European society for artificial organs, Porto, Portugal, September 2011
TERMIS	Tissue engineering and regenerative medicine international society, Granada, Spain, June 2011
JPSS	The 22nd International Symposium on Paediatric Surgical Research, Genoa, Italy, September 2009
TERMIS	Tissue engineering and regenerative medicine international society, Seoul, South Korea, September 2009

Languages

German	Mother language
English	Excellent
French	Good

Interests

Playing and writing music, sports (sailing, dancing, jogging), reading, travelling.

7 PUBLICATIONS

First author:

Marino D and Luginbühl J, Scola S, Meuli M, Reichmann E. Bioengineering dermo-epidermal skin grafts with blood and lymphatic capillaries. Sci Transl Med. 2014 Jan 29;6(221):221ra14. doi: 10.1126/scitranslmed.3006894.

Luginbühl, J., Marino, D., Hartmann-Fritsch, F., Scola, S., Meuli, M., Reichmann, E. Rapid perfusion directs the healing of prevascularized dermo-epidermal skin substitutes from scar formation towards regeneration. Under revision (2014).

Co-author:

Simonetta Scola, Joachim Luginbühl, Alberto Giovanni Busetto, Thomas Biedermann, Daniela Marino, Luca Pontiggia1 & Ernst Reichmann1*. An inexhaustible source of self-renewing keratinocytes: active stem cells of suprabasal layers retro-differentiate into basal quiescent stem cells. [in preparation]

Agnieszka S. Klar, Sinan Güven, Thomas Biedermann, Joachim Luginbühl, Sophie Böttcher-Haberzeth3, Claudia Meuli-Simmen4, Martin Meuli3, Ivan Martin2, Arnaud Scherberich2 and Ernst Reichmann1*. Tissue-engineered dermo-epidermal skin grafts prevascularized with adipose-derived cells. 2014 Mar 27. pii: S0142-9612(14)00205-1. doi: 10.1016/j.biomaterials.2014.02.049. [Epub ahead of print]

Hartmann-Fritsch, F., Biedermann, T., Braziulis, E., Luginbühl, J., Pontiggia, L., Bottcher-Haberzeth, S., van Kuppevelt, T.H., Faraj, K.A., Schiestl, C., Meuli, M., et al. Collagen hydrogels strengthened by biodegradable meshes are a basis for dermo-epidermal skin grafts intended to reconstitute human skin in a one-step surgical intervention. J Tissue Eng Regen Med. [Epub ahead of print]

Hartmann-Fritsch, F., Hosper, N., Luginbühl, J., Biedermann, T., Reichmann, E., and Meuli, M. Human amniotic fluid derived cells can competently substitute dermal fibroblasts in a tissue-engineered dermo-epidermal skin analog. Pediatr Surg Int 29:61-69.

Kottmann, J., Rey, J.M., Luginbühl, J., Reichmann, E., and Sigrist, M.W. Glucose sensing in human epidermis using mid-infrared photoacoustic detection. Biomed Opt Express 3:667-680.

Braziulis, E., Diezi, M., Biedermann, T., Pontiggia, L., Schmucki, M., Hartmann-Fritsch, F., Luginbühl, J., Schiestl, C., Meuli, M., and Reichmann, E. Modified plastic compression of collagen hydrogels provides an ideal matrix for clinically applicable skin substitutes. Tissue Eng Part C Methods 18:464-474.

Montano, I., Schiestl, C., Schneider, J., Pontiggia, L., Luginbühl, J., Biedermann, T., Bottcher-Haberzeth, S., Braziulis, E., Meuli, M., and Reichmann, E. Formation of human capillaries in vitro: the engineering of prevascularized matrices. Tissue Eng Part A 16:269-282. -derived cells

8 CONTRIBUTIONS

I conributed to the following publications as indicated:

Publication I:

Bioengineering dermo-epidermal skin grafts with blood and lymphatic capillaries

- Experimental outline
- Performance of experiments
- Preparation of figures
- Manuscript writing
- Revision of the manuscript

Publication II:

Rapid perfusion directs the healing of prevascularized dermo-epidermal skin substitutes from scar formation towards regeneration

- Experimental outline
- Performance of experiments
- Preparation of figures
- Manuscript writing
- Revision of the manuscript